USGS
science for a changing world

Arc-Related Porphyry Molybdenum Deposit Model

Chapter D of
Mineral Deposit Models for Resource Assessment

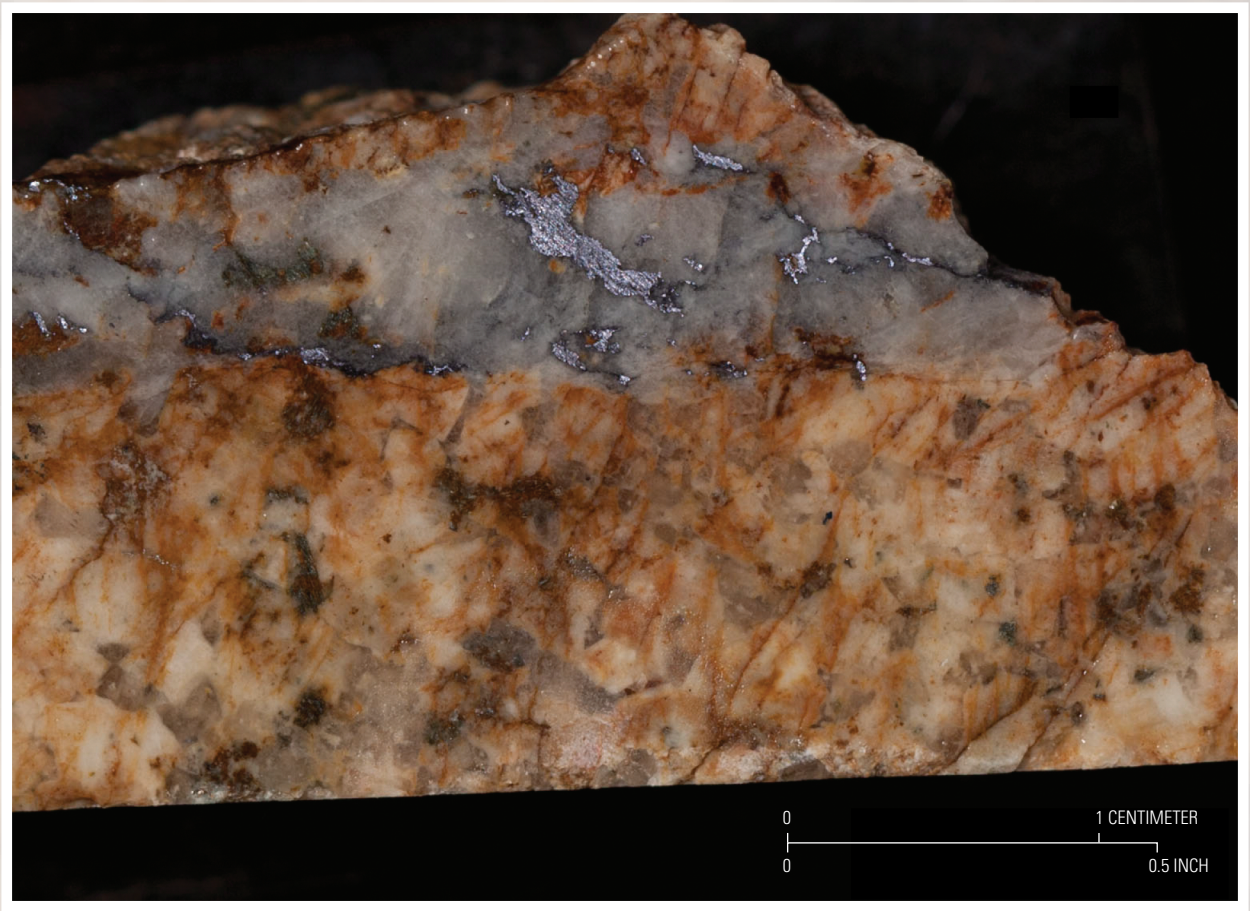

Scientific Investigations Report 2010–5070–D

U.S. Department of the Interior
U.S. Geological Survey

COVER: Quartz-molybdenite vein cutting through potassically altered granite. Photograph by Ryan D. Taylor, U.S. Geological Survey.

Arc-Related Porphyry Molybdenum Deposit Model

By Ryan D. Taylor, Jane M. Hammarstrom, Nadine M. Piatak, and Robert R. Seal, II

Chapter D of
Mineral Deposit Model for Resource Assessment

Scientific Investigations Report 2010–5070–D

U.S. Department of the Interior
U.S. Geological Survey

U.S. Department of the Interior
KEN SALAZAR, Secretary

U.S. Geological Survey
Marcia K. McNutt, Director

U.S. Geological Survey, Reston, Virginia: 2012

Suggested citation:
Taylor, R.D., Hammarstrom, J.M., Piatak, N.M., and Seal, R.R. II, 2012, Arc-related porphyry molybdenum deposit model, chap. D *of* Mineral deposit models for resource assessment: U.S. Geological Survey Scientific Investigations Report 2010–5070–D, 64 p.

Contents

Figures

Appendix Figures

Tables

Appendix Tables

Conversion Factors

SI to Inch/Pound

Multiply	By	To obtain
	Length	
centimeter (cm)	0.3937	inch (in.)
millimeter (mm)	0.03937	inch (in.)
meter (m)	3.281	foot (ft)
kilometer (km)	0.6214	mile (mi)
kilometer (km)	0.5400	mile, nautical (nmi)
meter (m)	1.094	yard (yd)
	Volume	
cubic meter (m^3)	6.290	barrel (petroleum, 1 barrel = 42 gal)
liter (L)	33.82	ounce, fluid (fl. oz)
liter (L)	2.113	pint (pt)
liter (L)	1.057	quart (qt)
liter (L)	0.2642	gallon (gal)
cubic meter (m^3)	264.2	gallon (gal)
cubic meter (m^3)	0.0002642	million gallons (Mgal)
cubic centimeter (cm^3)	0.06102	cubic inch (in^3)
liter (L)	61.02	cubic inch (in^3)
cubic meter (m^3)	35.31	cubic foot (ft^3)
cubic meter (m^3)	1.308	cubic yard (yd^3)
cubic meter (m^3)	0.0008107	acre-foot (acre-ft)
liter per second (L/s)	15.85	gallon per minute (gal/min)
cubic meter per day (m^3/d)	264.2	gallon per day (gal/d)
cubic meter per day per square kilometer [$(m^3/d)/km^2$]	684.28	gallon per day per square mile [$(gal/d)/mi^2$]
cubic meter per second (m^3/s)	22.83	million gallons per day (Mgal/d)
cubic meter per day per square kilometer [$(m^3/d)/km^2$]	0.0006844	million gallons per day per square mile [$(Mgal/d)/mi^2$]
cubic meter per hour (m^3/h)	39.37	inch per hour (in/h)
millimeter per year (mm/yr)	0.03937	inch per year (in/yr)
kilometer per hour (km/h)	0.6214	mile per hour (mi/h)
	Mass	
kilogram (kg)	2.205	pound avoirdupois (lb)
metric ton per year	1.102	ton per year (ton/yr)

Temperature in degrees Celsius (°C) may be converted to degrees Fahrenheit (°F) as follows:

$$°F=(1.8×°C)+32$$

Temperature in degrees Fahrenheit (°F) may be converted to degrees Celsius (°C) as follows:

$$°C=(°F–32)/1.8$$

Vertical coordinate information is referenced to the North American Vertical Datum of 1988 (NAVD 88).

Horizontal coordinate information is referenced to the North American Datum of 1983 (NAD 83).

Specific conductance is given in microsiemens per centimeter at 25 degrees Celsius (µS/cm at 25°C).

Concentrations of chemical constituents in water are given either in milligrams per liter (mg/L) or micrograms per liter (µg/L).

Arc-Related Porphyry Molybdenum Deposit Model

Ryan D. Taylor, Jane M. Hammarstrom, Nadine M. Piatak, and Robert R. Seal, II

Abstract

This report provides a descriptive model for arc-related porphyry molybdenum deposits. Presented within are geological, geochemical, and mineralogical characteristics that differentiate this deposit type from porphyry copper and alkali-feldspar rhyolite-granite porphyry molybdenum deposits. The U.S. Geological Survey's effort to update existing mineral deposit models spurred this research, which is intended to supplement previously published models for this deposit type that help guide mineral-resource and mineral-environmental assessments.

Arc-related porphyry molybdenum deposits are a substantial resource for molybdenum metal and may have anomalous concentrations of tungsten. The deposits contain low-grade ore (0.03–0.22 percent molybdenum) as molybdenite, but are large-tonnage, making them amenable to bulk mining open-pit techniques. The mineralizing system usually has fluorine contents of less than 0.1 percent. The cogenetic intrusion is a differentiated calc-alkaline granitoid, typically granodiorite to quartz monzonite in composition, with low rubidium and niobium, and moderate to high strontium concentrations. Metals and hydrothermal fluids are sourced from these intrusions, with an additional meteoric fluid component contributing to peripheral alteration but not adding more metal. The lithology of the surrounding country rocks is not important to the formation of these deposits, but a surrounding carbonate unit may be altered to skarn that contains economic mineralization. The creation of contact-metamorphosed hornfels adjacent to the intrusion is common.

Formation of arc-related porphyry molybdenum deposits typically occurs within a continental arc environment related to arc-continent or continent-continent collision and subduction. Few deposits are found in an island arc setting. Most classified arc-related porphyry molybdenum deposits are located in the western cordillera of North America, notably in British Columbia and Alaska.

Hydrothermal alteration provides a key component to the identification of a deposit. Alteration usually is zoned from a core of potassic plus/minus silicic alteration outwards through phyllic to propylitic alteration. Argillic alteration may be irregular in shape and will overprint earlier hydrothermal alteration.

Exploration should be limited to magmatic arc belts that have been unroofed and eroded to levels of a few kilometers depth. Important geological vectors toward areas of higher grade mineralization include intensity of hydrothermal alteration, veining, and faulting. Anomalous levels of molybdenum, tungsten, copper, lead, or zinc in soils, tills, stream sediments, and drainage waters may indicate the presence of an arc-related porphyry molybdenum deposit. Geophysical exploration techniques have been met with minimal success because of the overall low concentration of associated sulfide and oxide minerals.

Geoenvironmental concerns are generally low because of low volumes of sulfide minerals. Most deposits are marginally acid-generating to non-acid-generating with drainage waters being near-neutral pH because of the acid generating potential of pyrite being partially buffered by late-stage calcite-bearing veins. The low ore content results in a waste:ore ratio of nearly 1:1 and large tailings piles from the open-pit method of mining.

Introduction

Arc-related porphyry molybdenum deposits form in the same tectonic environment as many porphyry copper deposits (Seedorff and others, 2005; John and others, 2010), but are mined principally for molybdenum (Mo) and not for copper (Cu). The principal ore mineral containing molybdenum is molybdenite (MoS_2). Deposits are typically large, commonly greater than 50 million tonnes (Mt) and low-grade (0.03 to 0.22 percent Mo). They are hosted by hydrothermally altered porphyritic intermediate to felsic granitoid plutons and the flanking country rocks. These calc-alkaline granitoid intrusions are genetically, temporally, and spatially related to the molybdenum mineralization.

Numerous classification schemes for porphyry molybdenum deposits have been proposed (Mutschler and others, 1981; Westra and Keith, 1981; Wallace, 1995; Seedorff and others, 2005). Alkali-feldspar rhyolite-granite porphyry molybdenum deposits (Kamilli and others, written commun.), previously termed high-fluorine molybdenum or Climax-type molybdenum deposits, have received more attention than arc-related porphyry molybdenum deposits in the literature because of their higher-grade. Comparatively, arc-related porphyry molybdenum deposits are more numerous in North America and thus may be more important when molybdenum prices are high. Many of the known arc-related porphyry molybdenum occurrences are sub-economic at the current 2011 metal price or are found in environmentally sensitive areas and are not mined. Arc-related porphyry molybdenum

and alkali-feldspar rhyolite-granite porphyry molybdenum deposits may be two end-member systems within the porphyry molybdenum field, with certain hybrid deposits displaying characteristics intermediate between the two end-member deposit types. Nevertheless, many features are distinct enough such that two different deposit types are preferred.

In the past, arc-related porphyry molybdenum deposits had a variety of names. Most notably, they have been referred to as low-fluorine stockwork molybdenum deposits by some workers (for example, see Ludington and others, 2009). However, the lack of fluorine (F) concentration data for many deposits and the reliance on this single parameter has caused concern regarding this designation. Undoubtedly, fluorine does exert a strong effect on the properties of silicate melts in processes such as crystal fractionation, magma degassing, and melt-vapor interactions, so the presence or absence of fluorine-bearing minerals may qualitatively help to distinguish between the two end-member types of porphyry molybdenum deposits. The term arc-related porphyry molybdenum is preferred because it relates the mineralization to its tectonic environment and helps to delineate tracts of land that this deposit type may be found in.

Molybdenum has a melting temperature of over 2,600 degrees Celsius (°C) and is used to create stable and hard carbides (Northcott, 1956). These characteristics make molybdenum favorable for the creation of hardened steel alloys. Molybdenum use in armor and airplanes has helped shape the economic viability of mining molybdenite based on demand brought about by international conflicts.

This report of arc-related porphyry molybdenum deposits is part of an effort by the U.S. Geological Survey Mineral Resources Program to update existing models and develop new descriptive mineral deposit models that will be used for an upcoming national mineral-resource assessment and is intended to supplement previously published models such as those of Cox and Singer (1986). Anticipated uses are for mineral-resource and mineral-environmental assessments.

Deposit Type and Associated Commodities

Name

Arc-related porphyry molybdenum deposits.

Synonyms

Many different names have been used to describe the same type of deposit. These different names have focused mainly on distinctive geochemical or petrographic features of the system. Synonyms for arc-related porphyry molybdenum deposits include low-fluorine stockwork molybdenum, fluorine-poor, granodiorite-type, calc-alkaline-type, differentiated monzogranite class, Endako-type, subduction-related porphyry molybdenum, arc-related calc-alkaline, and porphyry molybdenum. However, the classification “porphyry molybdenum” can relate to arc-related porphyry molybdenum and alkali-feldspar rhyolite-granite porphyry molybdenum deposit types.

Brief Description

Arc-related porphyry molybdenum deposits are targeted for their appreciable amounts of contained molybdenum and occasionally have tungsten or base metal enrichments hosted in adjacent co-genetic skarn or peripheral vein deposits. Compared to other types of porphyry ore deposits, there is a distinctive overall lack of copper and tin enrichment in the mineralized system, and these are not considered to be recoverable metals. However, although the copper concentration is far less than what is noted within porphyry copper deposits, the copper content of arc-related porphyry molybdenum deposits can vary and may be more elevated in these deposits than in barren intrusions. The large tonnage and low molybdenum grade of these deposits is in contrast to the higher grade of alkali-feldspar rhyolite-granite porphyry molybdenum deposits (see figure A1 in the appendix). Copper is not considered a recoverable metal and when porphyry molybdenum deposits have recoverable quantities of copper, they are relegated to molybdenum-rich porphyry copper deposits and are not included in this report. Examples include Hall and Buckingham, Nevada, and Mount Tolman, Washington (none of these are shown in the location figures), which were once considered low-fluorine stockwork molybdenum deposits, but have since been shown to have similar metal grades to the more molybdenum-rich porphyry copper deposits of the world (Ludington and others, 2009, and references therein).

Formation of arc-related porphyry molybdenum deposits occurs within a magmatic arc, typically continental, related to arc-continent accretion/subduction or continent-continent collision (Sinclair, 1995); however, some deposits may be postsubduction (Wolfe, 1995). The intrusion of calc-alkaline magma into the upper crust differentiates and forms intermediate to felsic intrusive rocks ranging from tonalite to granite in composition. Most of the productive intrusions are classified as granodiorite and quartz monzonite (Westra and Keith, 1981). The magma is the source of the metals and much of the fluid in the hydrothermal system. Additional fluids are of meteoric origin, with magmatic fluid dominant in the core of the system and an increasing meteoric fluid component away from the intrusion.

The metalliferous stockwork seals fractures that were forcibly developed by hydrofracturing after metal-bearing solutions in the carapace of the crystallizing intrusion reached fluid pressures that exceeded the lithostatic pressure and tensile strength of the surrounding rock units. Preexisting structures do not necessarily dictate the creation of the stockwork veining. However, preexisting structures and zones of structural weakness may be preferred sites for initial pluton emplacement. Examples include local strike-slip faults within a regionally compressive tectonic regime of a continental magmatic arc.

The fluorine (F) content of the system is characteristically low, with no appreciable hydrothermal fluorite and the mineralizing intrusion containing less than 0.1 percent F. Low rubidium (less than 300 parts per million or ppm) and niobium (less than 30 ppm), and moderate to high strontium (greater than 100 ppm) concentrations of the associated igneous rocks help to geochemically distinguish this class of molybdenum deposit from the alkali-feldspar rhyolite-granite porphyry molybdenum type (Westra and Keith, 1981). The rare earth element (REE) patterns of the mineralizing intrusions are similar to those of normal and barren arc-related calc-alkaline intrusions and porphyry copper-bearing intrusions found throughout the world (for example, see Lawley and others, 2010). If a europium (Eu) anomaly exists, then it is typically minor and can be either positive or negative (for example, see Whalen and others, 2001; U.S. Geological Survey Headwaters Province Project Team, 2007; Lawley, 2009; Lawley and others, 2010).

The intrusion(s) responsible for mineralization are commonly porphyritic, but some are equigranular in texture. The main igneous minerals can include quartz, plagioclase, potassium feldspar, biotite, and hornblende, with additional minor and trace minerals such as apatite, magnetite, and zircon. Intrusions are commonly cylindrical and only a few hundred meters in diameter. The lithology of the country rocks has little effect on the formation of these deposits.

Both pervasive and vein selvage hydrothermal alteration is prevalent. A central core of potassic alteration with or without silicic alteration is surrounded by adjacent phyllic alteration and an outer zone of propylitic alteration. An irregular area of argillic alteration may overprint earlier hydrothermal alteration.

Associated Deposit Types

Many other deposit types are genetically associated to arc-related porphyry molybdenum deposits or are formed in similar tectonic environments. Genetically related deposits include molybdenum-bearing skarns (Meinert and others, 2005) in the adjacent country rocks that may contain appreciable amounts of tungsten commonly in the form of scheelite ($CaWO_4$). Peripheral silver-lead-zinc veins also may form as a result of the same hydrothermal system.

Porphyry copper deposits (John and others, 2010) also form in magmatic arc environments and may contain mineable amounts of molybdenum, but many are not major molybdenum producers and likely represent types of deposits found within the spectrum of porphyry mineralization that includes molybdenum, copper, and gold. Porphyry tungsten-molybdenum deposits, such as Logtung, Yukon and Mount Pleasant, New Brunswick (neither are shown), also may host molybdenum as a byproduct or as a primary commodity (Sinclair, 2007). Alkali-feldspar rhyolite-granite porphyry molybdenum deposits are another substantial source of molybdenum.

Primary Commodities

Molybdenum is the primary commodity recovered from arc-related porphyry molybdenum deposits. Commodity-wise, they are distinguished from porphyry copper plus or minus (±) molybdenum deposits by having no recoverable copper.

Byproduct Commodities

Tungsten ore in the form of scheelite may be economically substantial in peripheral skarn deposits genetically associated with some arc-related porphyry molybdenum deposits (for example, at Cannivan Gulch, Montana; Thompson Creek, Idaho; and MAX, British Columbia). Tungsten in other mineral forms is rarer, but can be found as wolframite [$(Fe,Mn)WO_4$, found for example at Davidson, British Columbia] or powellite, a form of scheelite with partial molybdenum substitution for tungsten (found for example at Boss Mountain, British Columbia). The Pine Nut, Nevada molybdenum deposit has associated tungsten skarn deposits that vary from scheelite- to powellite-dominated ore zones with increasing depth (Doebrich and others, 1996).

Trace Constituents

Anomalous metallic trace constituents found in arc-related porphyry molybdenum deposits include copper, lead, silver, tin, and zinc. Molybdenite in porphyry deposits may be a source for rhenium because molybdenite is the only major sulfide with substantial quantities of rhenium within its crystal structure. Only rare rhenium-sulfides have been documented. Bismuth also is elevated in some deposits and can be found in the form of native bismuth or bismuthinite (Sinclair, 2007).

Example Deposits

Many of the world's molybdenum deposits, including ores in both porphyry molybdenum deposit types, are located in the western cordillera of North America (fig. 1). Nevertheless, many other igneous-related molybdenum deposits or occurrences exist throughout the world, including elsewhere in North America (Ayres and others, 1982; Duke, 2007; Kerr and others, 2009), eastern Europe (Janković, 1982), Australia (Witcher, 1975), China (Mao and others, 2008), Russia (Sutulov, 1973), and elsewhere in Asia (Heinhorst and others, 2000) (fig. 2). However, many of these deposits do not have sufficient published data to definitively classify them as arc-related porphyry molybdenum deposits. In fact, some display characteristics that would preclude them from this classification (for example, Stein and others, 1997; Mao and others, 2008). Because of this, some deposits that may be classified as arc-related porphyry molybdenum deposits with additional research in the future are given limited discussion in this report.

Anduramba is one of the larger porphyry-style molybdenum prospects in the central part of the New England fold belt, southeastern Queensland, Australia (Witcher, 1975). Published

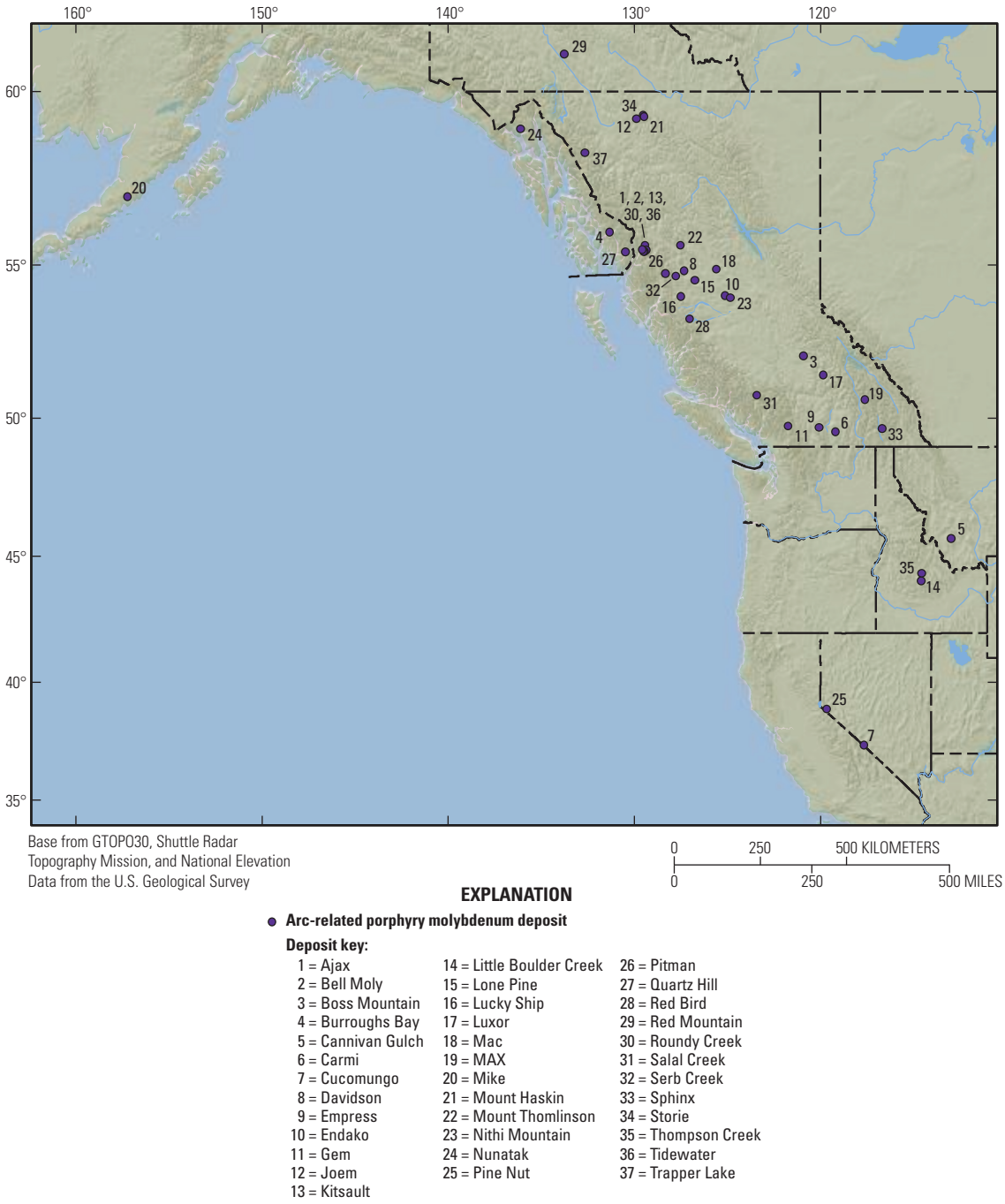

Figure 1. Distribution of arc-related porphyry molybdenum deposits in the western cordillera of North America. Latitude and longitude coordinates of the deposits listed in table A1.

geochemistry is lacking, but it is interpreted to have formed within a Permo-Triassic island arc setting (Horton, 1978). More work is needed to determine the specific tectonic regime of the arc and the classification of Anduramba.

Eastern European porphyry molybdenum deposits, such as Mackatica, Serbia, are associated with the Tertiary Alpine metallogenic epoch in the Serbo-Macedonian metallogenic province (Janković, 1982). These deposits lack published geochemical data, but have been briefly described in the western literature (Janković, 1982; Simic, 2001). Other molybdenum deposits in the vicinity of Mackatica, which might be classified in the future as arc-related, include Borovik, Kucišnjak, Groznatova Dolina, Troskacka Dolina, Cokanova Dolina, Pavlova, and Meca Dolina (none are shown in location figures).

A few deposits in eastern Canada also have been described as arc-related porphyry molybdenum, but lack required data for definitive classification. The Setting Net Lake (Ayres and others, 1982) and Pidgeon-Lateral Lake (Duke, 2007) deposits in Ontario are hosted by Archean rocks, whereas the Moly Brook, Newfoundland (Kerr and others, 2009) deposit is related to the

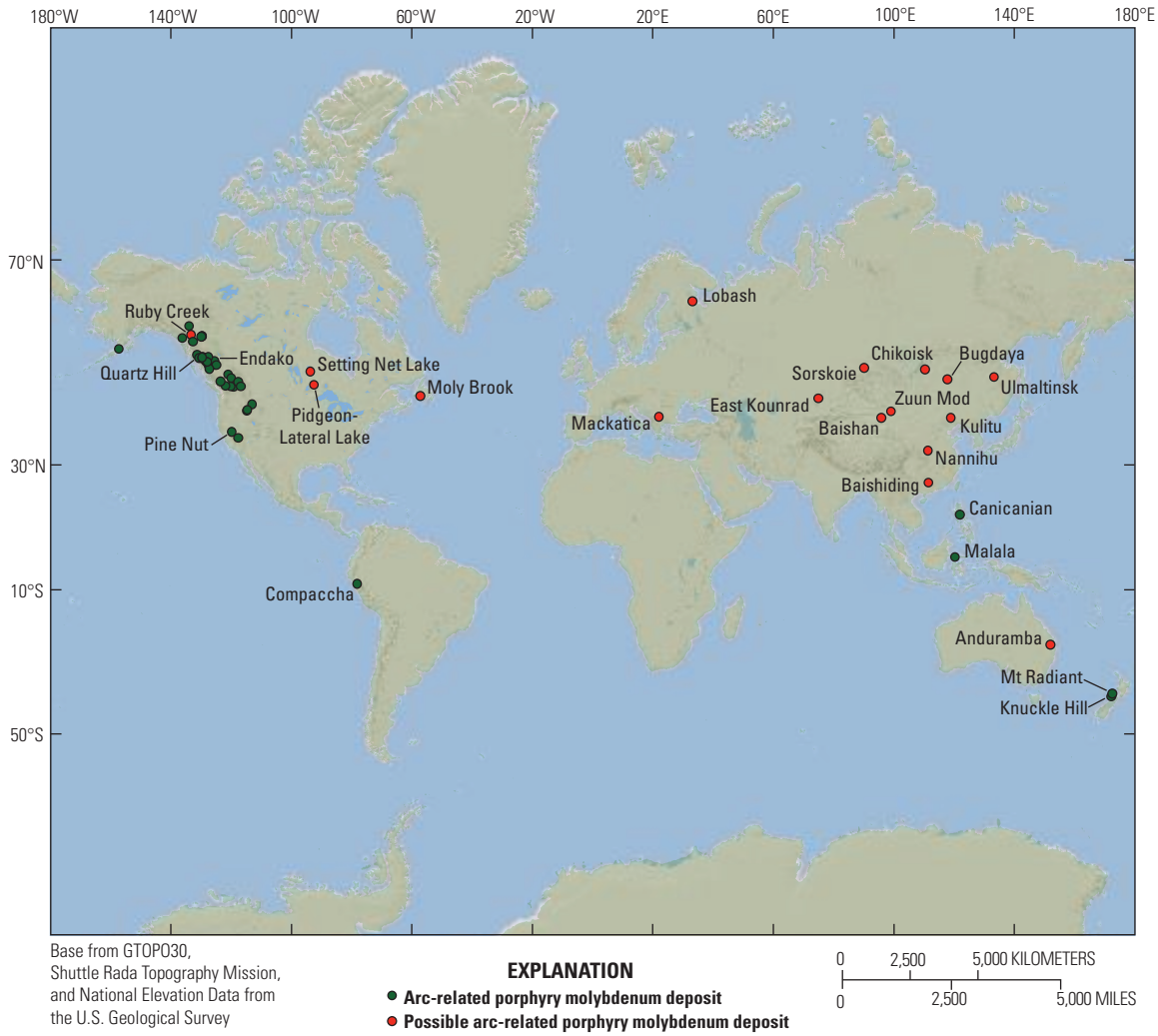

Figure 2. Global distribution of known arc-related porphyry molybdenum deposits and examples of possible arc-related porphyry molybdenum deposits. Additional porphyry molybdenum deposits exist near the labeled possible arc-related porphyry molybdenum deposits, but the best examples are displayed to show tracts of land that may contain arc-related porphyry molybdenum deposits.

late Precambrian to Devonian evolution of the Appalachians. If the older deposits are indeed classified as arc-related in the future, then we also will need to consider Precambrian terranes for this deposit type; presently (2012), definitive examples of this deposit type are restricted to the Phanerozoic. Other molybdenum occurrences have been noted in Newfoundland, but many contain copper as a secondary commodity, which would exclude them from this model.

Asia contains numerous porphyry molybdenum deposits. Unfortunately, most of these deposits also lack detailed geological and geochemical descriptions in the Western literature. In particular, China is the world leader in the production of molybdenum, mainly from porphyry and related skarn deposits. Whereas many deposits have been classified as porphyry molybdenum types, they have not been differentiated as arc-related or as alkali-feldspar rhyolite-granite porphyry molybdenum types. Based on the limited detail in the Chinese literature, many of the large molybdenum deposits, such as Jinduicheng (not shown) in the East Qinling-Dabie orogenic belt, appear better classified as alkali-feldspar rhyolite-granite porphyry molybdenum type (Stein and others, 1997; Mao and others, 2008). Deposits such as Baishan in the eastern Tianshan, northwestern China (Zhang and others, 2005), Baishiding in northeastern Guangxi, southern China (Li and others, 2010), Nannihu in the Qinling orogen, southeastern China (Changming and others, 2008), and Kulitu in the Xilamulun belt in eastern Inner Mongolia, northeastern China (Zeng and others, 2011) possibly may be classified as arc-related porphyry molybdenum; however, further research is necessary to verify this classification. Furthermore, many more deposits throughout China are simply lacking the necessary data and interpretations to give more detailed classifications beyond “porphyry molybdenum”.

Kazakhstan contains a few molybdenum deposits located in magmatic arc terranes (Heinhorst and others, 2000). East Kounrad is the most well-known of these and has been

described as an arc-related porphyry deposit by some researchers (Sinclair, 1995), and as a postmagmatic pegmatite vein-associated greisen-type deposit by others (Burmistrov and others, 1990; Chen and others, 2010). Unfortunately, many of the English-language papers regarding molybdenum deposits in Kazakhstan give poor chemical data and are typically regional overviews.

Russia also contains numerous porphyry molybdenum deposits. Bugdaya in the Eastern Transbaikal region (Laznicka, 1976), Chikoisk in the Buriat region of south-central Siberia (Sutulov, 1973; 1978), Lobash in the Kola-Karelia region (Gorelov and others, 1997), Sorskoie in the Chakasija region of south-central Siberia (Sutulov, 1978), and Ulmaltinsk in the Sakha region of Far East Russia (Sutulov, 1973) are all classified as porphyry molybdenum deposits and some are found in a continental arc tectonic setting (Sinclair, 2007). Most of the English-language literature only gives mention of them, with little to no geological interpretation or geochemical data.

Other deposits that previously had been categorized as arc-related porphyry molybdenum deposits recently have been reclassified through continued work within the last decade. As stated above in the Brief Description section of the Introduction, some deposits that have recoverable amounts of copper may be better classified as molybdenum-rich porphyry copper deposits. Other deposits, notably Ruby Creek (previously known as Adanac), which were once considered to have characteristics dominated by those of arc-related porphyry molybdenum deposits, may be better classified as alkali-feldspar rhyolite-granite porphyry molybdenum deposits, or as some hybrid between the two, based on the associated intrusive rock geochemistry (Ray and others, 2000; Arehart and others, 2006). The Zuun Mod project in Mongolia, located about 100 kilometers (km) from the border of China, was originally determined to be an arc-related porphyry molybdenum deposit, but is now (2012) interpreted to be more transitional to the alkali-feldspar rhyolite-granite porphyry molybdenum type (Clark and Baudry, 2011).

Most known and identified arc-related porphyry molybdenum deposits are found within the western cordillera of North America, in the United States and Canada (fig. 1). Recognized deposits of this type that are found elsewhere throughout the world (fig. 2) include Compaccha, Peru in the Andean continental arc (Hollister, 1975) and extremely rare occurrences within island arc environments in the Philippines and Indonesia (Knittel and Burton, 1985; van Leeuwen and others, 1994). Subeconomic deposits that are found on the South Island of New Zealand include Mt Radiant and Knuckle Hill (Tulloch and Rabone, 1993; Christie and Brathwaite, 1995). Notably, although the Andean arc contains abundant porphyry copper deposits, arc-related porphyry molybdenum deposits are not widely recognized.

Representative deposits within the United States include Quartz Hill, Alaska; Thompson Creek, Idaho; Little Boulder Creek (White Cloud), Idaho; and Cannivan Gulch, Montana. Of the more than 50 molybdenum occurrences in Idaho and Montana, only the Thompson Creek arc-related porphyry molybdenum deposit has had substantial production (Worthington, 2007). Many other productive deposits are spread across the western cordillera of Canada, notably the Endako, Kitsault (formerly known as Lime Creek), and Boss Mountain deposits in British Columbia.

Many small molybdenum occurrences are found scattered throughout Alaska (for example, see Cobb and Elliot, 1980; Cobb, 1981; Ashleman and others, 1997), and presumably elsewhere in the western United States and Canada. Most of these are uneconomic prospects or geochemical anomalies, and also may include such small deposits as Triangle Island, Alaska (not shown) that contained less than a couple hundred kilograms of molybdenite, which was likely mined out within a single day (Cobb, 1981). These minor occurrences, typically with too little data for deposit type classification, are not shown in figure 1 or 2, listed in table A1, or considered in grade-tonnage calculations.

Historical Evolution of Descriptive and Genetic Knowledge and Concepts

The Knaben mine in Norway (not shown) became the first modern mine to produce molybdenum when it opened on a continuous basis in 1885 (Sutulov, 1978). The discovery, during World War I, that molybdenum could be used as effectively as tungsten in strengthening steel for use in armor and high-speed machinery led to increased demand for the metal and started an intensive search for molybdenite. Major molybdenum production of arc-related porphyry molybdenum mines in Canada began in 1965 with production at the Endako and Boss Mountain mines (Soregaroli and Sutherland Brown, 1976). The Quartz Hill deposit in southeastern Alaska is currently the largest known arc-related porphyry molybdenum deposit in the world based on size and contained molybdenum, but it was not mined because of environmental concerns, low molybdenum prices, and obstacles to mining because of the creation of the Misty Fiords National Monument (Ashleman and others, 1997).

Arc-related porphyry and alkali-feldspar rhyolite-granite porphyry molybdenum deposits were at one time lumped together as “stockwork molybdenum deposits” (Clark, 1972). In later work, porphyry molybdenum deposits have been separated into two major types, now (2012) defined by the U.S. Geological Survey as arc-related porphyry molybdenum deposits and rift-related alkali-feldspar rhyolite-granite porphyry molybdenum deposits. Arc-related porphyry molybdenum deposits are considered by some workers to be an end-member and, thus, transitional to the spectrum of porphyry copper deposits (for example, Sillitoe, 1980; Theodore and Menzie, 1984). As such, the historical development of genetic

models for arc-related porphyry molybdenum deposits mirrors the development in the latter one-half of the twentieth century for models of porphyry copper deposits. More importantly, arc-related molybdenum deposits are characterized by many of the same exploration and assessment tract-defining criteria as porphyry copper deposits (John and others, 2010), except particular trace element chemistry and sulfide mineralogy.

The Buckingham, Nevada stockwork molybdenum deposit (not shown) was originally considered a type locality for arc-related porphyry molybdenum deposits (Theodore, 1986). However, it is now considered a molybdenum-rich porphyry copper deposit and has been shown not to be more molybdenum-rich or copper-poor than several porphyry copper deposits used in the modeling of that type of deposit (Ludington and others, 2009). The Copper Basin, Nevada deposit (not shown) consists of a supergene enriched chalcocite blanket derived from disseminated copper in the distal parts of the Buckingham deposit (Theodore and others, 1992).

Regional Environment

Geotectonic Environment

Arc-related porphyry molybdenum deposits form primarily in subduction-related magmatic arcs at convergent plate margins and share many of the same geological characteristics as porphyry copper deposits. Close association with continental magmatic arcs of calc-alkaline nature are nearly ubiquitous and deposits form almost exclusively within continental crust, whereas island arc environments are rare. Some deposits that are interpreted to have been underlain by a slab gap or slab window during magmatism and mineralization include Kitsault and Davidson (formerly known as Glacier Gulch, Hudson Bay Mountain, and Yorke-Hardy) in British Columbia (Kirkham, 1998). Most of the porphyry molybdenum deposits within the Canadian Cordillera are restricted to a tectonic setting that reflects Cretaceous through Tertiary development of younger continental margin arcs within previously accreted Triassic island arc terranes (McMillian and others, 1996).

Some deposits are interpreted to have formed in somewhat atypical postsubduction tectonic environments, such as the 27 million year old (Ma) Quartz Hill, Alaska (Wolfe, 1995), and the 4 Ma Malala, Indonesia (van Leeuwen and others, 1994) deposits. The Quartz Hill tectonic regime is interpreted to be post-orogenic and locally extensional along strike-slip faults, but the mineralizing intrusion was nevertheless emplaced within the central part of an older Late Jurassic through Eocene subduction-related calc-alkaline arc (Ashleman and others, 1997). At Quartz Hill, the cogenetic stock is calc-alkaline and has trace element characteristics similar to other arc-related porphyry molybdenum deposits. The exceptional characteristics and large size of Quartz Hill may have been effected by local rift-related emplacement of the calc-alkaline stock within the older calc-alkaline magmatic arc (Ashleman and others, 1997). Another example of an atypical tectonic regime for an arc-related porphyry deposit is found at Malala and is interpreted to be postsubduction, but still collisional at the time of molybdenum mineralization (van Leeuwen and others, 1994).

A postsubduction tectonic environment of porphyry formation, such as is found at Quartz Hill, increasingly has been recognized for porphyry copper deposits worldwide (Richards, 2009), and thus has implications for arc-related porphyry molybdenum deposits. This type of environment still indirectly involves subduction processes in that porphyry generation occurs by the later remelting of subduction-modified lithosphere and does not change the type of broad convergent margin tectonic setting that hosts these deposits.

The Malala deposit in Sulawesi, Indonesia is an example of an arc-related porphyry molybdenum deposit located in an island arc environment; however, the local geology is complex and displays many characteristics typical of a continental magmatic arc (van Leeuwen and others, 1994). The region consists of Mesozoic and Cenozoic volcanic and sedimentary formations that overlay metamorphic rocks. One interpretation is that western Sulawesi rifted away from Sundaland, creating the Makassar Straits that are underlain by thinned continental crust and not oceanic basement (Situmorang, 1982; van Leeuwen and others, 1994), creating a geological environment that is lithologically similar in many aspects to a continental margin (van Leeuwen and others, 1994). The geochemical characteristics of the ore hosting intrusions at the Malala deposit have continental affinity, such that Soeria-Atmadja and others (1999) suggest involvement of continental crust was necessary for the formation of the Malala molybdenum deposit and of all arc-related porphyry molybdenum deposits.

Another example of a deposit occurring within an island arc setting is Canicanian in the Philippines. The related intrusions at Canicanian display abnormally elevated levels of rubidium compared to typical arc-related porphyry molybdenum deposits and strontium isotopes that do not indicate involvement of old sialic continental crust melt in the magma (Knittel and Burton, 1985).

Temporal (Secular) Relations

The greatest concentration of arc-related porphyry molybdenum deposits are found in the western cordillera of North America and are Late Jurassic through Tertiary in age (table 1). The well-documented deposits of the western cordillera of North America range in age from ~148 Ma (Endako) to ~8 Ma (Salal Creek). The arc-related porphyry molybdenum deposits are mainly products of the subduction of the Kula and Farallon plate beneath western North America.

The Archean Setting Net Lake molybdenum occurrence (2,643 Ma; Nunes and Ayres, 1982) in the Superior Province of northwestern Ontario is an example of one of the older

Table 1. Geologic data on selected arc-related porphyry molybdenum deposits.

[Abbreviations: Ma, million years ago; m, meter; km, kilometer; ±, plus or minus. Geochronology method abbreviations: K-Ar, potassium-argon; Ar-Ar, argon-argon; Rb-Sr, rubidium-strontium; Re-Os, rhenium-osmium]

Deposit (fig. 1)	Location	Mineralizing rock-type	Mineralization age and method	Mineralizing intrusion dimensions
Bell Moly	British Columbia, Canada	Quartz monzonite porphyry	~52 Ma (K-Ar)	670 m × 335 m elongate
Boss Mountain	British Columbia, Canada	Monzogranite stock	102±4 Ma (K-Ar)	800 m × 650 m elliptical
Cannivan Gulch	Montana	Quartz monzonite porphyry	59.1 Ma (K-Ar muscovite)	900 m × 500 m irregular elongated
Compaccha (Tamboras)	Peru	Quartz monzonite porphyry	Neogene (inferred from determined ages of other local plutons)	Irregular elongated. Largely fault-controlled and silled along bedding in country rock.
Davidson (Glacier Gulch, Hudson Bay Mountain, or Yorke-Hardy)	British Columbia, Canada	Quartz monzonite to granodiorite stock	~70 Ma (K-Ar)	340 m diameter plug
Endako	British Columbia, Canada	Quartz monzonite	148 to 145 Ma (Re-Os and Ar-Ar)	24.4 km × 4.8 km elongate
Kitsault (Lime Creek)	British Columbia, Canada	Diorite to quartz monzonite	52.6 Ma (K-Ar)	450 m × 600 m
Little Boulder Creek (White Cloud)	Idaho	Biotite granite porphyry	84 Ma (Ar-Ar)	425 m × 250 m
Malala	Indonesia	Granite, quartz monzonite, granodiorite porphyries	~4 Ma (K-Ar, biotite)	
Max (Trout Lake)	British Columbia, Canada	Granodiorite to tonalite stock	80 Ma (Re-Os, molybdenite)	120 m × 300 m at surface
Quartz Hill	Alaska	Quartz monzonite porphyry stock	26.9 Ma (Rb-Sr)	5 km × 3 km elliptical composite stock
Red Mountain	Yukon, Canada	Quartz monzonite porphyry	87.3±2.0 Ma (K-Ar)	1,450 m × 650 m elliptical
Salal Creek	British Columbia, Canada	Quartz monzonite stock	8 Ma (K-Ar, biotite)	~60 km^2
Thompson Creek	Idaho	Quartz monzonite porphyry	88.4±3 Ma (K-Ar, biotite)	overall stock approximately 2.5 km × 1 km. Exposed on surface 300 m × 460 m.

molybdenum occurrences on Earth. It has been attributed to porphyry-style mineralization (Ayres and others, 1982), and has even been formally assigned to the low-fluorine stockwork molybdenum deposit model (for example, Sinclair, 1995). However, published geochemical data for the associated intrusive rocks is lacking and, therefore, it remains uncertain as to whether this is an arc-related porphyry molybdenum deposit. In fact, Richards and Kerrich (2007) question the applicability of Phanerozoic-style porphyry models to the Setting Net Lake molybdenum deposit because of the inferred postarc timing of magmatism. If future research determines that Setting Net Lake is indeed an arc-related porphyry molybdenum deposit, then this will greatly expand the permissive age range for these deposits to arc settings back beyond the Mesozoic.

The Spinifex Ridge project, Western Australia (not shown), defines a prospect area located within the Archean granite-greenstone terrane of the Pilbara Craton. Geochemical data are sparse, but mineralization has been classified as low-fluorine stockwork molybdenum type (Fisher, 2009). The prospect's association with a granodiorite intrusion is promising in warranting this classification, but because it contains about twice as much copper as molybdenum, and substantial economic silver in its total mineral resource (Fisher, 2009), it may be better classified as a molybdenum-rich porphyry copper deposit.

Duration of Magmatic-Hydrothermal System

The duration of a magmatic-hydrothermal system depends upon many factors, including depth of emplacement, initial magmatic temperature, conductive compared to convective cooling, volume of magma, type of magma, and permeability of the surrounding environment. Under optimal conditions that allow for a single intrusion to produce a long-lived geothermal system, Cathles and others (1997) deduced through numerical modeling that a geothermal system of temperatures greater than 200°C is commonly sustained for no longer than 800,000 years. As shown by the formation of porphyry copper deposits from multiple intrusions, the lifetime of some hydrothermal systems with multiple magma sources is well in excess of 1 million years (Myr) (John and others, 2010, and references therein).

Table 1. Geologic data on selected arc-related porphyry molybdenum deposits.—Continued

[Abbreviations: Ma, million years ago; m, meter; km, kilometer; ±, plus or minus. Geochronology method abbreviations: K-Ar, potassium-argon; Ar-Ar, argon-argon; Rb-Sr, rubidium-strontium; Re-Os, rhenium-osmium]

Deposit (fig. 1)	Deposit shape	Structural control on emplacement?	References
Bell Moly	Crescent around eastern part of stock	Yes. Elongated stock localized at structural intersections.	1, 2
Boss Mountain	Elongate breccia pipe with umbrella of quartz-molybdenite veins	Maybe. Many faults are located in the area, but are interpreted to be post-mineral. Pre-mineral faults likely exist, though.	1, 3, 4
Cannivan Gulch	Two ore shells, one irregular and the other an inverted cup	Yes, located in a NE-trending regional zone of strike-slip faulting.	5, 6, 7, 8
Compaccha (Tamboras)	Wide inverted cup	Yes, Compaccha fault for intrusion and intersections of N45E and N50W fractures for molybdenum mineralization.	9, 10
Davidson (Glacier Gulch, Hudson Bay Mountain, or Yorke-Hardy)	Tabular sheet	Maybe. Faults are located in the immediate vicinity of the deposit.	1, 11
Endako	Elliptical in plan view	Yes. Francois Lake Intrusions focused along suture between Cache Creek and Stikine terranes.	1, 12, 13
Kitsault (Lime Creek)	Ellipsoidal annular	Likely because of deep-seated faults and fractures.	2, 14, 15
Little Boulder Creek (White Cloud)	Arched tabular body	Yes, located in a NE-trending regional zone of strike-slip faulting.	16, 17, 18, 19
Malala	Elongated shell; main zone 1,850 m long, 30–300 m wide	Yes, faulting likely active before, during, and after batholith emplacement.	20
Max (Trout Lake)	Two ore zones, the larger of which is irregular, vertically attenuated	Yes, intrusion emplaced along the N-S trending Z Fault.	21, 22, 29
Quartz Hill	Roughly tabular to somewhat convex, elongate in NNW direction; 2,800 m × 1,500 m	Yes, Coast batholith emplaced in suture between two masses of accreted terranes. Mineralizing stock aligned with a major NNE-trending fault active in the early Tertiary.	23, 24
Red Mountain	Badly segmented by faults, sills, and dikes	Yes. Major pre-emplacement faults likely controlled location of porphyry.	25, 26, 31
Salal Creek	Irregular	Possibly. Projection of the strike-slip Nootka fault plate boundary underneath North America intersects the deposit.	27, 30
Thompson Creek	Tabular 3,400 m × 900 m	Yes, located in a NE-trending regional zone of strike-slip faulting.	8, 19, 28

References: 1: Soregaroli and Sutherland Brown, 1976, and references within; 2: Woodcock and Carter, 1976; 3: Christopher and Carter, 1976; 4: MacDonald and others, 1995; 5: Armstrong and others, 1978; 6: Hammitt and Schmidt, 1982; 7: Darling, 1994; 8: Hildenbrand and others, 2000; 9: Hollister, 1975; 10: Heintze, 1985; 11: Atkinson, 1995; 12: Bysouth and Wong, 1995; 13: Villeneuve and others, 2001; 14: Seraphim and Hollister, 1976; 15: Hodgson, 1995; 16: Theodore and Menzie, 1984; 17: Hall, 1995; 18: Winick and others, 2002; 19: Worthington, 2007; 20: van Leeuwen and others, 1994; 21: Linnen and others, 1995; 22: Lawley and others, 2010; 23: Wolfe, 1995; 24: Ashleman and others, 1997; 25: Stevens and others, 1982; 26: Brown and Kahlert, 1995; 27: Hyndman and others, 1979; 28: Hall and others, 1984; 29: British Columbia minfile 082KNW087; 30: British Columbia minfile 082JW 005; 31: Hunt and Roddick, 1987.

Relations to Structures

Stockwork veining commonly forms when the magmatic fluid pressure builds in the carapace of the intrusion and exceeds that of the lithostatic pressure and the tensile strength of neighboring rock units. Thus, the intense fracturing of the country rock associated with pluton emplacement and hydrofracturing from the exsolution of magmatic fluids help develop stockwork mineralization.

Direct structural control on pluton emplacement is not characteristic of all deposits, although localized lithospheric weaknesses are definitely favorable for magmatic emplacement. Many deposits, such as Red Mountain, Yukon (Brown and Kahlert, 1995); Endako, British Columbia (Bysouth and Wong, 1995); and Quartz Hill, Alaska (Ashleman and others, 1997), are hosted by intrusive complexes that are clearly structurally controlled. Within compressional tectonic regimes, zones of lesser stress, such as local translational zones, will be preferential sites of magma emplacement. Molybdenum mineralization at Compaccha, Peru occurs at the intersection of two sets of orthogonal fractures, with the shape of the cogenetic quartz monzonite porphyry mainly controlled by the Compaccha fault (Hollister, 1975).

In the Alice Arm area, northwestern British Columbia, there are multiple arc-related porphyry molybdenum deposits and evidence exists for both forceful and passive emplacement of the individual mineralizing intrusions. Forceful emplacement is accompanied by deformation of the country rocks, whereas passive emplacement of intrusions is indicated by little disturbance to the country rocks (Woodcock and

Carter, 1976). As mapped, many deposits in the Alice Arm district are not spatially associated with surficial faulting; however, deep-seated faults and fractures are inferred to have localized the Alice Arm intrusions (Seraphim and Hollister, 1976). The elongated geometry of many plutons also suggests emplacement along major fault zones (Woodcock and Carter, 1976).

Relations to Igneous Rocks

Arc-related porphyry molybdenum deposits are directly related to the emplacement of magma into the shallow parts of the upper crust. These magmas are consistently subalkaline (fig. 3*A*), and are more specifically calc-alkaline in nature (fig. 3*B*). Many of the intrusions directly related to mineralization are probably stocks derived from larger plutons at depth. For example, the Malala porphyries are derived from the Dondo intrusive suite (van Leeuwen and others, 1994). The molybdenum-bearing stockwork quartz veins are a product of metal-bearing fluids that exsolved directly from the crystallizing magmatic body. These porphyritic intrusions range from granite through tonalite, with a large number of examples being quartz monzonite and granodiorite in chemical and mineralogical composition. Subduction-related processes are the ultimate generator of these igneous bodies.

Relations to Sedimentary Rocks

Sedimentary rocks are not directly related to the genesis of arc-related porphyry molybdenum deposits. However, local sedimentary rocks are not uncommon and carbonate units may be metamorphosed into skarn by the intrusion of the magma. The local sedimentary rocks also may affect the shape and cooling history of the pluton based on structural integrity, as defined by fractures and bedding, and permeability.

Relations to Metamorphic Rocks

Metamorphic rocks are not critical to the development of arc-related porphyry molybdenum deposits but may act as host rocks. Contact metamorphism of adjacent rock units may produce hornfels, marbles, and skarns within the contact metamorphic aureole. Massive contact metamorphic rocks will affect the circulation of later stage hydrothermal fluids through decreased permeability of the environment surrounding the pluton.

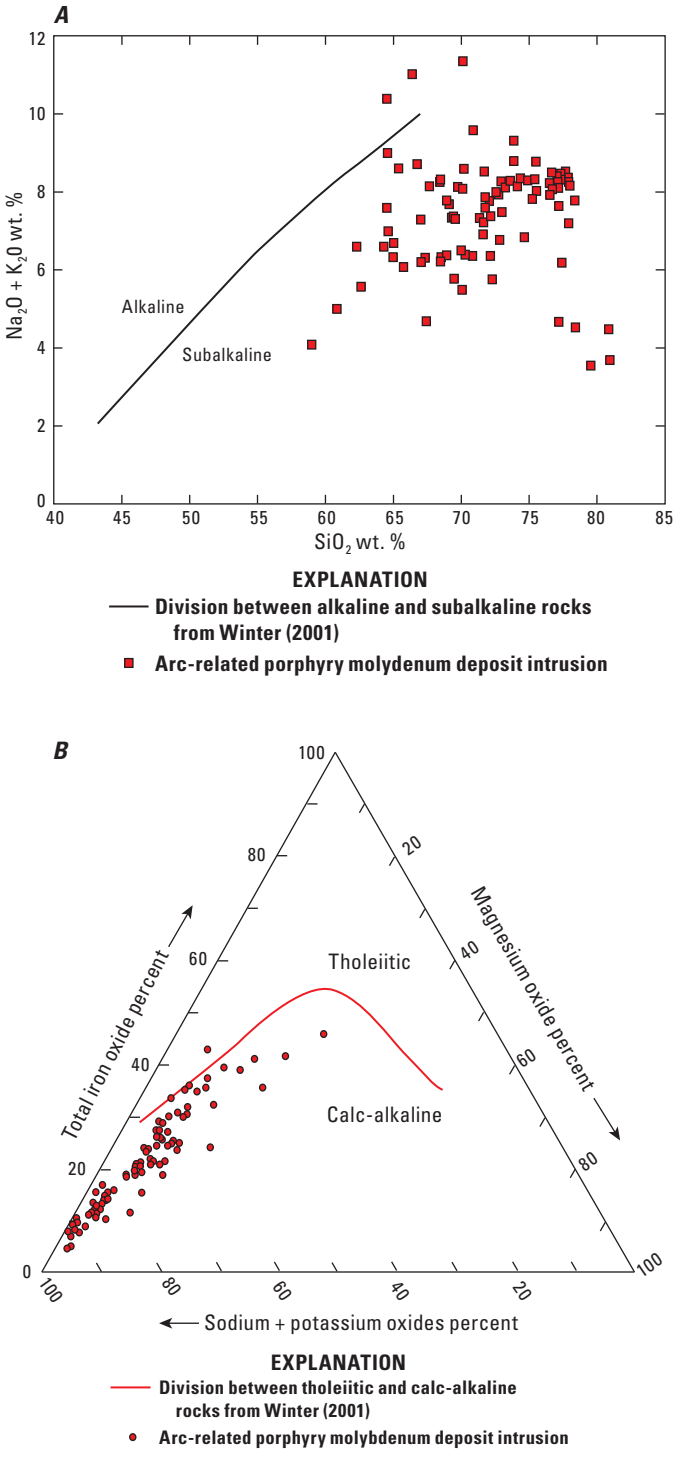

Figure 3. (*A*) Total alkalis vs. silica diagram and (*B*) alkali oxide-iron oxide-magnesium oxide (AFM) ternary diagrams show the subalkaline and more specifically calc-alkaline nature of the associated intrusive rocks for arc-related molybdenum deposits with divisions as shown in Winter (2001). Data points are from the following deposits: Quartz Hill (Hudson and others, 1981; Ashleman and others, 1997), Burroughs Bay (Hudson and others, 1981), Malala (van Leeuwen and others, 1994), Endako (Whalen and others, 2001), Kitsault (Steininger, 1985), Canicanian (Knittel and Burton, 1985), MAX (Lawley and others, 2010), Thompson Creek (Hall and others, 1984), altered rocks from Red Mountain (Brown and Kahlert, 1995), Little Boulder Creek (Mutschler and others, 1981), and Cannivan Gulch (Mutschler and others, 1981; U.S. Geological Survey Headwaters Province Project Team, 2007).

Physical Description of Deposit

Dimensions in Plan View

The mineralizing intrusions of arc-related porphyry molybdenum deposits are typically circular or elliptical in plan view and are generally 1,500 meters (m) or less in diameter (Soregaroli and Sutherland Brown, 1976). For example, the mineralizing intrusion at Red Mountain, Yukon is 1,450 m × 650 m (Brown and Kahlert, 1995) and the mineralizing intrusion at Kitsault is 600 m × 450 m (Hodgson, 1995). The Quartz Hill composite stock, which contains all of the molybdenum mineralization at the Quartz Hill deposit, is elliptical in shape and roughly 2 kilometers (km) across (Hudson and others, 1979).

Ore zones often are irregularly shaped, but can mimic the shape of the mineralizing intrusion and, therefore, can be circular or elliptical in plan view and are typically hundreds of meters in diameter (Sinclair, 1995). Highly irregular ore zones can occur because of the superposition of independently mineralized and altered zones (Sinclair, 2007). The mine at the Endako deposit is composed of three open pits arranged in a near linear fashion, with plans to combine the three pits into a single 3.5-km-long "super-pit" in order to mine the ~400 m × 3.5 km network of molybdenum veins (Ministry of Energy, Mines and Petroleum Resources, 2010a; Ministry of Energy, Mines and Petroleum Resources, 2010b; *http://www.thompsoncreekmetals.com/s/Home.asp*). The Quartz Hill deposit has a surface expression of ore of 2.8 km × 1.5 km (Ashleman and others, 1997).

Size of Hydrothermal System Relative to Extent of Economically Mineralized Rock

Intense alteration can form selvages adjacent to veining, but hydrothermal alteration also extends beyond economically mineralized zones of rock in the form of pervasive alteration. An outer halo of propylitic alteration can extend for hundreds of meters or even kilometers in extent beyond the central zone of potassic and silicic alteration into the regionally metamorphosed country rocks, such as at MAX, where the most intense and pervasive phyllic alteration is found peripheral to the high-grade molybdenum (Lawley and others, 2010).

Vertical Extent

The vertical extent of ore zones commonly ranges from tens to hundreds of meters (Sinclair, 1995). The Quartz Hill deposit extends from the surface to a depth of 500 m, with rare molybdenite-bearing veins extending to 1,000 m depth (Ashleman and others, 1997). The Endako deposit reaches a depth of 370 m (Selby and others, 2000). Molybdenum mineralization at MAX has a vertical extent of at least 1,000 m (Linnen and others, 1995). The mineralized zone at Red Mountain extends to a depth of more than 1,125 m (Yukon Geological Survey Yukon, minfile No. 105C 009).

Form/Shape

The ore is typically found on the top or sides of the mineralizing intrusion. Depending on the level of erosion, ore zones commonly can form as an inverted cup (for example, Compaccha: Heintze, 1985); be arcuate in plan view (for example, Gem: Young and Aird, 1969); or be present as an annular ring or cylinder with a barren core, if erosion has stripped away the upper part of mineralization (fig. 4; for example, Kitsault: Hodgson, 1995; Pine Nut: Doebrich and others, 1996). Ore zones also can form as tabular or lenticular orebodies (for example, Quartz Hill: Wolfe, 1995; Thompson Creek: Hall and others, 1984). However, the number, geometry, and timing of multiple mineralizing intrusions will affect the shape of an orebody and can create an irregular feature (for example, Endako: Selby and others, 2000), which will make it difficult to discern the shapes of the ores from individual mineralizing events. The ore is mainly present as a stockwork of veins, but breccia pipes and laminated veins of ribbon quartz with molybdenite also can be important (for example, Boss Mountain: Macdonald and others, 1995).

Host Rocks

Many deposits are hosted by the genetically related cylindrical porphyry stocks of calc-alkaline granitoids. Others are related to dike swarms, epizonal plutons, porphyritic sills, or batholiths (McMillan and others, 1996, and references within). Mineralization is dominantly hosted within these igneous intrusions and in the adjacent country rocks, generally restricted to within a few kilometers of the intrusions, which include contact-metamorphosed hornfels, other metamorphic rocks, volcanic rocks, older intrusive rocks, and sedimentary rocks. The lithochemistry of the country rocks that host the porphyritic intrusions is not an important control on mineralization.

Structural Setting(s) and Controls

Within the western cordillera of North America, the molybdenum mineralization and associated porphyry emplacement postdates accretion of island arc host terranes, but is broadly coeval with continental magmatic arc development. Addition of volatiles from the subducted slab induces partial melting of the mantle wedge and initiates magmatic processes that result in the emplacement of the mineralizing intrusions into the upper crust during formation of the continental arc. Remelting of subduction-induced metasomatized lithosphere during a subsequent tectonic event also may lead to relatively late emplacement of ore-forming intrusions following development of much of the continental arc. When available, structural weaknesses in the lower and upper crust present favorable paths for the ascent of the buoyant magma.

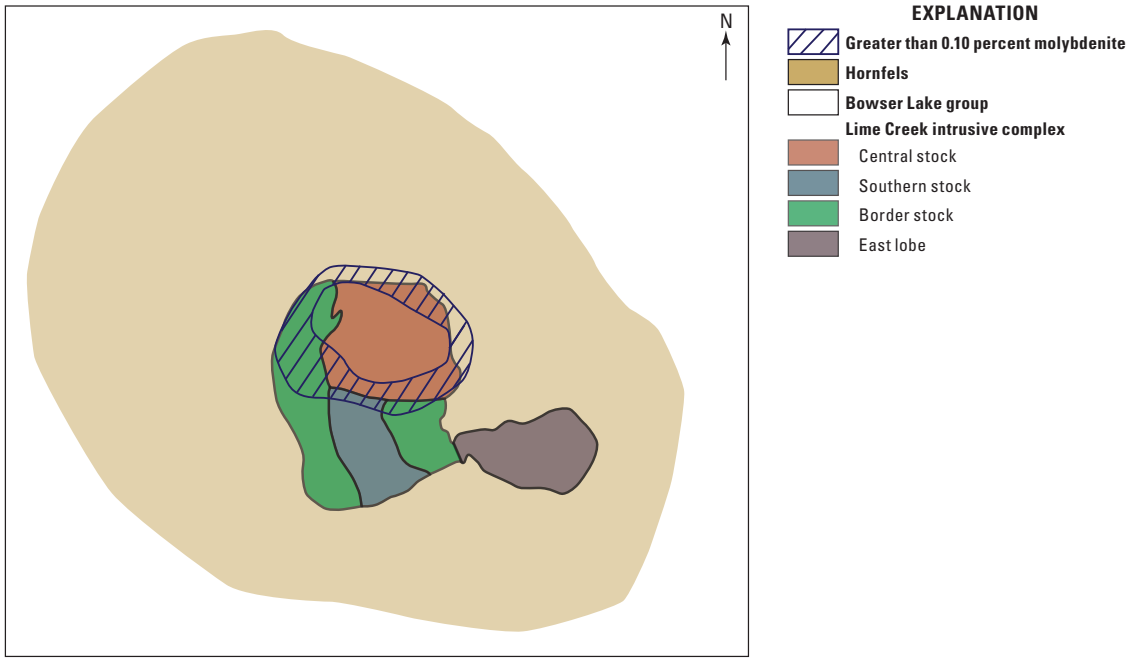

Modified from Steininger, 1985

Figure 4. Simplified geologic plan view of the Kitsault deposit displaying an annular geometry of the molybdenum ore zone and its relation to the location of the intrusive complex.

Hypogene Ore Characteristics

Mineralogy

Molybdenite is the principal economic mineral in arc-related porphyry molybdenum deposits. If tungsten is produced as a by-product in adjacent skarn, then scheelite and powellite can be of significance. Deposits are characteristically low-grade (0.03–0.22 percent Mo), but large (commonly >50 Mt), which makes them amenable to bulk-mining open-pit methods. Molybdenum mineralization is notably associated with potassic alteration and extends into the phyllic alteration zone (see the Hydrothermal Alteration section below). Molybdenite-bearing quartz veinlets in the form of a stockwork define most ores (fig. 5). Other sulfide and oxide minerals, such as galena, sphalerite, chalcopyrite, pyrrhotite, hematite, and magnetite, may be present, but are not of economic significance, except in cases when present in peripheral base metal-bearing zones (fig. 6; table 2).

Mineral Assemblages

Minerals associated with molybdenite can vary, but molybdenite-bearing veinlets typically are dominated by quartz or alkali feldspar or both. The mineral assemblage at Cannivan Gulch consists of quartz, molybdenite, and hydrothermal potassium feldspar and muscovite within the stock, whereas the same generation of veins found within the adjacent country rocks contain more pyrite, magnetite, and chlorite (Darling, 1994). Of the moderately and strongly mineralized quartz veins examined by Linnen and Williams-Jones (1990) at MAX, 72 percent also contained pyrite or pyrrhotite or both and 61 percent contained feldspar; the percentage of barren veins containing feldspar, pyrite, or pyrrhotite is much lower. Nearly 85 percent of the rocks at Quartz Hill that contain molybdenite also contain pyrite, and nearly 50 percent also contain magnetite, both as disseminations within the host rock and within the quartz veins (Ashleman and others, 1997).

Paragenesis

An initial barren or weakly mineralized stage of quartz or quartz-potassium feldspar veining typically precedes a later molybdenum mineralizing stage. Pyrite deposition typically overlaps that of the molybdenite, but also continues into later stages. A final barren stage of quartz veining is also common. Evidence for multiple episodes of molybdenite mineralization can be found at many deposits.

Four main stages of mineralization and alteration have been documented at the Malala deposit (fig. 7). Stage I consisted of barren quartz veining; stage II is characterized by potassic alteration, additional quartz veining and molybdenum and pyrite mineralization; stage III is dominated by sericite-chlorite-carbonate (phyllic) alteration and local molybdenite and pyrite; and stage IV is represented by clay and carbonate (argillic) alteration with no molybdenite or pyrite mineralization (van Leeuwen and others, 1994).

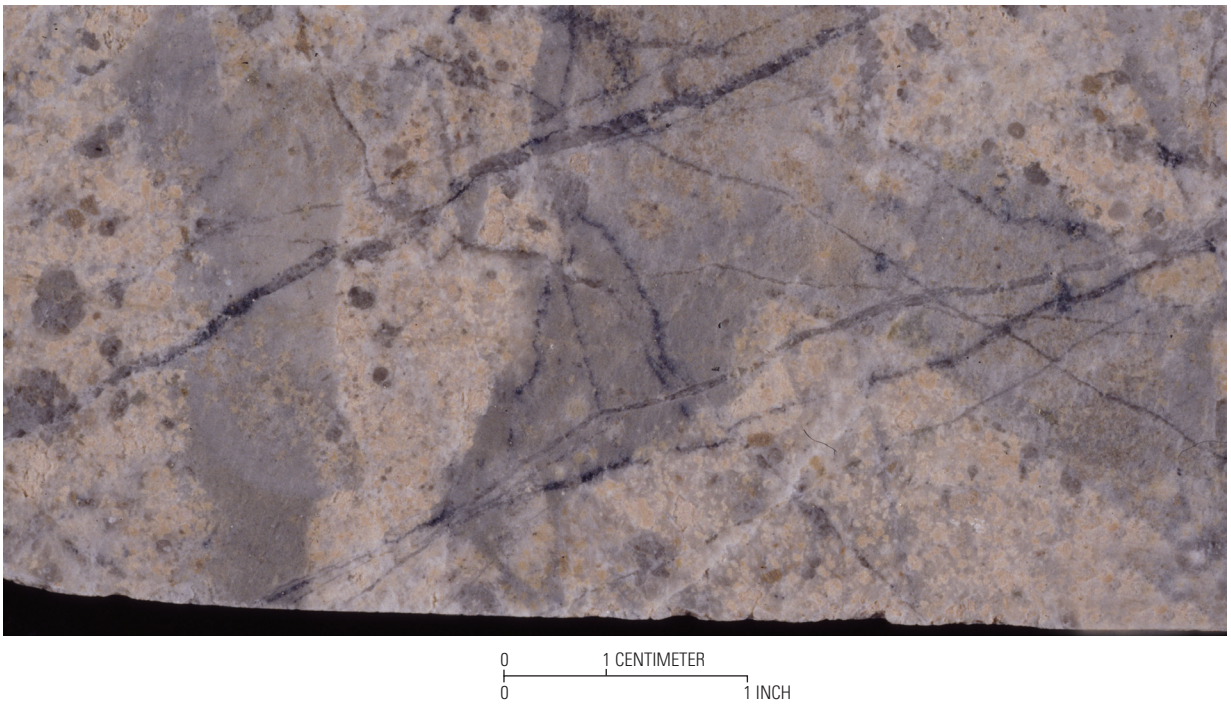

Figure 5. Example of quartz-molybdenite stockwork veining through a potassically and silicically altered sample of granodiorite, Red Mountain, Yukon. Photograph is courtesy of W.D. Sinclair.

The veinlet paragenesis at Quartz Hill also follows the barren-productive-barren mineralization style. An initial barren quartz stage was followed by a quartz–molybdenite–pyrite ± magnetite ± chlorite ± Fe oxide stage, followed by another barren quartz stage, followed by a new productive molybdenite stage, and a final zeolite ± anhydrite ± fluorite ± pyrite ± calcite stage (Ashleman and others, 1997).

At least four episodes of molybdenum mineralization occurred at Red Mountain. These occurred with or without pyrite in the early period of the quartz veining sequence (Brown and Kahlert, 1995).

Zoning Patterns

Molybdenum mineralization is associated most closely with potassic and phyllic alteration in space and time (figs. 7, 8). The highest molybdenum concentrations are located near the contact of, and within the inner potassic alteration zone and the adjacent quartz-sericite-pyrite zone (Westra and Keith, 1981). The ore zone geometry closely mirrors the zone of potassic alteration. The inner molybdenum zone may be surrounded or even cut by late silver-lead-zinc veining in some deposits. At MAX, a positive correlation exists between amount of veins that contain feldspar and molybdenum grade, but there is no correlation with molybdenum grade and iron-sulfide content (Linnen and Williams-Jones, 1990). In fact, a negative correlation exists between molybdenum grade and pyrite concentration at Red Mountain (Brown and Kahlert, 1995).

Ore Textures

Molybdenum mineralization generally is restricted to the stockwork veinlets that are of less than or equal to a few centimeters (cm) in width (figs. 5, 9). The veinlets of quartz ± molybdenite are generally a few centimeters in width, whereas veinlets of solely molybdenite may be only 1 millimeter (mm) or less. Often, the molybdenum is localized along the margins of quartz ± feldspar veins. Quartz-molybdenite veinlets at the Cannivan Gulch deposit are narrow and concentrated within the stock, and when found in the country rocks are wider, as much as 5 cm, but less abundant (Darling, 1994). At MAX, the bulk of mineralization is found within quartz veins mostly 0.5 to 5 cm in width, but the highest grade ore, locally greater than 0.6 percent Mo, is present as disseminated molybdenite within pervasively quartz-feldspar-muscovite altered intrusive rocks (Linnen and Williams-Jones, 1990). Veinlets of molybdenite at Quartz Hill are generally less than 1 mm in width (Ashleman and others, 1997). The stockwork veins at Endako are 1 to 5 cm in width, whereas the ribbon-textured quartz veins that represent most of the ore are often greater than 5 cm in width and can be as wide as 1 m (Selby and others, 2000).

Ribbon veins are commonly wider than stockwork veins and are composed of numerous laminations of fine-grained quartz, sulfide, and incorporated wall rock. Molybdenite is distributed along thin seams within the laminations parallel to the vein walls. Periodic episodes of crack-seal vein growth lead to the formation of ribbon veins. Boss Mountain, Red Mountain, Endako, and Malala are important deposits that contain ribbon-textured quartz veins.

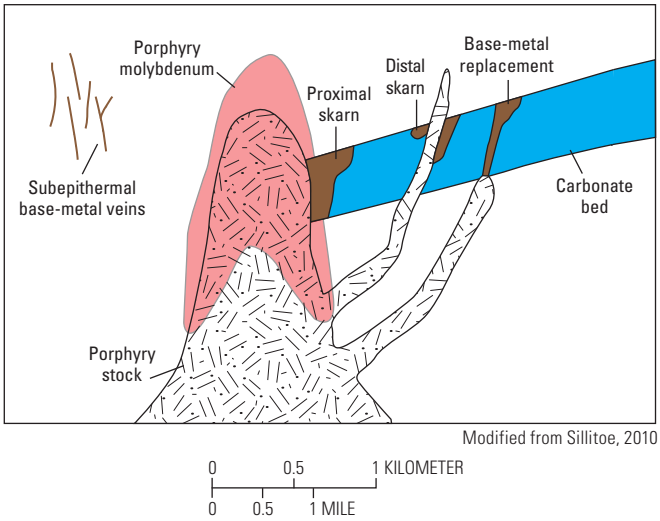

Figure 6. Schematic cross section through a porphyry deposit and the spatial relations with associated skarn and base metal occurrences. Subepithermal base metal veins occur in noncarbonate rocks, whereas base metal replacement and skarn mineralization occur within carbonate rocks. The porphyry deposit is centered on the apex of the porphyry stock.

Grain Size

Molybdenite crystals typically form with a rosette or a platy habit and are generally fine grained, less than 1 mm in diameter. The Quartz Hill deposit contains fine-grained molybdenite ranging from 0.008 to 0.09 mm in diameter within the quartz stockworks (Ashleman and others, 1997). Molybdenite crystals at Endako are less than 2 mm long (Selby and others, 2000). Davidson contains rosettes of molybdenite within pegmatite veins that are as much as 5 cm in length and that grow perpendicular to the vein walls (Atkinson, 1995). Greater than 80 percent of the total molybdenite at Kitsault is in the form of individual grains that are smaller than 0.05 mm in diameter, but crystals as large as 5 mm in diameter are present with aggregates of molybdenite as much as 2 cm wide (Steininger, 1985).

Pyrite may be the most abundant sulfide associated with arc-related porphyry molybdenum deposits and is generally fine-grained. Individual pyrite crystals at Kitsault range in size from 0.05–3 mm with aggregates of pyrite as much as 2 cm wide (Steininger, 1985).

Table 2. Mineralization related information for selected arc-related porphyry molybdenum deposits.

[Mineral abbreviations: mo, molybdenite; py, pyrite; cp, chalcopyrite; gn, galena; sp, sphalerite; sch, scheelite; ana, anatase; aik, aikinite; bth, bismuthinite; bo, bornite; spc, specularite; wul, wulfenite; wof, wolframite; po, pyrrhotite; ttr, tetrahedrite; asp, arsenopyrite; ney, neyite; en, enargite; hub, hubnerite; st, stibnite. Elemental abbreviations: Mo, molybdenum; Ag, silver; Pb, lead; W, tungsten; Zn, zinc; Bi, bismuth; Cu, copper; Sb, antimony. Mt, million tonnes]

Deposit	Location	Grade/tonnage	Major sulfides and tungstates	Minor metallic minerals	Related mineralization	References
Red Mountain	Yukon, Canada	187.24 Mt @ 0.1% Mo	mo, py	cp, gn, sp, sch	late and minor base metal veining	1
Boss Mountain	British Columbia, Canada	63 Mt @ 0.074% Mo	mo, py	cp, sp, gn, sch, ana, aik, bth	none	2
Endako	British Columbia, Canada	777.26 Mt @ 0.053% Mo	mo, py	cp, bo, bth, sch, gn, spc, wul	none	3
Quartz Hill	Alaska	1600 Mt @ 0.076% Mo	mo, py	gn, sp, cp		4, 5
Max (Trout Lake)	British Columbia, Canada	42.94 Mt @ 0.12% Mo	mo, po	py, cp, sch	Ag-Pb-W-Zn skarn and later Pb-Zn-Ag veins	6, 7
Davidson (Glacier Gulch, Hudson Bay Mountain, Yorke-Hardy)	British Columbia, Canada	75.28 Mt @ 0.177% Mo	mo, sch	wof, py, po, cp	outer base metal zone, W	8, 9
Kitsault (Lime Creek)	British Columbia, Canada	701.8 Mt @ 0.071% Mo	mo, py	sch, gn, po, sp, cp, ttr, ney	base metal sulfides, Pb-Bi sulphosalts	10, 11
Cannivan Gulch	Montana	324.3 Mt @ 0.06% Mo	mo, py	cp, sp	skarn Mo	12
Thompson Creek	Idaho	326.4 Mt @ 0.068% Mo	mo	py, gn		13
Little Boulder Creek (White Cloud)	Idaho	181 Mt @ 0.12% Mo	mo	sch, gn, sp, cp, asp, py	locally Ag is found	14, 15
Malala	Indonesia	100 Mt @ 0.084% Mo	mo, py	cp, gn, sp, po		16
Compaccha (Tamboras)	Peru	4.6 Mt @ 0.072% Mo	mo, py	en, hub, gn, sp, cp, ttr, st, wof	Cu, Pb, Zn, Sb zoning around Mo core	17
Salal Creek	British Columbia, Canada	n/a	mo, py	cp, gn, sp		18
Bell Moly	British Columbia, Canada	32.53 Mt @ 0.06% Mo	mo, py	po, gn, sp	Ag-Pb-Zn veins	11, 19

Grade and tonnage data from table A1. Other references are as follows: 1: Brown and Kahlert, 1995; 2: MacDonald and others, 1995; 3: Bysouth and Wong, 1995; 4: Wolfe, 1995; 5: Ashleman and others, 1997; 6: Linnen and others, 1995; 7: Lawley and others, 2010; 8: Bright and Jonson, 1976; 9: Atkinson, 1995; 10: Hodgson, 1995; 11: Woodcock and Carter, 1976; 12: Darling, 1994; 13: Hall and others, 1984; 14: Kirkemo and others, 1965; 15: Hall, 1995; 16: van Leeuwen and others, 1994; 17: Hollister, 1975; 18: British Columbia Geological Survey, minfile 082JW 005; 19: British Columbia Geological Survey, minfile 103P 234.

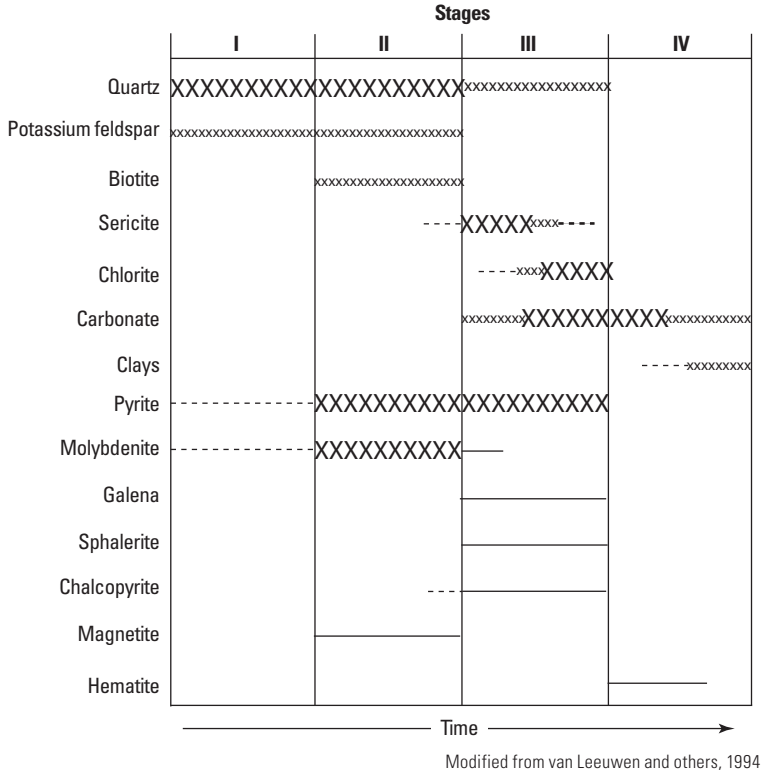

Figure 7. A generalized paragenetic sequence for Malala, Indonesia, with timing and relative abundance indicated for each mineral. The overall sequence of alteration and mineralization for Malala reflects what is typically encountered within arc-related calc-alkaline porphyry molybdenum deposits.

Hypogene Gangue Characteristics

Mineralogy

Quartz is ubiquitous and almost always the most abundant gangue mineral. It is found in most veins, stockworks, breccias, and locally replaces host rock within the silicic alteration zone. Potassium feldspar is also a common gangue mineral. Quartz and potassium feldspar may account for 90 percent of hypogene gangue (Soregaroli and Sutherland Brown, 1976). Other gangue minerals include carbonates, sericite, biotite, chlorite, gypsum, epidote, clays, anhydrite, and hornblende. Pyrite and magnetite are the most common metallic gangue minerals. Sodic alteration in the form of secondary albite is rarer.

Mineral Assemblages

Hypogene gangue minerals include hydrothermal alteration minerals, which will be discussed within the hydrothermal alteration mineral assemblages section below. Because the mineralizing intrusions are granitic in composition, quartz, potassium feldspar, plagioclase, hornblende, and biotite, and trace minerals such as apatite and zircon, commonly are found together in varying proportions in least altered parts of the intrusions. Common metallic gangue minerals such as pyrite and magnetite commonly are found along with quartz.

Paragenesis

Because molybdenite is the only ore mineral associated with arc-related porphyry molybdenum deposits, gangue paragenesis is included with discussions of molybdenite and is summarized in the above Hypogene Ore Paragenesis section.

Zoning Patterns

When iron-rich country rocks surround the arc-related porphyry molybdenum deposit, a pyritic or pyrrhotitic halo may form. At Red Mountain, this occurred when sulfur-bearing hydrothermal fluids interacted with the iron in the country rocks to produce pyrite. This does not always occur, as at Malala, which is an example of a deposit that does not have a well-developed pyrite halo but still contains disseminated pyrite associated with molybdenite mineralization. Other hypogene zoning will be discussed in the Alteration section.

Textures, Structures, and Grain Size

Textures of the host granitoids generally are inherited from the original intrusion that is later modified by the mineralizing event(s). Feldspar crystals and mafic minerals that are altered by the hydrothermal event may retain the complete

original relict shape of the primary crystal. However, the alteration minerals themselves may be an agglomeration of smaller minerals that replace a larger mineral. An example of this would be when sericite replaces a large phenocryst of feldspar during phyllic alteration. When altered rocks are weathered at the surface, the soft replacement minerals, such as clays from argillic alteration, may preferentially weather out and leave the relict shape of the original mineral as an open space on the weathered face of the rock.

Unidirectional solidification texture (UST) is a common texture created by quartz or feldspar growth within the intrusion. Euhedral crystals grow in one direction from a solid substrate inward, commonly emanating from the top or sides of a porphyry stock and indicate the direction of crystal growth into the younger rock. When multiple intrusive rocks are in contact with each other, the observation of UST's can geologically confirm the relative ages between the igneous rocks. This texture is not universal, but is present in some arc-related porphyry molybdenum deposits such as MAX (Lawley, 2009).

Vein selvages of varying nature occur in association with quartz veins. In the potassic alteration zone, selvages of biotite and potassium feldspar are present. Selvages of muscovite can be observed in the phyllic alteration zone.

Hydrothermal Alteration

Relations Between Alteration, Gangue, and Ore

Molybdenite ore deposition, quartz veinlet formation, and hydrothermal rock alteration are all products of a hydrothermal system with components of meteoric and magmatic fluids in varying proportions. As the magmatic volatiles move upward in the cupola of the host intrusive rock, changes in pressure, temperature, and the chemistry of the host rocks and hydrothermal solution will cause ore and gangue minerals to precipitate within fractures that are filled to create the stockwork and ribbon veining. Ionic substitutions within the minerals of the host rock during the flow of hydrothermal fluids through these rocks are the cause of the various alteration zones. Pervasive rock matrix alteration and vein selvage alteration can be prevalent in arc-related porphyry molybdenum deposits. Endako is an example of a deposit with vein selvage alteration, but without pervasive rock matrix alteration (Selby and others, 2000).

Mineralogy

The primary mineral sites within the host igneous intrusion that are most susceptible to hydrothermal alteration include the feldspars and mafic minerals, such as hornblende, biotite, and pyroxene. These primary minerals may be altered by ionic substitution and hydrolytic alteration to produce secondary potassium feldspar, biotite, chlorite, epidote, clay, sericite, and apatite.

The most abundant sulfide minerals are molybdenite and pyrite. Minor to rare crystals of chalcopyrite, galena, sphalerite, and tungstate minerals also can be observed. Other metallic minerals include magnetite and hematite. Pyrrhotite may be found in some deposits, mostly associated with hornfels country rocks. Quartz, carbonate, anhydrite, and gypsum are locally present within veins or vein selvages.

Mineral Assemblages

Different mineral assemblages relate to different alteration types and the evolution of hydrothermal fluids through space and time, with alteration assemblages of arc-related porphyry molybdenum deposits being similar to those of porphyry copper deposits. Alteration of surrounding rocks commonly begins with contact metamorphism associated with initial magma intrusion. Hydrothermal alteration of potassic and silicic nature follow. Phyllic alteration follows, with propylitic, and argillic alteration as the final stages of hydrothermal alteration.

Potassic alteration zones are dominated by variable amounts of potassium feldspar, biotite, quartz, and possibly anhydrite. Phyllic alteration is also common, and usually contains quartz, sericite or muscovite, pyrite, and also may have carbonate, magnetite, and chlorite. Propylitic alteration zones can contain chlorite, epidote, carbonates, and quartz. Argillic alteration consists of clay minerals such as kaolinite and illite. Sodic metasomatism is rare, but can be found at some deposits such as Davidson (Atkinson, 1995). See Seedorff and others (2005) for a comprehensive listing of hydrothermal alteration assemblages of porphyry ore deposits.

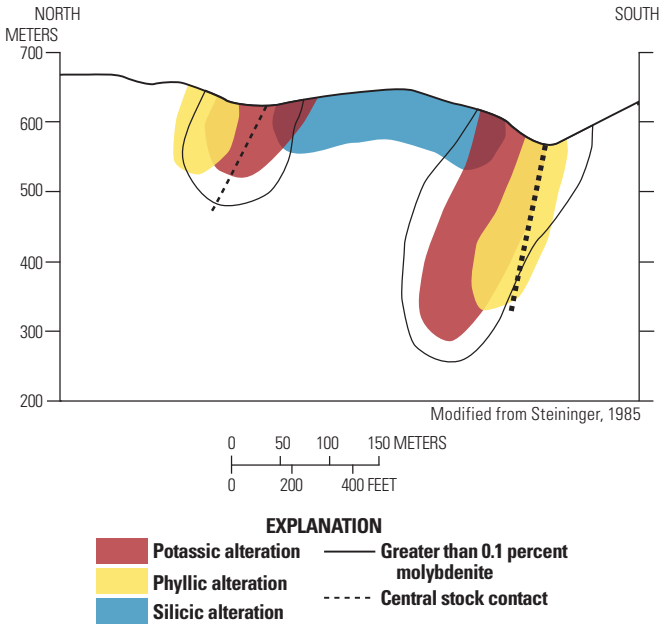

Figure 8. Generalized cross section of hydrothermal alteration distribution through the Kitsault deposit. Note the correlation between potassic alteration and concentration of molybdenum mineralization, which forms an annular ring in plan view. The central stock is in contact with peripheral hornfels country rocks.

Silicic and potassic alteration form the core of the hydrothermal alteration. Laterally adjacent is the zone of phyllic alteration. Propylitic alteration forms in the periphery of the system and argillic alteration may overprint earlier phases of alteration (fig. 10). The geometry of the alteration zoning is highly variable because of differences in emplacement depth, zones created by structures.

Lateral and Vertical Dimensions

Hydrothermal alteration extends well beyond the molybdenum orebodies but its extent will be highly variable in size for different deposits. Zones of silicic, potassic, and phyllic alteration are each commonly on the order of a couple hundred meters or less in width. Propylitic alteration is the most extensive, and when present can extend for kilometers beyond the regions of silicic, potassic, and phyllic alteration. Argillic alteration typically overprints earlier alteration zones.

The potassic biotite alteration at Boss Mountain extends for 1,500 m to the west beyond the Main Breccia Zone of molybdenum mineralization (Soregaroli and Nelson, 1976). An extensive area of alteration and mineralization at Malala covers an area of 4 square kilometers (km^2) (van Leeuwen and others, 1994). During discovery of Quartz Hill, assay results indicated anomalous molybdenum values as high as 168 ppm over a 35 km^2 area through stream-sediment analysis and later work showed quartz-molybdenite stockworks outcropping over a much more limited 2 km^2 area (Ashleman and others, 1997). Surface mineralization and related hydrothermal alteration at Thompson Creek covers an area of 760 × 2,400 m (Schmidt and others, 1983).

Selvages

When closely spaced veinlets produce stockworks, vein selvage alteration can overlap to form contiguous areas of pervasive alteration. These selvages appear to envelope barren and productive veins (for example, Endako: Bysouth and Wong, 1995). Potassic alteration generally occurs as vein selvages, but can appear pervasive because of closely spaced veining. Phyllic alteration is generally also fracture and vein controlled, but is more likely to appear pervasive because of wider alteration envelopes.

The most prominent alteration at Endako formed as vein selvages. Potassium feldspar vein selvages of greater than 95 percent modal abundance range from 3 mm to 5 cm surrounding quartz veins at Endako. Other potassic alteration selvages contain less potassium feldspar, although greater than 60 percent, and variable amounts of biotite and quartz and are generally 5 to 60 cm in width, but can form vein haloes as great as 5 m (Kimura and others, 1976). Phyllic alteration selvages at Endako consist of quartz (50–60 percent), sericite (30–50 percent), pyrite (1–5 percent), and occasional magnetite or chalcopyrite. They form selvages 3-mm- to 5-cm-wide (Kimura and others, 1976). Kaolinite selvages also occur and can be as wide as 2 m, with the alteration intensity proportional to the amount of brecciation associated with the encompassed vein (Selby and others, 2000).

The vein selvage alteration at Davidson is usually less than 1 m in width (Atkinson, 1995). Where this veining is more concentrated, overlapping alteration forms zones of pervasive alteration. The same appearance is found at Boss Mountain where quartz-sericite-pyrite vein selvages can reach as much as 1.5 m and may overlap to form pervasively altered zones.

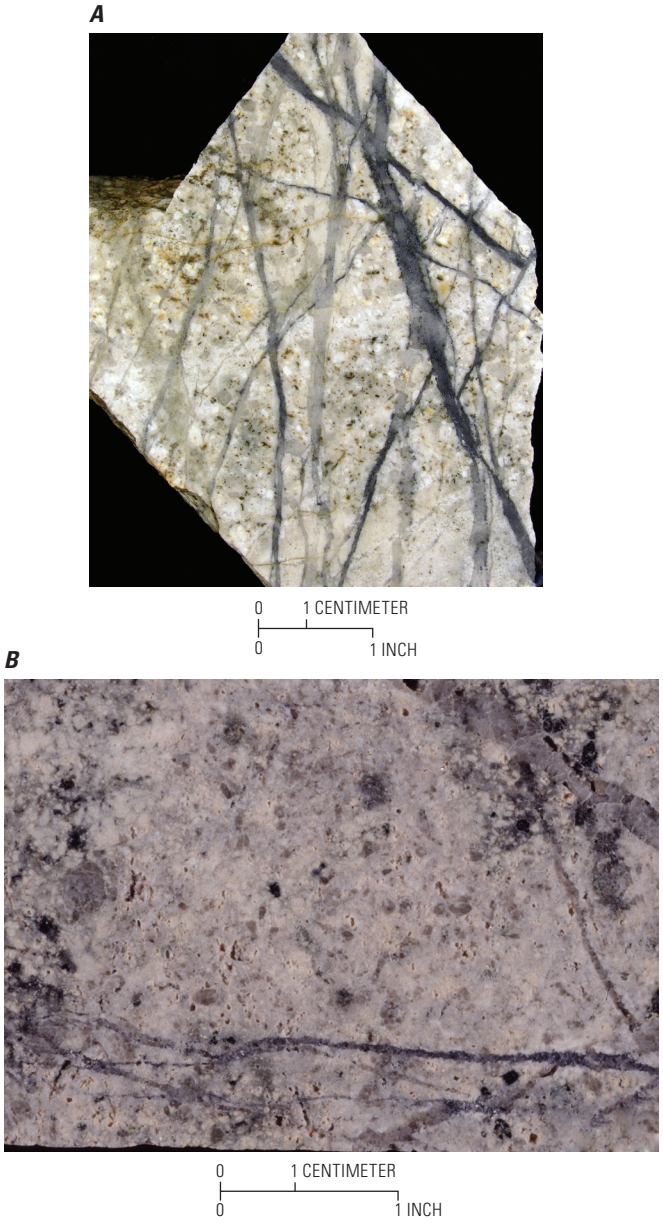

Figure 9. Examples of different types of alteration associated with arc-related porphyry molybdenum deposits. In both photographs, notice the offset and crosscutting veins that indicate development through multiple events. (*A*) Sericitized granodiorite with quartz-molybdenite veins, Roundy Creek, British Columbia. (*B*) Potassically altered granodiorite with pervasive pink potassium feldspar and isolated fine-grained hydrothermal black biotite, Red Mountain, Yukon. Both photographs are courtesy of W.D. Sinclair.

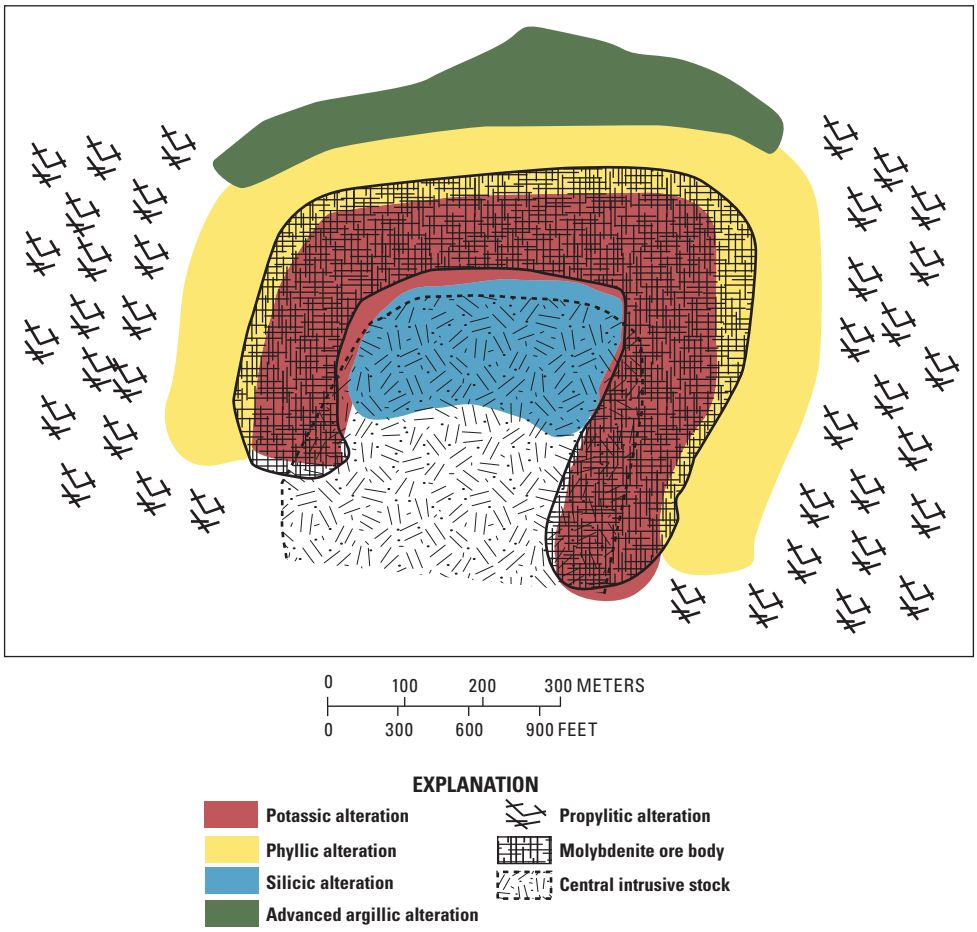

Figure 10. A conceptual diagram illustrating the spatial relations between plutonism, hydrothermal alteration, and molybdenum mineralization. Individual deposits will vary in shape and size, but the overall spatial pattern of alteration will be similar. The advanced argillic alteration may overprint other alteration packages besides propylitic and phyllic. The central silicic zone is not always present. Propylitic alteration can extend for kilometers. Dimensions of each alteration zone are approximate.

Rock Matrix Alteration

Although vein selvage alteration is more common, pervasive rock matrix alteration also is frequently noted. Argillic, phyllic, and propylitic alteration assemblages are more likely to be pervasive than potassic assemblages; however, examples of pervasive potassic alteration are noted in some deposits (figs. 5, 9).

Pervasive argillic alteration at the Endako deposit in the form of kaolinization can be weak, moderate, or intense. It is characterized by clays replacing feldspar (Kimura and others, 1976).

Intense and pervasive silicic and potassic alteration is recognized at Quartz Hill (Wolfe, 1995). Locally, hydrothermal potassium feldspar replaced the aphanitic rock matrix near microfractures and along the boundaries of magmatic potassium feldspar phenocrysts, and replaces plagioclase phenocrysts (Ashleman and others, 1997).

Most of the alteration at Malala is pervasive, with lesser amounts of fracture controlled vein selvage alteration (van Leeuwen and others, 1994). In the potassic alteration zone, hydrothermal biotite is dominant as it replaces primary biotite and primary feldspar. Carbonate is the most widespread alteration product and replaces all primary silicates except quartz. Red Mountain notably contains pervasive potassic, phyllic, and propylitic alteration (Brown and Kahlert, 1995).

Textures

Hydrothermal fluids form high densities of quartz veins and veinlets resulting in stockwork and less common ribbon-textured orebodies. The ribbon-textured quartz veins are laminated by numerous layers of molybdenite. At Endako, the ribbon-textured quartz-molybdenite ore veins commonly

contain five to ten laminations of molybdenite (Selby and others, 2000). Stockwork veining can be extensive; at MAX, greater than 60 percent of the rock volume within the stockwork mineralized zone consists of planar hydrothermal veining (Linnen and Williams-Jones, 1990). In contrast, only 20 percent of the rock volume within the mineralized zone at the Mac deposit consists of stockwork veining (Cope and Spence, 1995).

Hydrothermal "shreddy" biotite texture helps differentiate between hydrothermal and primary biotite. During hydrothermal growth of biotite, the biotite crystals tend to be abundant, small, and grow in random orientations. This is in contrast to primary igneous biotite that is likely to form euhedral six-sided books.

Potassic alteration also forms potassium feldspar that may need to be differentiated from primary potassium feldspar. Field evidence for replacement of plagioclase crystals to secondary potassium feldspar relies on interpretation of crystal shape. Plagioclase commonly is more elongate than potassium feldspar. So if abundant potassium feldspar is found that resembles the elongate crystal form of plagioclase, this may indicate hydrothermal replacement.

Zoning Patterns

Zoning patterns of hydrothermal alteration largely reflect changing temperature, pressure, fluid/rock interaction, and potassium ion/hydrogen ion (K^+/H^+) ratios within the cooling ore-forming fluid (fig. 11; Hemley and Jones, 1964). A typical alteration pattern consists of a core of potassic alteration with or without pervasive silicic alteration, surrounded by a phyllic alteration zone, an outer propylitic halo, and an irregular argillic alteration zone that overprints earlier alteration packages.

Temporally, the alteration follows a similar pattern with early interior alteration and later exterior alteration. An example is Quartz Hill, with early silicic and potassic alteration followed by a phyllic quartz-sericite-pyrite assemblage, and late propylitic and argillic alteration (Ashleman and others, 1997).

Some deposits do not display a prominent zonation pattern. Hydrothermal alteration is fracture controlled at Davidson and deposit scale zonation has not been established (Atkinson, 1995).

Supergene Ore Characteristics

Molybdenum ore is not substantially concentrated by supergene processes. Thus, a major difference between arc-related porphyry molybdenum deposits and porphyry copper deposits is the lack of supergene enrichment in the former. Molybdenite does oxidize to molybdite (MoO_3), ilsemannite [$Mo_3O_8 \bullet n(H_2O)$], and ferrimolybdite [$Fe_2(MoO_4)_3 \bullet 8H_2O$], which can all be mechanically dispersed through erosion. A shallow zone of ferrimolybdite is locally present at Quartz Hill at depths of 1–2 m (Ashleman and others, 1997). An oxidized surficial zone at Red Mountain contains ferrimolybdite as fracture coatings that are generally within 30 m of the surface (Brown and Kahlert, 1995). Surface leaching of molybdenite at the Mac property can reach a depth of 50 cm (Cope and Spence, 1995). The soft nature of molybdenite causes preferential weathering and wide dispersion of molybdenum that may cause anomalies in stream sediments far from orebodies, such as at Quartz Hill (Ashelman and others, 1997).

Supergene Gangue Characteristics

Common supergene minerals are hematite, limonite, and ferrimolybdite. Other phases, such as powellite, pyrolusite, wulfenite, and copper-bearing minerals are noted at Endako (Selby and others, 2000). Copper is not economically important in arc-related porphyry molybdenum deposits and trace amounts of copper-bearing oxide minerals, such as malachite, which are important in porphyry copper deposits, are not recovered and are considered gangue minerals in the present deposit type.

Pyrite is one of the most abundant hypogene sulfides and oxidizes to produce limonite, one of the more common supergene gangue minerals. The formation of a broad limonitic gossan may be weak or nonexistent if the pyrite content of the deposit is low, or may be strongly limonitic or even jarositic if the pyrite content is high. At Boss Mountain, limonite is found as a staining in fractures to an average depth of 12 m, but can be found as deep as 150 m in some postmineralization faults (Soregaroli and Nelson, 1976).

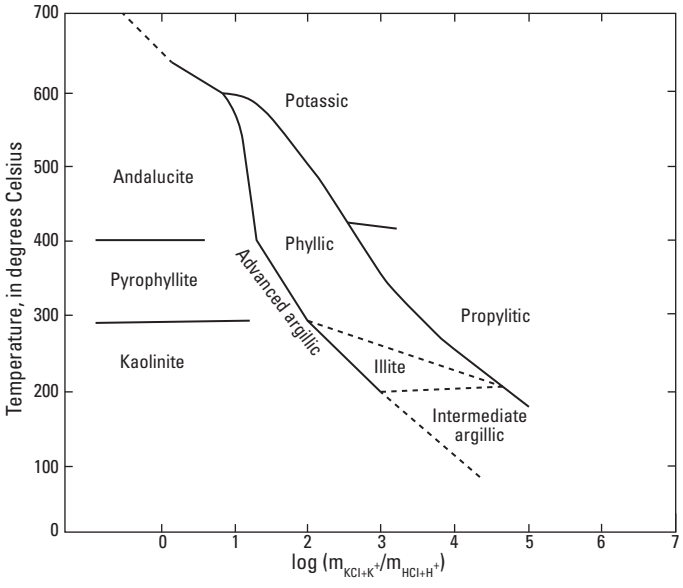

Modified from Seedorff and others, 2005

Figure 11. Alteration mineral phase diagram for the system K2O-Al2O3-SiO2-H2O-KCl-HCl at P(H2O)=1 kilobar. The phase boundaries correspond to limits of the alteration types.

Weathering/Supergene Processes

Weathering and supergene enrichment are economically unimportant in arc-related porphyry molybdenum deposits. The oxidation of molybdenite to yellow ferrimolybdite does not create enriched ore, unlike supergene processes that concentrate copper in porphyry copper deposits and create a chalcocite blanket.

Modern weathering processes associated with arc-related porphyry molybdenum deposits and their mine wastes are dominated by the balance between the acid-generating potential associated with minor amounts of pyrite and the acid-neutralizing potential offered by minor amounts of carbonate and silicate minerals. Ludington and others (1995) have reviewed the geoenvironmental characteristics of alkali-feldspar rhyolite-granite porphyry molybdenum (Climax-type or high-fluorine) porphyry molybdenum deposits, which share some geologic and mineralogical features with arc-related porphyry molybdenum deposits. The oxidation of pyrite and other sulfide minerals proceeds with either dissolved oxygen (O_2) or dissolved ferric iron (Fe^{3+}) as the oxidizing agent. Dissolved oxygen is the most important oxidant at pH values more than four, whereas ferric iron dominates at less than four (Williamson and others, 2006). The aqueous oxidation of pyrite by dissolved oxygen is described by reaction 1:

$$FeS_2 + 7/2\ O_2 + H_2O \rightarrow Fe^{2+} + 2\ SO_4^{2-} + 2\ H^+. \quad (1)$$

Reaction 1 actually represents the overall action of numerous intermediate reactions. The aqueous oxidation of pyrite by ferric iron is described by reaction 2:

$$FeS_2 + 14\ Fe^{3+} + 8\ H_2O \rightarrow 15\ Fe^{2+} + 2\ SO_4^{2-} + 16\ H^+. \quad (2)$$

For reaction 2, where ferric iron is the oxidant, ferrous iron must be oxidized to ferric iron to perpetuate the reaction:

$$Fe^{2+} + ¼\ O_2 + H^+ \rightarrow Fe^{3+} + ½\ H_2O. \quad (3)$$

The rate of the oxidation of ferrous iron to ferric iron is greatly enhanced by the iron oxidizing bacterium *Acidithiobacillus ferrooxidans*. Singer and Stumm (1970) observed that *A. ferrooxidans* increased the rate of oxidation of ferrous iron to ferric iron by a factor of 100,000 relative to the abiotic rate. In the case of both sets of reactions for pyrite, additional acid is generated by the oxidation and hydrolysis of the aqueous ferrous iron as described by the reaction:

$$Fe^{2+} + ¼\ O_2 + 5/2\ H_2O \rightarrow Fe(OH)_3 + 2\ H^+, \quad (4)$$

which also produces the orange and brown precipitates that typify acid-mine drainage.

Molybdenite, the primary molybdenum ore mineral in all porphyry molybdenum deposits, is generally considered to be fairly unreactive in the weathering environment (Plumlee, 1999). Nevertheless, its dissolution can be described by the reaction:

$$MoS_2 + 3\ H_2O + 9/2\ O_2 \rightarrow MoO_4^{2-} + 2\ SO_4^{2-} + 6\ H^+. \quad (5)$$

Gangue minerals in the host rocks generally react to consume the acid generated by the oxidation of sulfides. Carbonate minerals, such as calcite, consume acid as described by reaction:

$$CaCO_3 + H^+ \rightarrow Ca^{2+} + HCO_3^-. \quad (6)$$

Aluminosilicate minerals, such as plagioclase, can consume acid, although they are not as reactive as carbonate minerals (Plumlee, 1999; Jambor and others, 2002). Reactions involving these minerals typically add major element dissolved constituents, such as aluminum, to the water and produces secondary phases, such as clays.

The geochemical mobility of molybdate anions increases with alkalinity in contrast to the geochemical mobility of metallic cations, such as copper. At low pH conditions where metallic cations are mobile, the molybdate ion is stable because it sorbs or co-precipitates with iron oxyhydroxides at low pH (Ludington and others, 1995). Under acidic or weakly acidic to alkaline weathering conditions, molybdenite oxidizes to form Mo-bearing iron hydroxides or the mineral ferrimolybdite. Oxidation of pyrite in unmined deposits, or in tailings and waste rock during their weathering, can lead to acid-rock drainage and development of limonite-rich gossans.

Geophysical Characteristics

Literature on geophysical characteristics of arc-related porphyry molybdenum deposits is minimal. In some locations where geophysical methods have been applied, such as at the Endako and MAX deposits, difficulty was encountered in delineating the deposit relative to unmineralized intrusions and the surrounding country rocks. Hypothetically, certain aspects of a deposit can be identified because of the associated physical and chemical characteristics, if these characteristics differ substantially from those of the adjacent barren rock. Such properties include magnetic susceptibility, electrical resistivity, and density. Common hydrothermal minerals found in arc-related porphyry molybdenum deposits that are relevant to geophysical detection include magnetite, pyrite, biotite, potassium feldspar, clays, and sericite. Overall low total sulfide content (generally <5 volume percent) in arc-related porphyry molybdenum deposits reduces the usefulness of many geophysical methods and, in many aspects, signatures of barren intrusions resemble those of productive intrusions.

Magnetic, Gravity, and Electrical Signatures

The magnetite- and ilmenite-series intrusions are associated with arc-related porphyry molybdenum deposits and the difference between the two series will greatly affect the magnetic susceptibility of the rock. However, a ring or arc of high magnetic anomalies surrounding the deposit may be produced if the periphery of the deposit has pyrrhotite- or magnetite-bearing skarn or hornfels. Scattered anomalies caused by the pyrrhotite-bearing skarns adjacent to the MAX deposit were successfully defined by magnetometer surveys (fig. 12; Linnen and others, 1995).

Molybdenite is relatively dense, with a specific gravity of 4.62–4.73. This value is substantially higher than most igneous, sedimentary, and metamorphic rocks, and the quartz (specific gravity of 2.65) gangue that typically hosts the molybdenite. However, the overall low molybdenite volume found in ore-related intrusions, coupled with the low density of the hosting quartz veins, precludes detection of a substantial gravity anomaly associated with zones of ore. Gravity surveys can detect intrusions, but simply being able to detect an intrusion does not reflect whether it is mineralized or not.

Induced polarization (I.P.) is an electrical method that measures how well materials in the earth retain an electrical charge, with disseminated metallic minerals and clay minerals producing the best responses. Disseminated sulfide mineralization and secondary clays produced from hydrothermal fluids are common in arc-related porphyry molybdenum deposits. Thus an I.P. anomaly may not necessarily reflect mineralization, but instead could be a sulfide barren zone with an abundance of hydrothermal clays such as found in an advanced argillic zone of alteration that could aid in vectoring into a deposit location during exploration. An I.P. survey over the molybdenite ore zone at the Endako deposit found only normal background values, although with a weak anomaly occurring over the pyritic zone (Bysouth and Wong, 1995).

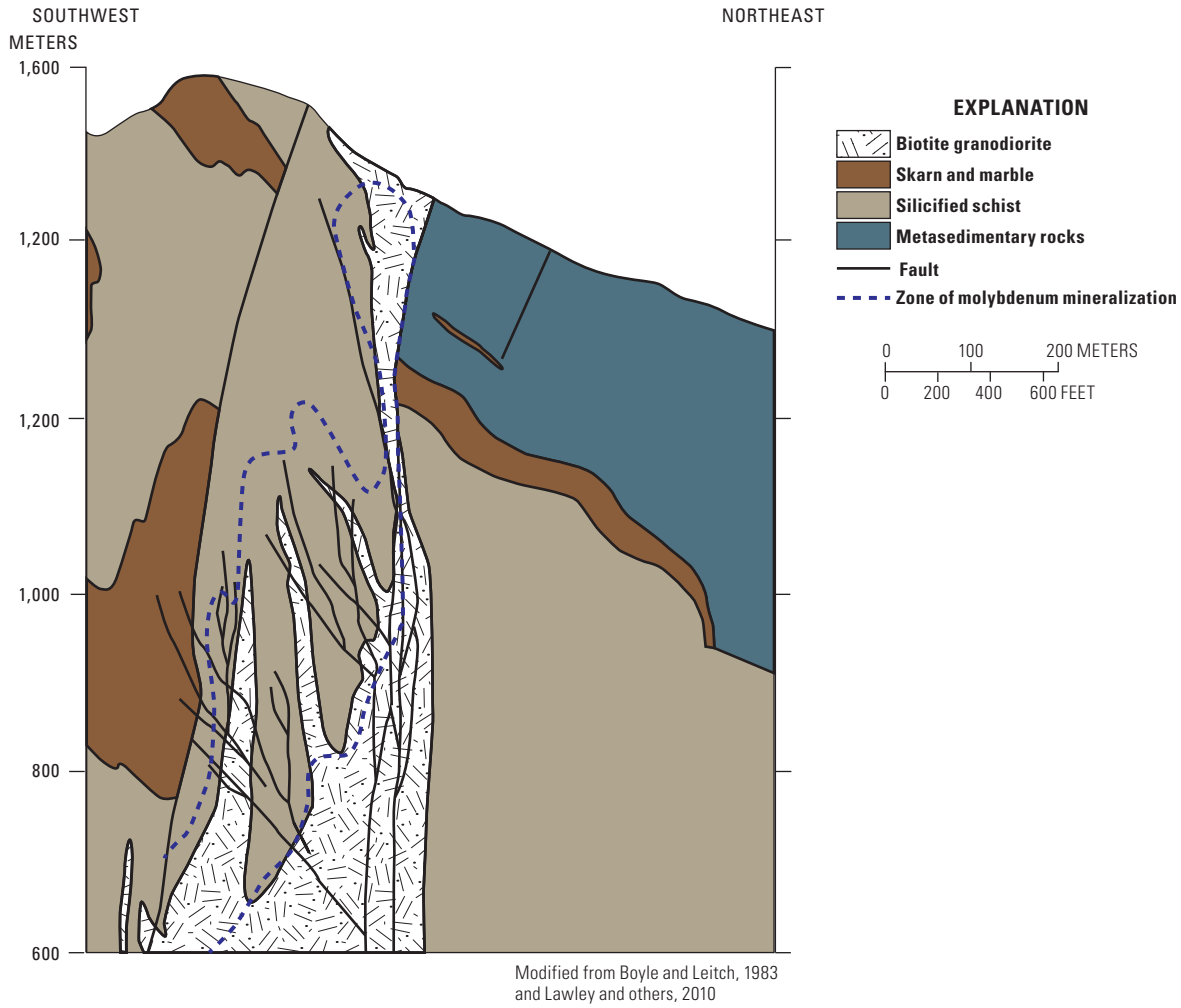

Figure 12. The spatial relation between pyrrhotite-bearing skarn, molybdenum mineralization, and the Trout Lake biotite granodiorite. Scattered anomalies were defined by magnetometer surveys around the MAX deposit that were caused by the pyrrhotite-bearing skarn.

Radiometric Signature

Abundant and naturally occurring radioactive elements include potassium (K), thorium (Th), and uranium (U). Potassium is a major component of hydrothermal potassium feldspar and biotite. Gamma ray spectrometry surveys could be used to outline the zone of potassic alteration temporally and spatially associated with molybdenum mineralization, which has been accomplished for porphyry copper deposits in Canada (Ford and others, 2007). These airborne surveys measure the concentrations of radioactive elements contained within the upper few centimeters of the Earth's surface, meaning that these data should be interpreted in terms of surface geochemistry. This method is incapable of discovering concealed deposits.

This technique may prove troublesome in some regions. By using airborne surveys, it may be difficult to distinguish anomalies associated with potassic alteration from that associated with normal rocks with high potassium contents. Using element ratios may be helpful in this differentiation. For example, low Th/K ratios are suggestive of potassium enrichment associated with biotite and potassium feldspar alteration and can be used to distinguish alteration from any primary high potassium concentrations in the area (Ford and others, 2007). Clearly, careful geological consideration and mapping must be considered before jumping to conclusions based on a radiometric signature.

Geochemical Characteristics

Trace Elements and Element Associations

Molybdenum has an estimated abundance in continental crustal rocks of 1.5 ppm (Taylor and McClennan, 1985), an estimated abundance of 0.059 ppm in the mantle (Newsom and Palme, 1984), and has a high affinity for sulfur such that it is a chalcophile element (Soregaroli and Sutherland Brown, 1976). Within arc-related porphyry molybdenum deposits, the molybdenum is concentrated in quantities that are economically viable for past, present, or future mining because molybdenum and tungsten strongly partition into an aqueous phase from an evolving and crystallizing magma chamber and reach their maximum ore-fluid concentrations in the late stages of vapor evolution (Candela, 1989). Arc-related porphyry molybdenum deposits may locally contain anomalous fluorite, but fluorine enrichments are low within the overall system (generally less than 0.1 percent F) and comparable to levels associated with porphyry copper deposits (Westra and Keith, 1981).

Substantial concentrations of rhenium have been reported in only one major sulfide mineral, molybdenite, although a number of rare rhenium sulfide minerals are known that include rheniite (ReS_2), dzhezkazganite ($ReMoCu_2PbS_4$), and tarkianite ($(Cu,Fe)(Re,Mo)_4S_8$). Substantial levels of rhenium also may be concentrated in minerals such as uraninite and gadolinite. Within porphyry deposits, molybdenite from gold-rich porphyry copper deposits have the highest levels of rhenium, whereas molybdenum-rich porphyry copper deposits have lower values, and porphyry molybdenum and porphyry tungsten-molybdenum deposits have the lowest levels (for example, see Sinclair and others, 2009). Rhenium enrichment in molybdenite is useful in geochronological studies of ore deposits and has been utilized to date the Endako deposit (Villeneuve and others, 2001) and the MAX deposit (Lawley and others, 2010).

Zoning Patterns

In plan view, molybdenum mineralization is found at the core of arc-related porphyry molybdenum deposits, dominantly hosted within intrusive rocks but also within surrounding country rocks. When present, tungsten or lead-zinc-silver mineralization is found on the periphery and occasionally cross cutting the molybdenum mineralization. Outlying lead-zinc-silver prospects are found mainly in a belt lying 5–10 km away from the MAX deposit (Boyle and Leitch, 1983), whereas the MAX deposit itself contains adjacent tungsten-bearing skarns that are cut by additional lead-zinc-silver veins found within the contact metamorphic aureole of the Trout Lake stock (Boyle and Leitch, 1983; Lawley and others, 2010). These lead-zinc-silver veins are interpreted to be late stages of the magmatic-hydrothermal system (Lawley and others, 2010). Anomalous arsenic concentrations as high as 500 ppm within the rock are found outward from the tungsten skarns at MAX (Boyle and Leitch, 1983). Peripheral tungsten-bearing skarns also are noted at Cannivan Gulch and Thompson Creek. In the metamorphic country rocks marginal to the molybdenum zone at Red Mountain is an area of anomalous tungsten (greater than or equal to 50 ppm), lead (as high as 1,500 ppm), and copper (as high as 1,500 ppm), with a distal zinc anomaly (150–1,500 ppm) (Brown and Kahlert, 1995). Fluorine is coincident with tungsten at Red Mountain. Metal zoning in quartz veins at Compaccha goes from central molybdenum to copper (enargite-bearing) to lead-zinc-silver (sphalerite- and galena-bearing) to most distal anomalous antimony (stibnite-bearing) (fig. 13). Base metal zoning, however, can be absent in deposits, as is noted at Quartz Hill (Ashleman and others, 1997).

Fluid-Inclusion Microthermometry and Geochemistry

A fundamental difference exists between fluid inclusions of the arc-related porphyry molybdenum deposits and the alkali-feldspar rhyolite-granite porphyry molybdenum deposits. As shown in table 3, molybdenum mineralization in arc-related porphyry molybdenum deposits are typically associated with low to moderate salinity [less than 16 weight (wt) percent NaCl equivalent (equiv.)], moderate temperature

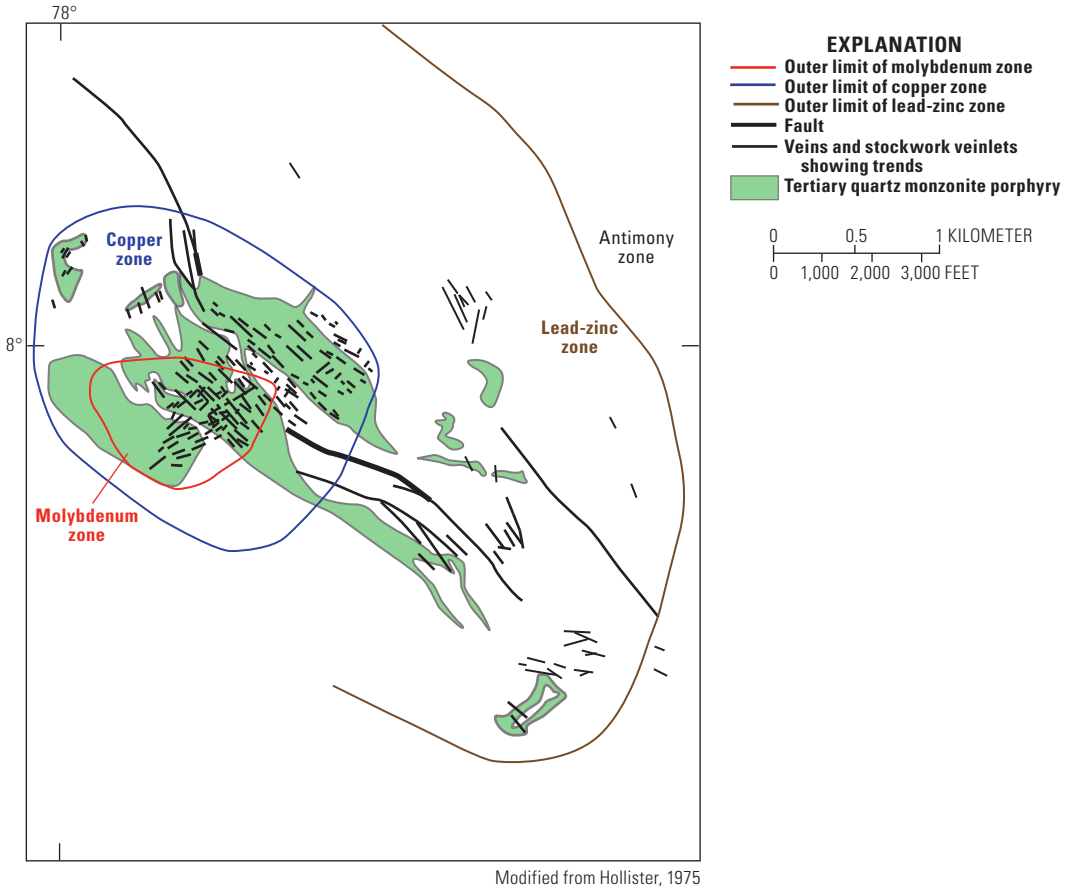

Figure 13. District map of Compaccha, Peru showing sulfide metal zonation of molybdenum (Mo), copper (Cu), lead-zinc (Pb-Zn), and antimony (Sb). Most stockwork veinlets are concentrated within the Mo zone.

(commonly 250–400°C) fluids, and CO_2-bearing inclusions (Theodore and Menzie, 1984; Linnen and others, 1995). In contrast, alkali-feldspar rhyolite-granite porphyry molybdenum deposits usually contain molybdenite-associated primary fluid inclusions with hypersaline fluids and homogenization temperatures from 400 to greater than 600°C (Ludington and Plumlee, 2009). However, both of these differing types of fluid inclusions may occur in either deposit type. Compositions of fluid inclusions from porphyry copper deposits are highly variable and dependent on variables such as pressure and temperature during entrapment, with hypogene ore deposition occurring at high and low temperatures within different deposits (Seedorff and others, 2005).

Many different types of fluid inclusions exist within all deposits associated with magmatic activity, but the numerous primary inclusions are the ones that are most important to the genetic study of arc-related porphyry molybdenum deposits. These primary fluid inclusions may contain components of magmatic and meteoric fluids. Primary fluid inclusions can be hosted in many different minerals, such as quartz, carbonate, fluorite, feldspar, epidote, apatite, and sulfides. The primary fluid inclusions most commonly studied are hosted within quartz, as these are widespread, paragenetically associated with molybdenite, and abundant. Fluid inclusions can be liquid-rich, vapor-rich, or multi-phase, and may or may not contain daughter crystals that include halite, sylvite, hematite, apatite, anhydrite, or sulfides.

Magmatic fluids will at one time be in equilibrium with minerals and melt at magmatic pressures and temperatures, but not necessarily at those pressures or temperatures at the time the fluid inclusions were trapped. Many fluid inclusions with a major magmatic fluid component have a high homogenization temperature (>500°C) and high salinity (Bodnar, 1995). However, fluid inclusions that record lower homogenization temperatures and salinities may still be magmatic in origin, dependent on the conditions when the fluid was trapped. These characteristics also may indicate a component of meteoric water in addition to magmatic fluid.

Variability in the characteristics of magmatic fluid inclusions can be a function of depth of emplacement and the stage of crystallization of the magma (Bodnar, 1995). Macdonald (1983) and Macdonald and others (1995) note a fundamental change in the characteristics of fluid inclusions occurs at the 1,353 m mine level within the Boss Mountain deposit. Fluid inclusions in samples from above this level have highly variable fluid/vapor ratios and homogenize to liquid-H_2O and

Table 3. Examples of characteristics of primary quartz-hosted fluid inclusions related to molybdenite mineralization within arc-related porphyry molybdenum deposits.

[°C, degrees Celsius; wt% NaCl, weight percent sodium chloride; X_{CO2}, molar proportion of carbon dioxide]

Deposit	Homogenization temperature (°C)	Salinity (wt% NaCl equivalent)	X_{CO2}	Reference
Cannivan Gulch	196–272	1.8–6.8	0.02–0.08	Darling, 1994
Davidson	300–440	2–15	present	Bloom, 1981
Endako	type 1: 250–440 type 3: 375–420	type 1: 5.3–14.8 type 3: 30–40	absent	Selby and others, 2000
MAX	type 1: mostly 190–270 type 2: mostly 260–340	type 1: mostly 6–10 type 2: max 6–16	absent 0.08–0.20	Linnen and Williams-Jones, 1990
Malala	400–600	40–55	present	van Leeuwen and others, 1994
Thompson Creek	180–300	6–11	present	Hall and others, 1984

vapor-CO_2 phases. Below this level, there is no substantial molybdenum mineralization, the fluid inclusions have consistent fluid/vapor ratios, and are three phase consisting of water, liquid CO_2, and vapor CO_2. This fundamental change in fluid inclusion composition is a product of CO_2 unmixing once the molybdenum-bearing fluids estimated to be composed of 94 percent H_2O, 4 percent CO_2, and 2 percent NaCl equiv. intersect the solvus within the H_2O-CO_2-NaCl system (Macdonald and others, 1995).

Although CO2 is found in fluid inclusions from porphyry copper deposits (John and others, 2010), it may be more important in porphyry molybdenum deposits. As emphasized in the above paragraph, CO_2 unmixing accompanied molybdenum mineralization at the Boss Mountain, alkali-feldspar rhyolite-granite porphyry Climax, and molybdenum-rich porphyry copper Buckingham deposits (Macdonald and others, 1995, and references therein). This change in CO_2 content of the fluids may cause molybdenum deposition under certain conditions. Aqueous-carbonic fluid inclusions are common in fluorine-poor arc-related porphyry molybdenum deposits (Linnen and Williams-Jones, 1990), yet also are locally observed, but are not abundant, and are less substantial in alkali-feldspar rhyolite-granite porphyry molybdenum deposits (Keith and others, 1993). For example, CO_2 is not observed in fluid inclusions from the Henderson, Colorado alkali-feldspar rhyolite-granite porphyry molybdenum deposit (location not shown in figures) (Macdonald and others, 1995, and references therein).

Not unexpectedly, different types of fluid inclusions can be associated with different types of alteration. At Davidson, early fluids associated with potassic alteration are shown to be hypersaline brines that contain halite and sylvite daughter crystals (Bloom, 1981). Later, more dilute fluids coincide with the initiation of phyllic alteration. At MAX, aqueous inclusions predominate within the zone of potassic alteration and aqueous-carbonic inclusions predominate within muscovite-ankerite alteration, whereas both types are common within quartz-feldspar-muscovite alteration (Linnen and Williams-Jones, 1990).

Stable Isotope Geochemistry

The most commonly studied stable isotopic systems within arc-related porphyry molybdenum deposits are oxygen, and sulfur (table 4). The main uses have been to trace fluid and sulfur sources and determine temperatures of mineralizing fluids.

Oxygen isotope data support the involvement of a meteoric water component along with magmatic fluids within the hydrothermal fluid regime. At Malala, a shift in $\delta^{18}O_{H2O}$ oxygen isotopic values from early magmatic values of approximately 7–10‰ to late hydrothermal fluid negative values is interpreted to be the result of a waning magmatic component and an increased meteoric water component (van Leeuwen and others, 1994). Using quartz-potassium feldspar and quartz-biotite pairs, Selby and others (2000) indicated that oxygen isotopes support the involvement of meteoric and magmatic fluids at Endako, where ore-forming fluids had calculated temperatures ranging from 200°C to 490°C.

Based on oxygen isotope data for quartz and muscovite in equilibrium, Linnen and Williams-Jones (1990) calculated fluid temperatures of 371–400°C for mineral pairs associated with molybdenum at MAX and a temperature of 384°C for fluids associated with muscovite-ankerite alteration. These ore-forming fluids were calculated to have values of $\delta^{18}0$ of 8.0–8.4 ‰. Broader temperature ranges are reported for quartz-potassium feldspar pairs (200–460°C) and quartz-biotite pairs (290–490°C) at Endako (Selby and others, 2000). The higher temperatures are in agreement with values of trapping temperatures for primary fluid inclusions in quartz veins within zones of potassic alteration, whereas the lower temperatures suggest not all mineral pairs were in equilibrium.

Sulfur isotopes generally support a mantle origin for the sulfur (Westra and Keith, 1981). For example, sulfur isotope values from Kitsault (formerly Lime Creek) have values of 0.0±1.6 per mil (‰) for sulfides and are consistent with derivation from a mantle source (Giles and Livingston, 1975). However, in contrast to data from most deposits, sulfur isotope analyses of molybdenite, pyrite, and arsenopyrite at Thompson Creek cluster between positive (+)9.6 and +11.4 ‰ and suggest a lower crustal source for sulfur (Hall and others, 1984).

Petrology of Associated Igneous Rocks

Rock Names

The mineralizing magma has compositions ranging from diorite to granite, most typically ranging in SiO_2 content from 65–77 wt percent (Sinclair, 2007). Quartz monzonite and granodiorite compositions are the most common compositions. Magmas generally generate peraluminous I-type granitoids. In some areas, mafic to rhyolitic intrusions are present locally, but they are not genetically related to molybdenum mineralization.

Forms of Igneous Rocks and Rock Associations

Multiple intrusive stocks are present at most deposits, not all of which host or are associated with mineralization. Other spatially associated intrusive rocks can be in the form of breccias (Boss Mountain), stocks and plutons (MAX), dikes and sills (Davidson), and batholiths (Endako).

Mineralogy

Intrusive rocks associated with arc-related porphyry molybdenum deposits are granitoids that, by definition of being calc-alkaline in nature, contain plagioclase crystals. Quartz and potassium feldspar also are universally found as major rock-forming minerals within the associated igneous rocks. The most common mafic mineral present is biotite, with lesser numbers of deposits containing amphibole. Phenocrysts within the porphyry are commonly plagioclase, quartz, or potassium feldspar, and rarely biotite (for example, Red Mountain: Brown and Kahlert, 1995). Some deposits are associated with reduced, ilmenite-bearing intrusions (fig. 14), but many others are associated with oxidized, magnetite-bearing intrusions. Common trace minerals include apatite, sphene, zircon, and magnetite. Monazite has been documented at Kitsault (Steininger, 1985), and allanite and ilmenite have been recognized at Quartz Hill (Wolfe, 1995). The mineral assemblages of the mineralizing intrusions of selected arc-related porphyry molybdenum deposits are listed in table 5.

Textures and Structures

Intrusions responsible for mineralization are typically porphyritic, but not always. The Endako quartz monzonite is generally equigranular, but some larger potassium feldspar crystals, as long as 7 mm, may visibly suggest a porphyritic texture within the 3–4 mm “groundmass”. Nevertheless, the crystals are not widespread enough to justify the term “porphyritic” (Kimura and others, 1976).

Equigranular, sugary aplite dikes and aplitic groundmass within porphyritic intrusions mainly consist of fine-grained quartz and alkali feldspar crystals. Formation of aplitic texture is regarded as a quenching feature because of rapid ascent and loss of volatiles from the magma causing rapid crystallization of

Table 4. Isotope values of select arc-related porphyry molybdenum deposits.

[‰= [(isotopic ratio of sample/isotopic ratio of standard)-1]×1000; ‰-CDT, per mil relative to the Canyon Diablo troilite standard; ‰-SMOW, per mil relative to the Standard Mean Ocean Water standard; ‰-PDB, per mil relative to the Pee Dee Belemnite standard. nd, no data]

Deposit	Sample description	Sulfur (‰-CDT)	Oxygen (‰-SMOW)	Carbon (‰-PDB)	$^{87}Sr/^{86}Sr$ (initial)	Reference
Malala	Vein quartz	nd	6.4–10.7	nd	nd	van Leeuwen and others, 1994
	Late-stage dolomite vein	nd	6.4–11.2	nd	nd	
	Whole rock, fresh porphyry	nd	6.3–8.1	nd	nd	
	Whole rock, potassic alteration	nd	7.1–7.6	nd	nd	
	Whole rock, phyllic alteration	nd	1.8–3.0	nd	nd	
Endako	Whole rock, least altered porphyry	nd	2.7–6.9	nd	nd	Selby and others, 2000
	Whole rock, potassic alteration	nd	6.3–7.5	nd	nd	
	Whole rock, argillic alteration	nd	5.2–7.2	nd	nd	
	Vein quartz	nd	6.7–9.5	nd	nd	
	Late-stage calcite vein	nd	–16.5	4.2	nd	
MAX	Vein quartz	nd	12.3–12.8	nd	nd	Linnen and Williams-Jones, 1990
	Vein muscovite	nd	9.6–10.0	nd	nd	
	Quartz from pervasive alteration	nd	12.5–12.7	nd	nd	
	Muscovite from pervasive alteration	nd	9.7–9.8	nd	nd	
Thompson Creek	Pyrite	9.6–9.9	nd	nd	nd	Hall and others, 1984
	Arsenopyrite	10.4	nd	nd	nd	
	Molybdenite	10.3–11.4	nd	nd	nd	
	Vein quartz	nd	10.7–11.2	nd	nd	
Kitsault	Hydrothermal sulfides	–1.6–1.6	nd	nd	nd	Giles and Livingston, 1975
	Plutonic rocks	nd	nd	nd	0.705	
Canicanian	Plutonic rocks	nd	nd	nd	0.7035–0.7037	Knittel and Burton, 1985
Quartz Hill	Plutonic rocks	nd	nd	nd	0.705	Hudson and others, 1981
Burroughs Bay	Plutonic rocks	nd	nd	nd	0.7049–0.7051	Hudson and others, 1981

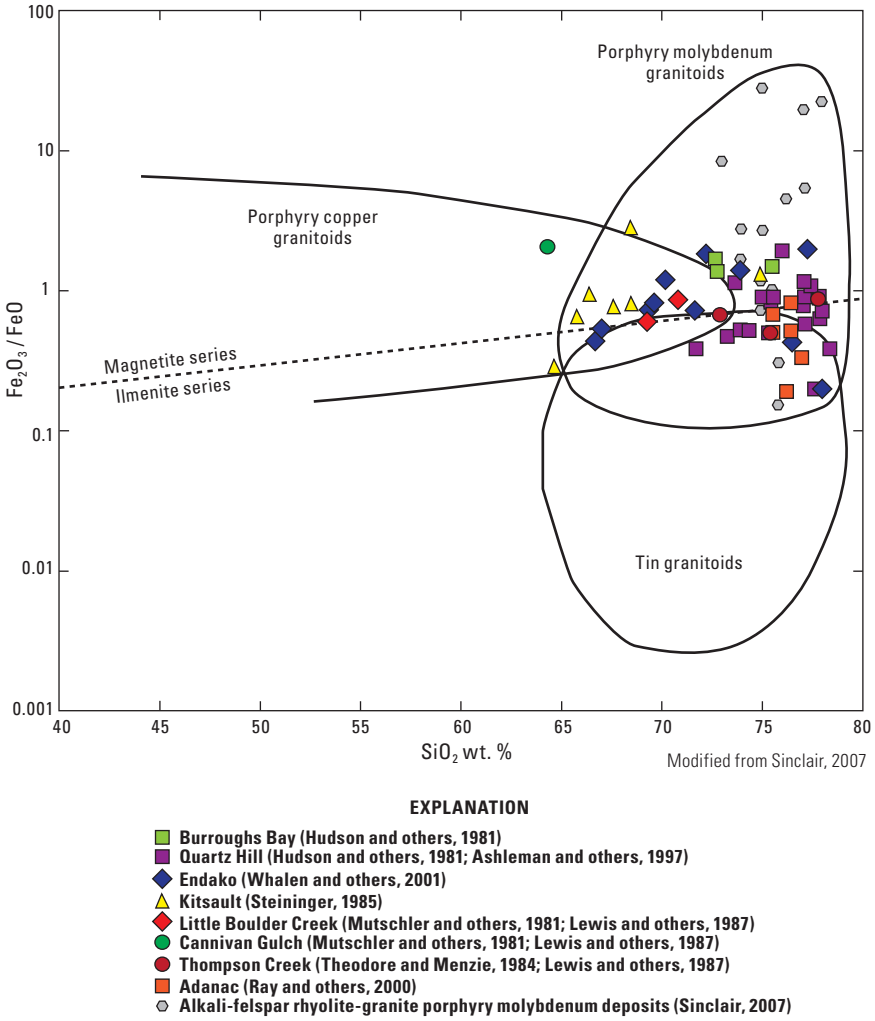

Figure 14. Silica (SiO_2) compared to iron (II) oxide/iron (III) oxide (Fe2O3/FeO) variation diagram for granitoids related to porphyry mineral deposits.

the viscous melt. Aplitic texture is recognized at the top of the granodiorite sheet at Davidson and aplite dikes can be observed at many deposits, including Kitsault.

A residual low-viscosity, H_2O-rich fluid is responsible for the formation of associated pegmatites. Pegmatite dikes are exceptionally coarse-grained and represent the last and most hydrous parts of a magma body. The coarse-grained nature is not a product of slow cooling rates, but is instead produced by poor nucleation and high chemical diffusivity in the volatile-rich fluid (Winter, 2001). Rare earth elements may be enriched within the pegmatites, however no arc-related deposits have reported economic values.

Forceful emplacement of magma or hydrothermal fluids may result in breccia formation. Intrusion breccias occur at the margins of the pluton and are characterized by fragments within a crystalline igneous breccia. Hydrothermal breccias commonly are related to mineralization. Quartz Hill contains an intrusive contact breccia, hydrothermal breccia, and tectonic breccia (Ashleman and others, 1997). Boss Mountain contains several breccias, a number of which are associated with mineralization.

Grain Size

Crystal sizes vary from fine-grained and aphanitic to coarse-grained. Many deposits, such as Nithi Mountain, Endako, and MAX, are medium-grained with crystals approximately equal to or less than 6 mm in length. Phenocrysts of orthoclase locally can reach lengths of 6 cm at Malala, but most phenocrysts of orthoclase, plagioclase, quartz, and biotite are smaller than 1.5 cm in size (van Leeuwen and others, 1994). Fine-grained aplite and coarse-grained pegmatites are relatively common.

Petrochemistry

Magmatic systems associated with arc-related porphyry molybdenum deposits can have high levels of magmatic differentiation or can be weakly differentiated. These calc-alkaline, peraluminous, I-type magmas predominantly generate hydrous forms of mafic minerals, such as biotite and hornblende, but are still likely to be leucocratic granitoids.

Table 5. Mineralogy of the mineralizing intrusions associated with selected arc-related porphyry molybdenum deposits.

[Mineral abbreviations: plag, plagioclase; qtz, quartz; kspar, potassium feldspar; bt, biotite; ap, apatite; spn, sphene; zrc, zircon; mnz, monazite; hbl, hornblende; op, opaques; mt, magnetite; py, pyrite; aln, allanite; ilm, ilmenite. nd, no data; cm, centimeter; mm, millimeter]

Deposit	Location	Mineralizing intrusion	Major minerals	Minor minerals	Trace minerals	Phenocrysts	References
Thompson Creek	Idaho	Weakly porphyritic quartz monzonite porphyry	plag, qtz, kspar, bt	nd	ap, spn, zrc, mnz	local kspar 1–2cm	Schmidt and others, 1983; Hall and others, 1984
Kitsault	British Columbia, Canada	Diorite to quartz monzonite	plag, qtz, kspar, bt, hbl	nd	spn, ap, zrc, mnz, op	plag, qtz, kspar	Steininger, 1985
Max	British Columbia, Canada	Equigranular to porphyritic granodiorite 0.5–2 mm equigranular	plag, qtz, kspar, bt	hbl subordinate to bt	ap, zrc, spn, op	2–5mm qtz, locally plag	Linnen and Williams-Jones, 1990; Lawley, 2009
Endako	British Columbia, Canada	Mostly medium-grained 1–6 mm, subporphyritic quartz monzonite	bt, plag, kspar, qtz	nd	mt, py, ap, spn	kspar up to 7 mm	Kimura and others, 1976; Bysouth and Wong, 1995
Quartz Hill	Alaska	Fine to medium-grained porphyritic quartz monzonite	plag, qtz, kspar	bt, hbl	py, ap, zrc, aln, mt, spn, ilm	qtz, kspar, plag	Wolfe, 1995; Ashleman and others, 1997
Boss Mountain	British Columbia, Canada	Boss Mountain stock quartz monzonite	equigranular kspar, qtz groundmass	bt, hbl	ap, spn, mt, zrc	qtz, kspar, plag	Soregaroli and Nelson, 1976
Malala	Indonesia	Malala granite, granodiorite, and quartz monzonite porphyries	plag, qtz, kspar	hbl subordinate to bt	ap, zrc, spn, mt	plag, qtz, bt, rapakivi textured kspar	van Leeuwen and others, 1994
Little Boulder Creek	Idaho	medium grained equigranular biotite granite porphyry	plag, qtz	kspar, hbl	nd	nd	Lewis and others, 1987

Intermediate to felsic magmas with SiO_2 contents typically ranging from 65–77 wt percent can produce tonalites, diorites, granodiorites, and quartz monzonites. These types of deposits typically contain low levels of fluorine within the intrusion, generally less than 0.1 percent F.

Geochemical differences between arc-related porphyry molybdenum deposits and alkali-feldspar rhyolite-granite porphyry molybdenum deposits are noted with major and trace elements. Westra and Keith (1981) based their distinction between the two deposit types on potassium oxide (K_2O) content at a given SiO_2 value. In their model, at 57.5 percent SiO_2, most arc-related porphyry molybdenum deposits have K_2O values of less than 2.5 percent and alkali-feldspar rhyolite-granite porphyry molybdenum deposits have higher K_2O values. Westra and Keith (1981) attribute this basic difference in geochemistry to be a result of the location within the subduction zone and depth of the subducted slab. However, Christiansen and Wilson (1982) question the validity of this model and instead suggest that differences in geochemistry result from deep crustal melting for alkali-feldspar rhyolite-granite porphyry molybdenum deposits. Differences in fluorine, niobium, rubidium, and strontium concentrations within these two different deposit types also is stressed as being important by Westra and Keith (1981).

Trace-Element Geochemistry

The overall trace element patterns for arc-related porphyry molybdenum deposits are similar to archetypal arc-related calc-alkaline rocks. This fact makes it difficult, if not impossible, to differentiate between barren and mineralized intrusive rocks based on trace element geochemistry alone. It is expected that large-ion lithophile element and fluid mobile element concentrations will be elevated in subduction-generated magmatic rocks. Also consistent with subduction-related magmatism are low-levels of TiO_2, but these are still generally greater than 0.1 percent.

Cogenetic intrusive rocks related to molybdenum mineralization in arc-related porphyry molybdenum deposits have low concentrations of rubidium and niobium (generally less than 300 and 30 ppm, respectively), and moderate to high concentrations of strontium (generally greater than 100 ppm), whereas alkali-feldspar rhyolite-granite porphyry molybdenum deposits are enriched in rubidium and niobium, but depleted in strontium, calcium, barium, and titanium (figs. 15, 16; Westra and Keith, 1981). Trace element data for the Adanac deposit indicate that it does not cleanly fit into either the arc-related porphyry or alkali-feldspar rhyolite-granite porphyry molybdenum end members. Strontium and niobium data for Adanac is similar to the large Quartz Hill deposit; however the cogenetic pluton for Adanac has been shown to be alkalic (Smith, 2009), which is uncommon for subduction-related magmatism. Quartz Hill and Adanac have some hybrid characteristics of arc-related porphyry and extensional alkali-feldspar rhyolite-granite porphyry molybdenum deposits, with Quartz Hill more resembling the former and Adanac more resembling the latter. Data for Adanac and Quartz Hill, and the overlap of

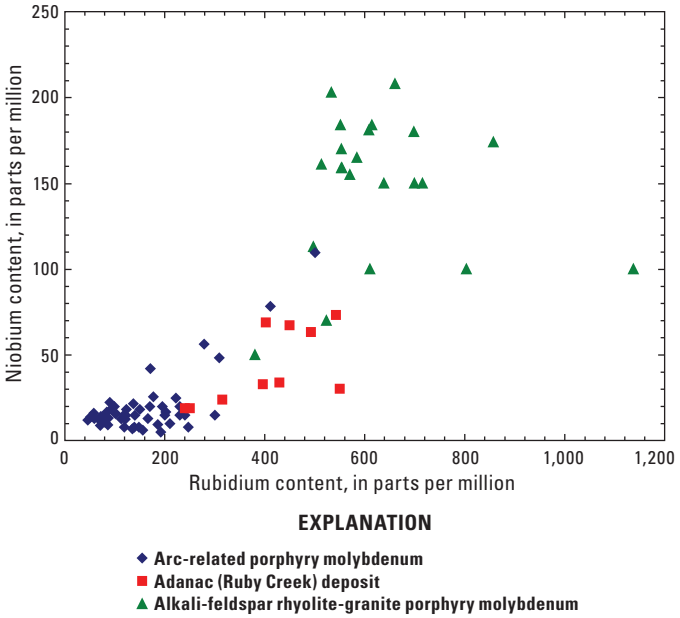

Figure 15. Niobium (Nb) and rubidium (Rb) contents of unaltered and least altered intrusive rocks associated with molybdenum mineralization. Data for arc-related porphyry molybdenum deposits include Malala (van Leeuwen and others, 1994), Kitsault (Steininger, 1985), Endako (Whalen and others, 2001), MAX (Lawley and others, 2010), Little Boulder Creek (Lewis and others, 1987), Thompson Creek (Lewis and others, 1987), Davidson (unpublished data, Sinclair, written commun., 2011), Red Mountain (unpublished data, Sinclair, written commun., 2011), Storie (unpublished data, Sinclair, written commun., 2011), and Mount Haskin (unpublished data, Sinclair, written commun., 2011). Data for alkali-feldspar rhyolite-granite porphyry molybdenum deposits includes Henderson, Colo. (Carten and others, 1988), Red Mountain, Colo. (Bookstrom and others, 1988), and Climax, Colo. (Bookstrom and others, 1988). Data for Adanac (Ray and others, 2000; unpublished data, Sinclair, written commun., 2011) shown for comparison.

trace element data points for deposits classified as arc-related porphyry molybdenum and alkali-feldspar rhyolite-granite porphyry molybdenum deposits supports the likely existence of a continuum between these two end-member deposit types. The tectonic location and petrochemistry of the hosting intrusion are likely the best methods of classifying a deposit into end-member porphyry molybdenum models.

Some newly studied molybdenum deposits in China, such as the Jinduicheng molybdenum porphyry, also have trace element concentrations of the associated mineralizing intrusion that are neither fully characteristic of arc-related porphyry molybdenum nor alkali-feldspar rhyolite-granite porphyry molybdenum deposits (Zhu and others, 2010; Ludington, written commun., 2011). However, many of these deposits are more reminiscent of the alkali-feldspar rhyolite-granite-type. Stein and others (1997) unequivocally characterized the large Jinduicheng deposit and others in the Qinling belt of China to be of the alkali-feldspar rhyolite-granite porphyry molybdenum type.

Quartz Hill intrusive rocks trace element concentrations as compiled by Hudson and others (1979) are lower in barium, cerium, chromium, cobalt, copper, lanthanum, vanadium, zinc and zirconium than the average I-type granite, but greater in lead (Winter, 2001). Climax, Henderson, and the Tertiary molybdenum deposits in Idaho, all examples of alkali-feldspar rhyolite-granite porphyry molybdenum deposits which are not displayed on the location figures, have strong negative europium anomalies indicating fractionation of plagioclase and its separation from the magma, whereas many arc-related porphyry molybdenum deposits, such as MAX, have no excessive europium anomalies (U.S. Geological Survey Headwaters Province Project Team, 2007; Lawley, 2009; Lawley and others, 2010). The europium trends for intrusive rocks from Endako are variable in intensity and direction (Whalen and others, 2001). The Quartz Hill composite stock does display a moderate negative europium anomaly (Ashleman and others, 1997), again suggesting some differences from most other deposits in this model.

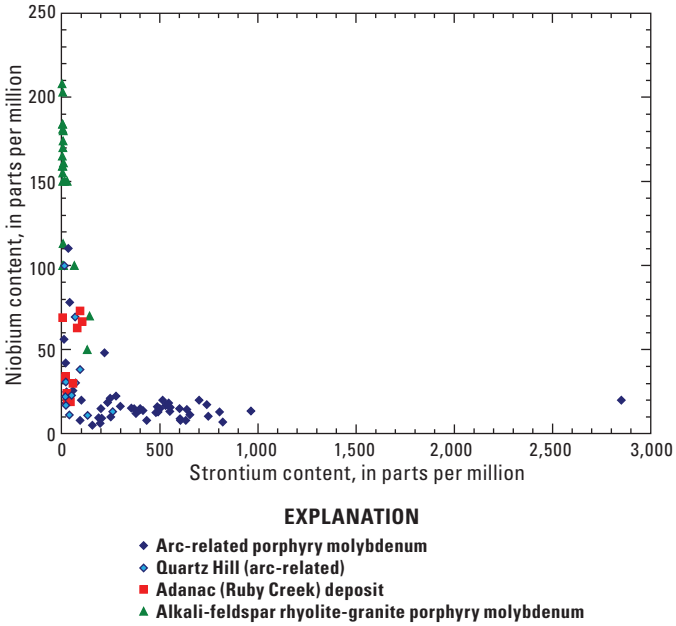

Figure 16. Niobium (Nb) and strontium (Sr) contents of unaltered and least altered intrusive rocks associated with molybdenum mineralization. Data for arc-related porphyry molybdenum deposits include Malala (van Leeuwen and others, 1994), Kitsault (Steininger, 1985), Endako (Whalen and others, 2001), MAX (Lawley and others, 2010), Little Boulder Creek (Lewis and others, 1987), Thompson Creek (Lewis and others, 1987), Quartz Hill (Hudson and others, 1979), Davidson (unpublished data, Sinclair, written commun., 2011), Red Mountain (unpublished data, Sinclair, written commun., 2011), Storie (unpublished data, Sinclair, written commun., 2011), and Mount Haskin (unpublished data, Sinclair, written commun., 2011. Data for alkali-feldspar rhyolite-granite porphyry molybdenum deposits includes Henderson, Colo. (Carten and others, 1988), Red Mountain, Colo. (Bookstrom and others, 1988), and Climax, Colo. (Bookstrom and others, 1988). Note the similarity in chemical composition for Quartz Hill and Adanac (Ray and others, 2000; unpublished data, Sinclair, written commun., 2011).

Isotope Geochemistry

Little isotopic research has been carried out on igneous rocks associated with arc-related porphyry molybdenum deposits. However, Whalen and others (2001) looked at neodymium isotopes of associated intrusive rocks to the Endako deposit and noted only positive epsilon neodymium (εNd) values, which varied slightly between the various intrusive phases, but ranged from +1.1 to +7.2. The overall positive εNd values suggest magmatic derivation from an isotopically depleted source, such as depleted asthenosphere.

Radiogenic neodymium and strontium values, compared to chondritic values, for ore-related cogenetic intrusive rocks in Idaho and Montana are generated from an isotopically enriched source(s) (U.S. Geological Survey Headwaters Province Project Team, 2007). This enriched source cannot be asthenospheric mantle, and is inferred to be ancient continental crust or lithosphere based on the tectonic location. Contamination of magma derived from the mantle wedge with melts from the lower crust through MASH (Melting Assimilation Storage Homogenization) processes would produce these isotopic values.

Strontium isotope values in other deposits also preclude a substantial crustal component in the magma (table 4). Initial $^{87}Sr/^{86}Sr$ values at Quartz Hill indicate little involvement of older sialic crust generating or even contaminating the magma (Ashleman and others, 1997). Instead, a primitive source with a low rubidium-strontium ratio likely produced these intrusive rocks. Initial $^{87}Sr/^{86}Sr$ of 0.7052±0.0002 for plutonic rocks at Kitsault suggests mantle derivation with minor crustal contamination of the magma (Giles and Livingston, 1975). The low initial strontium values at Canicanian of 0.70351–0.70374 also rule out substantial contribution of crustal melt (Knittel and Burton, 1985).

Depth of Emplacement

The development of arc-related porphyry molybdenum deposits is favored at greater depths than porphyry copper deposits because of differences in the behavior of molybdenum relative to copper during magmatic evolution (Candela and Holland, 1986; Misra, 2000). Copper behaves as a compatible element before water saturation of the magma, but acts as an incompatible element afterward, whereas molybdenum acts as an incompatible element throughout the crystallization process. Therefore, early vapor evolution at shallow depth is conducive to scavenging of copper into the exsolved fluid or vapor and formation of a porphyry copper deposit. A late vapor evolution at greater depth will create a porphyry molybdenum deposit because much of the copper would have been lost to crystallized phases, but would leave abundant molybdenum to concentrate in the magmatic fluid.

Unlike porphyry copper deposits, porphyry molybdenum deposits do not commonly occur within related volcanic rocks because of their greater depth of emplacement (Hollister, 1978). However, they are emplaced at relatively shallow

depths, as can be noted with the brittle nature of the stockwork veining. Arc-related porphyry molybdenum deposits can be generated from equigranular intrusions, which contrasts to the nearly ubiquitous porphyritic texture of porphyry copper deposits and can be a result of deeper emplacement of the magma.

Seedorff and others (2005) compiled data from some well-studied porphyry deposits and determined that most form between 1 and 6 km of the paleosurface, but some may form even deeper (for example, Butte, Montana; not shown in the location figures). Out of the six molybdenum-rich porphyry copper deposits that Seedorff and others (2005) presented depth of formation data for, five deposits show that molybdenum mineralization occurred at greater depths than copper mineralization, whereas only one deposit has molybdenum and copper mineralization at the same depth (see Seedorff and others, 2005; figure 9).

Linnen and Williams-Jones (1990) used fluid inclusion and stable isotope data to estimate a fluid pressure of 1.4–1.7 kilobars during mineralization. If this fluid pressure is assumed to equal the lithostatic pressure, this equates to entrapment at 4–5 km depth (Lawley and others, 2010). However, Linnen and Williams-Jones (1990) assumed a lithostatic pressure of 2 kilobars for the emplacement of the Trout Lake stock, which equates to a depth of emplacement of approximately 7 km.

Petrology of Associated Sedimentary Rocks

The sedimentary country rocks that the cogenetic intrusions are emplaced into will affect the convection of the hydrothermal system based on the permeability of the hosting sedimentary rock. Low permeability of the sedimentary rocks will hinder widespread hydrothermal fluid convection. If the adjacent country rocks are carbonates, then the formation of metal-bearing skarn deposits is possible.

Petrology of Associated Metamorphic Rocks

The intrusion of the magmatic bodies causes contact metamorphism or metasomatism of the surrounding country rocks to form hornfels, marble, or skarn. Skarn formation may be of economic significance in some deposits by hosting molybdenum or tungsten mineralization.

The makeup of the metamorphic country rock does not affect the formation of arc-related porphyry molybdenum deposits in any way beyond possible permeability issues for hydrothermal fluids as described in the Petrology of Associated Sedimentary Rocks section.

Theory of Deposit Formation

Ore Deposit System Affiliation(s)

Many types of other mineral deposits may be associated with arc-related porphyry molybdenum deposits and the hydrothermal system responsible for their formation. These are likely found peripheral to the central molybdenum orebody, but also may be found within the main deposit. Commodities of economic concern, other than molybdenum, are primarily tungsten, lead, zinc, and silver.

Veins that contain base metals may be spatially and genetically associated with molybdenum mineralization. Base metal veins containing sphalerite, galena, chalcopyrite, lead-bismuth sulphosalts, tetrahedrite, scheelite, and molybdenite are found scattered throughout the Kitsault molybdenum deposit. Paragenetically late, but minor, base metal veining can be found at Red Mountain. A peripheral base metal zone at Davidson surrounds the central molybdenum zone, and lead-zinc-silver veins at MAX extend outward further than molybdenum mineralization. Copper-, lead-, zinc-, and antimony-enriched zones surround the main molybdenum occurrence at Compaccha, but are not economically viable (fig. 13).

Tungsten-bearing skarns also are associated with molybdenum ores and may be of economic significance. Scheelite mineralization within skarn is developed at deposits such as MAX, Cannivan Gulch, and Thompson Creek.

Sources of Metals and Other Ore Components

The most consistent petrologic feature of arc-related porphyry molybdenum deposits is the cogenetic calc-alkaline intrusion. No pattern between development of a deposit and country rock characteristics is noted. This is suggestive of the molybdenum being mainly, if not totally, derived from the magmatic body and this is accepted by most researchers (for example, Soregaroli and Sutherland Brown, 1976). Geochemical confirmation of this is lacking in the literature; however, this link to magmatic activity has been illustrated for alkali-feldspar rhyolite-granite porphyry molybdenum deposits (Stein and Hannah, 1985) and also for arc-related porphyry copper deposits (John and others, 2010).

Possible sources within the Earth for the magma include the subducted slab, the asthenospheric mantle wedge above the subducted slab, the subcontinental mantle lithosphere, lower crust, and upper crust. The formation of adakite-like magmas from the direct melting of a subducted slab has been popularized as the cause of porphyry copper deposit formation (for example, Kay, 1978); however, the linkage between direct slab melting and porphyry mineralization is controversial and tenuous, and classical magmatic processes in a subduction zone can create these chemical characteristics (Richards and Kerrich, 2007). Considering the occurrence, albeit rare, of arc-related porphyry molybdenum deposits within an island

arc setting (for example, Malala and Canicanian), a model for derivation from thick middle to upper continental crust is not applicable. Instead, a model of principally subduction-derived magma from the mantle with possible assimilation of lower crustal material through MASH processes (Hildreth and Moorbath, 1988) is widely accepted (for example, see Richards, 2003).

Sources of Fluids Involved in Ore Component Transport

A magmatic-hydrothermal genetic model is most applicable, with metals derived from genetically associated intrusions. Fluids causing the hydrothermal alteration can be magmatic and meteoric, with larger proportions of meteoric water affecting the tops and peripheries of the system. Metals are derived from the magmatic fluids, whereas any meteoric or formation water will only add negligible amounts of molybdenum.

Magmatic fluids are extracted during the process of second boiling (Burnham, 1997). In this process, a saturated magma reacts to create crystals and an aqueous fluid concentrated in the carapace of the intrusive body. However, the process of second boiling is not sufficient in itself to produce some of the large ore deposits. Shinohara and others (1995) suggest that the small stocks associated with porphyry molybdenum deposits mainly remain liquid before and during the mineralizing process, when they are connected at depth to a larger batholith. In this model, volatile-rich magma ascends toward the cupola of the molten stock where it degasses. The denser degassed magma descends because of its lower volatile content and greater density. This convective model explains how undersized stocks can concentrate enough ore-forming fluids and metals to produce large porphyry deposits.

Fluid pressure induced fracturing of the surrounding rock will occur whenever this energy exceeds the tensile strength of the rock. This fluid escapes into the stockwork fractures, carrying with it the metals of economic interest. Episodic buildup of pressure, which will be followed by fracturing and sealing of the fractures, will lead to formation of multigeneration, crosscutting stockwork veins of differing mineralogies.

The proportion of nonmagmatic fluid in the system increases spatially away from the core intrusion. This meteoric water is derived from the surrounding country rocks and its circulation is initiated by thermal gradients caused by the intrusion and the escaping magmatic fluids. Meteoric fluids also will start to dominate in the waning periods of the hydrothermal cycle as magmatic fluids have cooled.

Sources of Ligands Involved in Ore Component Transport

Metal-transporting ligands of many species are found in natural hydrothermal systems. Common and important ligands in hydrothermal systems include Cl^-, F^-, HS^-, NH_3^-, and OH^-. Examples of ligands of lesser importance include Br^-, I^-, HSO_4^-, and SO_4^{2-}. Just as metals and fluids are sourced from the cogenetic intrusion, so are the ligands. Organically derived ligands are of no importance for these deposits.

Chemical Transport and Transfer Processes

Chloride and sulfide complexes are not substantial transporting species for molybdenum. Instead, most molybdenum is transported as $HMoO_4^-$ or H_2MoO_4 with lesser amounts being transported as MoO_3F^-, which shows that fluorine is not a necessary ion for transportation of molybdenum (Smith and others, 1980). In recent experiments, Ulrich and Mavrogenes (2008) suggest that H_2MoO_4 is the dominant complex in aqueous solutions, and Cl^- complexes are negligible in transportation, except possibly in high-salinity solutions. However, arc-related porphyry molybdenum deposits are characterized by low to moderate salinities.

Molybdenum precipitation may be facilitated by decreasing pH, fO_2, or fH_20, by an increase in fS_2, and by a drop in temperature of the transporting medium. Decompression and dropping fluid temperature can occur simply through stockwork fracturing of the host rock. Mixing of the molybdenum-bearing magmatic fluids with external meteoric fluids could cause the molybdenum to drop out of solution and precipitate. Reaction 7 is a simplistic reaction for molybdenite precipitation.

$$H^+ + HMoO_4^- + S_2 = MoS_2 + H_2O + 3/2O_2 \qquad (7)$$

At high temperatures, the partitioning of molybdenum into an aqueous solution is independent of CO_2, F, Cl, and S content. Ulrich and Mavrogenes (2008) indicated that molybdenum solubility is temperature dependent, with greater solubility at higher temperatures. In contrast, Candela (1992) emphasizes the compatibility of molybdenum between crystal and melt is dependent on the magmatic oxygen fugacity, with molybdenum acting more incompatibly under oxidizing conditions. However, arc-related deposits can still be generated from reduced ilmenite-series intrusions.

Fluid Drive, Including Thermal, Pressure, and Geodynamic Mechanisms

Pressure and temperature gradients are critical to the initiation of fluid drive. The major heat source in a porphyry system is from the magma emplacement. Magmatic fluids become over-pressurized and are then physically expelled into the solidified carapace and the surrounding country rocks. Cooler conditions outward from the central stock or pluton will cause the magmatic fluid to progressively cool as it interacts with country rock and meteoric fluids as it moves outward, upward, and even downward away from the intrusion (Beane, 1983; Carten and others, 1988). Through time, the magma is chilled through convection and more importantly through conductive cooling. This heat, in part, will be

transferred to the surrounding country rocks and will initiate convection of meteoric waters, as well as contact metamorphism of the adjacent rock units.

Pressures within these systems vary greatly and can change quickly. An interplay of factors such as lithostatic pressure, hydrostatic pressure, regional tectonic stresses, production of fluids from metamorphic reactions and the magma, and the dynamic action of magma emplacement affect the pressures and stresses on the system. During cooling and concentration of volatiles within the carapace of the pluton, pressures build and cause hydrofracturing when the fluid pressures exceed the tensile strength of the rock (Burnham and Ohmoto, 1980). Pressure build-up and subsequent fluid release will allow the fluids to move to the areas of lower pressure found in the newly formed fractures, creating breccias and stockwork veining of molybdenum mineralization.

Exploration/Resource Assessment Guides

Geological

To start, proper regional locations for arc-related molybdenum mineralization must be targeted. This mandates that identification of these deposits typically is limited to examination of magmatic belts that formed above subduction zones along convergent plate boundaries. Targeting in regions that already have discovered deposits and prospects should be given precedence.

Geologic mapping is extremely important in the discovery of deposits and delineating areas of higher grade molybdenum mineralization. Mapping of igneous rocks, their distribution patterns, and pervasiveness of veining, hydrothermal alteration, sulfide mineralization, faulting, and weathered products provide critical information. As an example, key determinants that were studied at Endako for potential of higher grade molybdenum zones include mineral assemblage, alteration intensity, and vein intensity (Bysouth and Wong, 1995).

Early discovery of some molybdenum deposits in British Columbia was in response to mineral prospectors noting geological anomalies in their search for gold or silver deposits. For example, Boss Mountain was originally discovered by gold prospectors who uncovered the molybdenite occurrence in 1911.

Geochemical

The most successful aqueous geochemical surveys focus on chemical indicators that are associated with the ore deposit type and are mobile in aqueous solutions. Groundwater interacts with buried deposits and rock formations and will inherit certain chemical characteristics of the ore and rocks, with the metallic levels partially dependent on the residence time of the fluids in an underground environment.

Advances in analytical techniques and instrumentation have affected the nature of geochemical surveys. Newer high-resolution inductively-coupled-plasma mass-spectrometers (HR-ICP-MS) allow for multiple element analyses with low detection limits of less than one part per trillion for some elements. Key aqueous pathfinder elements for porphyry molybdenum deposits include molybdenum, selenium, rhenium, and arsenic, with secondary pathfinder elements including lead and zinc (Leybourne, 2007). Mapping values of these pathfinder elements may show proximity and direction of the sample sites to a deposit when compared to local background values.

Stream-sediment surveys may unearth geochemical anomalies through mechanical dispersion of near surface materials, and through a hydromorphic component of metals transferred to the sediment through interaction of metal-bearing fluids, which links stream-sediment sampling with surface-water sampling. Common elements that are anomalous in stream sediments include molybdenum, tungsten, fluorine, copper, lead, zinc, and silver (Sinclair, 1995). Anomalous levels of molybdenum (most between 10–30 ppm), niobium (detectable), and beryllium (5 or 10 ppm) were noted in stream sediments at Quartz Hill in southeastern Alaska (Elliot and others, 1976). This led to detailed exploration and the discovery of silicified outcrop that contained molybdenite. A regional stream-sediment survey in Indonesia resulted in the discovery of the Malala molybdenum deposit through anomalous levels of copper (245 ppm), molybdenum (15 ppm), lead (390 ppm), and zinc (340 ppm) in the Takudan River sediments (van Leeuwen and others, 1994).

Cook (2000) analyzed lake sediments near known arc-related porphyry molybdenum prospects in the vicinity of Endako, British Columbia, with implications for regional exploration. Molybdenum values of as much as 165 ppm (median values of 7, 8, and 42 ppm molybdenum for the three individual lakes) greatly exceeded regional background values of 1–4 ppm. Large within-lake variations in molybdenum concentration are noted with the highest values occurring in central sub-basins within the lakes and lower values occurring in clastic-dominated nearshore environments. The molybdenum in the sediment is interpreted to be hydromorphic in nature with possible geobotanical accumulation within organic-rich sediments.

The Mac deposit was identified through lake sediment geochemical analyses that defined anomalous molybdenum, copper, and silver values compared to the background level found in regional lakes. This led to subsequent soil and silt sampling that identified other molybdenum prospects in the area (Cope and Spence, 1995).

Soil, silt, and glacial till sampling are methods that look for the mechanical dispersal of molybdenum. Geochemical surveys using these media may identify high-grade molybdenum mineralization. For example, a strong molybdenum soil anomaly overlies the Endako ore deposit and is dispersed by glacial processes as far as 5 km to the east. It is thought that in the early stages of exploration, geochemical soil sampling would have been beneficial here (Bysouth and Wong, 1995).

Geophysical

Geophysical detection of a mineral deposit requires different physical or chemical characteristics of sufficient magnitude between the deposit and the surrounding country rocks. Magnetic, gravity, and electrical methods are examples of the most commonly used methods for ore deposit detection (Ford and others, 2007).

Magnetic anomalies may define the presence of minerals such as magnetite and pyrrhotite located within the adjacent hornfels zone, but molybdenum mineralization itself would not be identified. Induced polarization (I.P.) surveys may note locations of high concentrations of pyrite alteration, but this is complicated by generally low sulfide concentrations within this deposit type. Most promising may be radiometric surveys looking for zones of potassic alteration. Airborne gamma-ray spectrometry surveys may delineate high potassium anomalies formed because of hydrothermal alteration, but these anomalies may be difficult to distinguish from anomalies produced simply by ordinary high potassium rock types. Overall, geophysical detection of arc-related porphyry molybdenum deposits has met with minimal success because of low sulfide and oxide contents of the deposit type.

At Endako, low sulfide contents rendered geophysical exploration useless. Over the molybdenum zone, I.P. anomalies lie within normal background levels (Bysouth and Wong, 1995).

A magnetometer survey at MAX showed a few anomalies related to pyrrhotite-bearing skarns. However, the porphyry deposit itself was not defined based on geophysical methods (Linnen and others, 1995).

Attributes Required for Inclusion in Permissive Tract at Various Scales

The future discovery of partially to completely concealed deposits requires knowledge of where these deposits may form in the first place. Determining regions likely to contain molybdenum mineralization will minimize geochemical and geophysical exploration expenses that are required to occur before costly drilling commences.

First of all, a magmatic belt located in a subduction zone setting at a convergent plate margin is necessary. Known arc-related porphyry molybdenum deposits are found in mountain belts where known porphyry copper mineralization also is located. However, many mountain belts where porphyry copper deposits are found do not contain any, as of yet discovered, arc-related porphyry molybdenum deposits.

Proximity to known deposits also is favored. Locating regional structures in areas known to have formed or currently are forming within subduction zones where intrusions can be focused is a priority. Next, finding those intrusions that are of permissible age to be related to subduction processes is required. Intrusions of the proper chemical makeup and mineralogy (in other words, I-type calc-alkaline intermediate to felsic intrusions) may then be favored for further detailed exploration. Furthermore, a location where potassic alteration grades outward or upward into phyllic alteration is a diagnostic feature (Hall, 1995).

Factors Affecting Undiscovered Deposit Estimates (Deposit Size and Density)

Many deposits with a surface expression have been discovered already, so future exploration and discoveries will focus mainly on covered deposits. Geological mapping of covered areas is much less likely to reveal a deposit than by applying geochemical or geophysical techniques to identify any ore-related anomalies. Nevertheless, knowledge of regional geologic, magmatic, and tectonic features permissible for definition of tracts of land that are most favorable for molybdenum mineralization remains essential before targeting with other methodologies. This, for example, will allow for focused geochemical surveys. In the late 1970s, the British Columbia Geological Survey published regional geochemical survey data that led to the discovery of multiple arc-related porphyry molybdenum deposits near the Alice Arm area; similar work in geologically favorable regions of Alaska and elsewhere in the United States may eventually lead to the discovery of new molybdenum deposits in remote or covered locations.

Geoenvironmental Features and Anthropogenic Mining Effects

Pre-Mining Baseline Signatures in Soil, Sediment, and Water

The enrichment of elements in soil, sediment, and water from the weathering of a mineral deposit depends on the deposit type, host-rock lithology, ore and gangue mineral assemblage, and environment. In addition to molybdenum, arc-related porphyry molybdenum deposits may have anomalous levels of tungsten, copper, gold, silver, lead, and zinc. Pre-mining baseline signatures generally are characteristic of a given deposit type.

Soils

The median concentration of molybdenum in soils is 6 ppm for samples from the western United States and 0.5 ppm for samples from the eastern United States, with a median value for the United States of 1 ppm (Kubota, 1977). According to Barceloux (1999), the typical range of molybdenum in soils in North America is between 1 and 2 ppm. Soils near arc-related porphyry molybdenum deposits commonly contain molybdenum concentrations that are substantially higher than the median values for the United States (table 6). For example,

Table 6. Concentrations of molybdenum (in ppm) in surface soils in the vicinity of arc-related porphyry molybdenum deposits.

[>, greater than; Mo, molybdenum; ppm, parts per million; <, less than; mm, millimeter]

Deposit	Description	Mo (ppm)	Reference
Kitsault	Pre-mining in region of deposit, <2mm size fraction	25–2,361	Price, 1989
Kitsault	Pre-mining in region of deposit, coarse size fraction	2–256	Price, 1989
Endako	Pre-mining in region of deposit	15≥81	Mathieu, 1995
Endako	Regional background	2	Mathieu, 1995
Endako	Mining-impacted soils	2.3–258	Mathieu, 1995
Luxor	Pre-mining soil anomaly	>25–942	Kingsman Resources Corp, 2009
Median United States soils		1	Kubota, 1977

naturally occurring soils in the region of the Kitsault deposit contain 25–2,361 ppm molybdenum in the less than 2 mm size fraction and 2–256 ppm in the coarse (greater than 2 mm) fraction (Price, 1989). A soil molybdenum anomaly overlies the Endako deposit, with a 5 km eastward glacial dispersion train (Bysouth and Wong, 1995). Soil samples within the anomaly contain between 15 and greater than 81 ppm molybdenum; regional background samples outside the anomaly contain 2 ppm molybdenum (Mathieu, 1995; table 6). A similar trend was noted for the Red Mountain deposit, with silt-size stream sediments containing as much as 330 ppm molybdenum in mineralized areas and containing 20–40 ppm molybdenum downstream from the mineralization for 1.6 km; background values in the area are 4 ppm (Brown and Kahlert, 1995). At the arc-related Luxor porphyry molybdenum property in British Columbia, a 100- to 400-m-wide × 1-km-long soil anomaly containing 25–942 ppm molybdenum prompted further exploration (Kingsman Resources Corp, 2009). The extent of the MAX deposit was delineated by trenching and sampling of B-horizon soils; a geochemically anomalous area was defined by a 100 ppm molybdenum contour that overlaps a more extensive area of anomalous tungsten, likely because of tungsten skarns adjacent to the molybdenum deposit (Linnen and others, 1995).

Sediments

As noted above in the Exploration/Resource Assessment Guide geochemistry section, Cook (2000) analyzed molybdenum in lake sediments in the Endako area of British Columbia and documented elevated molybdenum concentrations of as much as 165 ppm relative to regional background concentrations of 1–2 ppm molybdenum in small eutrophic lakes (table 7). In southwestern Montana, stream sediments were sampled along Cannivan Gulch proximal to the undeveloped Cannivan Gulch porphyry molybdenum deposit as part of a mineral-resource assessment of the Eastern Pioneer Mountains (Pearson and others, 1988). Sediments contained less than 500 ppm copper, less than 29 ppm molybdenum, less than 80 ppm arsenic, less than 1,600 ppm zinc, and 70–99 ppm lead (Berger and others, 1979; Pearson and others, 1988). Stream-sediment surveys in Challis National Forest, Idaho identified geochemical signatures associated with porphyry molybdenum deposits that included (1) bismuth, boron, copper, lead, molybdenum, tin, thorium, and tungsten for panned heavy mineral concentrates in the area of the Thompson Creek deposit; (2) bismuth, copper, molybdenum, silver, and tungsten for stream sediments from the same area; and (3) copper, lead, molybdenum, silver, and zinc for stream sediments from the White Cloud area. In Alaska, regional stream-sediment exploration led to the discovery of the Quartz Hill deposit based on a concentration of 168 ppm molybdenum obtained for a minus-80-mesh stream-sediment fraction from a tributary of a creek that drains the deposit area (Wolfe, 1995).

Waters

Waters draining the intrusive rocks that host arc-related porphyry molybdenum deposits and their surrounding alteration zones have distinct signatures. Commonly, stream waters draining the deposits exhibit molybdenum in concentrations greater than in unmineralized areas. Typical molybdenum background concentrations in water are approximately 1 micrograms per liter (µg/L) for freshwater systems of the United States (Chappell and others, 1979) and for surface waters of North America (Hem, 1985). The concentrations of molybdenum in natural freshwater in Canada are reported to range from less than 0.1 µg/L to 500 µg/L, whereas in groundwater they are reported to range from less than 0.1 µg/L to greater than 1,000 µg/L (MEND, 2008). Chappell and others (1979) suggested that waters with more than 10 to 20 µg/L molybdenum likely are affected by human activity such as mining, milling, smelting, coal-fired power plants, and agriculture. Voegeli and King (1969) suggested stream waters with molybdenum greater than 5 µg/L likely are draining molybdenum deposits and waters with molybdenum greater than 60 µg/L likely are draining areas of mining.

Waters associated with porphyry molybdenum deposits tend to be near-neutral; variable in concentrations of molybdenum (less than 2 to greater than 10,000 µg/L); below regulatory guidelines for copper, iron, lead, zinc, and mercury concentrations; and locally above guidelines for arsenic, cadmium, and selenium levels (appendix 2). The effects of other peripheral deposit types within drainage areas may explain much of the variability in the data.

Table 7. Concentrations of metals in stream, wetland, and lake sediment downstream from arc-related porphyry molybdenum deposits.

[Elemental abbreviations: As, arsenic; Cd, cadmium; Co, cobalt; Cr, chromium; Cu, copper; Fe, iron; Mo, molybdenum; Ni, nickel; Pb, lead; Sb, antimony; Zn, zinc. ppm, parts per million; %, percent; <, less than; nd, no data; n, number of samples]

Mining area	Description	As (ppm)	Cd (ppm)	Co (ppm)	Cr (ppm)	Cu (ppm)	Fe (%)	Mo (ppm)	Ni (ppm)	Pb (ppm)	Sb (ppm)	Zn (ppm)	Reference
White Cloud, Idaho	Little Boulder Creek about 0.5 miles downstream of the Baker adit	6.1	<2	22	250	20	4.9	nd	59	34	nd	91	Giles and others, 2009
Malala, NW Sulawesi, Indonesia	Tukudan River, downstream of undisturbed deposit	nd	nd	nd	nd	245	nd	15	nd	390	nd	340	van Leeuwen and others, 1994
Malala, NW Sulawesi, Indonesia	Tributary to Tukudan River, downstream of undisturbed deposit	nd	nd	nd	nd	nd	nd	567	nd	nd	nd	nd	van Leeuwen and others, 1994
Endako region, British Columbia, Canada	Median lake sediment concentrations—Hanson lake (n=44)	13	0.5	10	40	65.5	3.78	7	32	9	0.8	122	Cook, 2000
Endako region, British Columbia, Canada	Median lake sediment concentrations—Tatin lake (n=38)	2	0.3	6	22.5	35	2.02	8	17	4.5	0.65	77.5	Cook, 2000
Endako region, British Columbia, Canada	Median lake sediment concentrations—Counts lakes (n=63)	3	0.6	7	23	44	1.65	42	17	10	1.1	109	Cook, 2000
Probable Effect Concentrations (PEC)		33	4.98	nd	111	149	nd	nd	48.6	128	nd	459	MacDonald and others, 2000

Pre-mining molybdenum concentrations in waters draining the Endako deposit were substantially higher than the average background concentrations in freshwater systems in the United States (appendix 2); some concentrations were greater than 32 µg/L molybdenum. Samples upstream from mining activity also have elevated molybdenum concentrations, with values ranging from 10 to 340 µg/L molybdenum; mine-impacted waters contain 1,460–24,600 µg/L molybdenum (appendix 2) (Mathieu, 1995).

Wanty and others (2003) indicated that waters draining calc-alkaline porphyry molybdenum deposits in the western United States commonly have concentrations of aluminum, cadmium, copper, iron, lead, manganese, and zinc that exceed U.S. Environmental Protection Agency (USEPA) drinking water limits and concentrations of cadmium, copper, lead, and zinc that exceed water-hardness adjusted USEPA chronic and acute aquatic ecosystem criteria (U.S. Environmental Protection Agency, 2006; 2009). The major-element chemistry of such drainage waters generally is dominated by calcium or magnesium. The dominant anion is sulfate because of the weathering of the sulfide minerals of the deposit (Wanty and others, 2003).

Tuttle and others (2002) noted that the overall metal concentrations and pH of stream water did not change after flowing over an undisturbed section of the Buckingham molybdenum-rich porphyry copper deposit in Nevada. For example, the pH of a seep within the deposit boundary was 4.0 (appendix 2). Stream-water pH was between 7.6 and 8.4 along the stream's length, which includes areas upstream and downstream from the deposit boundary (appendix 2). Molybdenum concentrations were higher in the stream water than the seep water because the higher pH of the stream inhibited adsorption of dissolved molybdenum onto Fe-oxides (Tuttle and others, 2002).

Data from the undeveloped Cannivan Gulch and Buckingham deposits (appendix 2) represent the most comprehensive dataset for waters associated with arc-related porphyry molybdenum and molybdenum-rich porphyry copper deposits, respectively. Samples from both areas include those collected where no obvious mining-related disturbances are present upstream. Dissolved molybdenum concentrations increase with increasing sulfate concentrations at both sites; Buckingham samples contain an order of magnitude more sulfate than Cannivan Gulch waters (fig. 17*A*). All Cannivan Gulch samples and most Buckingham samples are near-neutral in pH (fig. 17*B*). Dissolved molybdenum concentrations in some samples where no obvious mining-related disturbances are present exceed the drinking water guideline of 70 µg/L (World Health Organization, 2008).

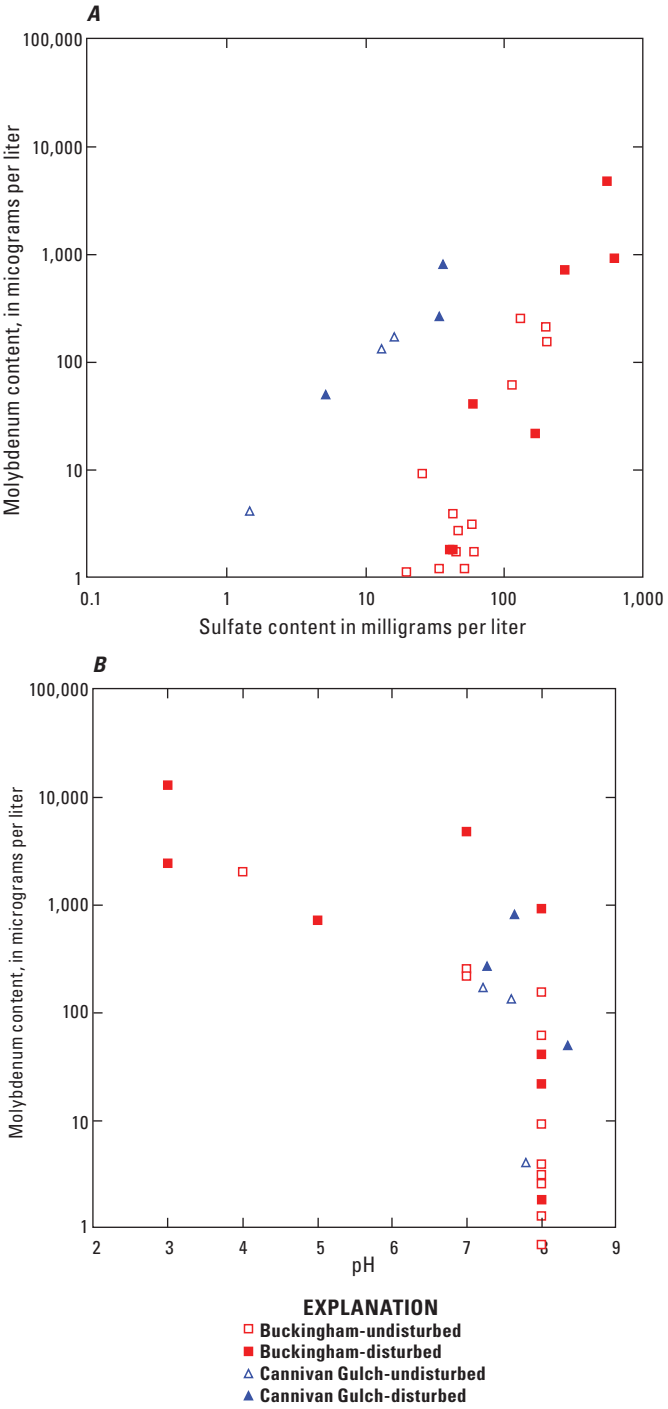

Figure 17. Concentrations of dissolved molybdenum in waters associated with the Cannivan Gulch, Mont. arc-related porphyry molybdenum deposit and the Buckingham, Nev. molybdenum-rich porphyry copper deposit for comparison, as a function of (*A*) sulfate concentration and (*B*) pH.

Past and Future Mining Methods and Ore Treatment

Most arc-related porphyry molybdenum deposits are presently mined by open-pit methods. However, early underground workings and later open pits are present at many sites. Ore is crushed on site and ground with added water using single semiautogenous (SAG) grinding mills with screens and ball mills. Mill output is passed to flotation cells after small amounts of reagents are added. The reagents include frothers, collectors to promote adherence of molybdenite to the air bubbles, and depressants to decrease the tendency of unwanted minerals to adhere to the air bubbles. Any trace copper would

be depressed. The molybdenite-laden froth is skimmed off the top and the waste material (tailings) is drawn from the bottom. The concentrate is then thickened and filtered to remove moisture and then shipped to offsite refineries (Hesse and Ellis, 1995).

At the Endako mine, the molybdenum sulfide recovered from flotation is roasted in a multi-hearth roaster to produce molybdic oxide (MoO_3), and the sulfur dioxide removed during roasting is collected, neutralized with tailings, and stored in the tailings pond. If the sulfide concentrate contains greater than 0.05 percent Pb or Bi, then it is passed through a leaching circuit before roasting to reduce the concentrations of these metals (Bysouth and Wong, 1995). At the Kitsault mine, Nokes reagent was added to the grinding and flotation stages and the final concentrate was leached with hot hydrochloric acid to produce a material that contained less than 0.02 percent Pb (Hodgson, 1995). Thompson Creek is a conventional open-pit mine that produces a molybdenite concentrate through crushing, grinding, and flotation. Tailings are floated to remove pyrite as a concentrate, which is pumped to subaqueous deposition in a tailings pond to prevent oxidation and acid generation. The methods for on-site processing are documented by Roscoe and others (2007). Rougher concentrate is processed through a series of cleaner flotation columns to produce different grades of product. Undersize material is dewatered and batch leached with hot ferric chloride to remove lead, copper, and uranium. Leach slurry is filtered and dried; filtrate is neutralized and discarded as tailings. Wet scrubbers process off-gases from driers before discharging to the atmosphere. Tailings are stored in a center line construction dam. The introduction of a pyrite circuit reduced acid-rock drainage on the downstream dam face and resulted in improved water quality in dam seepage of 300 to 4,200 liters per minute depending on the season.

Volume of Mine Waste and Tailings

The tonnages of tailings are essentially the same as the tonnages of the deposits, because of the low volumes of ore minerals. Waste to ore ratio for the life of the Boss Mountain mine, for example, was 1:1 (Macdonald and others, 1995). At full mill production, the Thompson Creek mine in Idaho produces about 5.7 million cubic meters of tailings each year.

The Quartz Hill deposit has not been mined, but it is estimated that, if developed, production could reach 72,600 tonnes per day, creating an open pit approximately 3.2 km by 2 km with a depth of as much as 570 m. Peak tailings disposal could reach 72,500 dry tonnes per day and average 63,400 tonnes per day. During a proposed 55-year life of the mine, nearly 1.4 billion tonnes of tailings could be generated (Hesse and Ellis, 1995). The volume of waste material would approximate 1 tonne of waste per tonne of ore mined.

Waste generated from the pit at the Kitsault mine amounted to 177 million tonnes, with the waste to ore stripping ratio ranging from 1 to 1.9 (Hodgson, 1995). From April 1981 to November 1982, 12,000 tonnes per day of tailings (4.38 million tonnes annually) were produced at Kitsault and were disposed in a nearby fjord by way of submarine tailings discharge (Odhiambo and others, 1996).

Mine Waste Characteristics

Chemistry

Pilot plant milling tests were done on ore from the Quartz Hill deposit. These pilot tests were done to not only determine optimal mill design and establish ore recovery values, but to characterize the waste produced. The concentrations of metals in concentrator tailings are well below USEPA environmental guidelines for the remediation of soils at contaminated sites and many elements, including chromium, copper, iron, manganese, nickel, selenium, and zinc, are present in concentrations near or below the average for the continental crust (table 8) (Hesse Associates, 1993; Hesse and Ellis, 1995). Metal concentrations that are higher than those reported for the continental crust include arsenic, cadmium, lead, molybdenum, and silver. The proposal for a mine suggests tailings could be disposed of in a submarine basin so the USEPA remediation guidelines may not be applicable (Hesse Associates, 1993; Hesse and Ellis, 1995).

Tailings from the Kitsault mine were deposited into a submarine basin on the bed of a fjord, similar to what was proposed as an option for the Quartz Hill tailings. The composition of tailings from Kitsault is similar to that reported for the test tailings from Quartz Hill (table 8). The concentrations of cadmium, lead, molybdenum, and zinc in the Kitsault tailings were substantially higher than reported for natural sediments in a nearby river and for the average composition of continental crust (Pedersen and others, 1995; Odhiambo and others, 1996). Representative composite assays of rougher tailings from the Thompson Creek mine (1991 data) contained 0.009 percent Mo, 0.002 percent Cu, and 0.002 percent Pb (U.S. Environmental Protection Agency, 1992).

Acid-Base Accounting

As previously discussed in the Weathering/Supergene Processes section, pyrite can produce acid upon oxidation and any late calcite commonly occurring as veins can neutralize the acid. The sum of these two processes is expressed as the net neutralization potential of a material. Macdonald and others (1995) stated that tailings from the Boss Mountain mine are nonacid generating. In contrast, at the Thompson Creek mine (U.S. Environmental Protection Agency, 1992), sulfur content of some intrusive rocks reached 1.13 per cent, representing minor acid-generating potential. At Thompson Creek, eight samples of intrusive rocks had neutralization potential/acid production potential (NP/AP) ranging from 0.63:1 to 6.85:1. These values span the range from marginally acid-generating to nonacid generating. Samples of 76 volcanic

Table 8. Concentrations of elements in mine waste from arc-related porphyry molybdenum deposits.

[Elemental abbreviations: Ag, silver; As, arsenic; Cd, cadmium; Cr, chromium; Cu, copper; Fe, iron; Hg, mercury, Mn, manganese; Mo, molybdenum; Ni, nickel; Pb, lead; Se, selenium; Zn, zinc. ppm, parts per million; nd, no data; <, less than; ~, approximately; n, number of samples; ±, plus or minus]

Deposit	Description	Ag (ppm)	As (ppm)	Cd (ppm)	Cr (ppm)	Cu (ppm)	Fe (ppm)	Hg (ppm)	Mn (ppm)	Mo (ppm)	Ni (ppm)	Pb (ppm)	Se (ppm)	Zn (ppm)	Reference
Quartz Hill, Alaska	Pilot test tailings[1]	0.13	10.9	2.4	10	69		0.05	462	120	17.7	47	0.1	46	U.S. Forest Service, 1988, in Hesse and Ellis, 1995
Quartz Hill, Alaska	Pilot test tailings[1]	nd	nd	nd	nd	10	9,400–21,300	nd	nd	46–142	nd	3–22	nd	17–42	U.S. Borax, 1982, in Hesse Associates, 1993
Quartz Hill, Alaska	Pilot test tailings	nd	<0.2	0.3	nd	40	10,000	nd	nd	160	26	30	nd	18	U.S. Borax, 1982, in Hesse Associates, 1993
Quartz Hill, Alaska	Pilot test tailings	nd	<5.0	<1.0	nd	20	10,000	nd	100	120	20	20	nd	<20	U.S. Borax, 1982, in Hesse Associates, 1993
Quartz Hill, Alaska	Pilot test tailings	nd	nd	nd	nd	22	14,900	nd	nd	62	nd	11	nd	30	U.S. Borax, 1982, in Hesse Associates, 1993
Quartz Hill, Alaska	Pilot test tailings	nd	0.61	0.5	nd	29.9	nd	nd	374	60.3	9.8	5.6	nd	20.1	U.S. Borax, 1982, in Hesse Associates, 1993
Kitsault mine, British Columbia, Canada	Tailings	nd	nd	~9	nd	nd	nd	nd	nd	95	nd	52	nd	314	Pendersen and others, 1995
Kitsault mine, British Columbia, Canada	Tailings (n=16)	nd	nd	16.2±11.2	nd	56.3±25	19,500±4,800	nd	365±170	nd	nd	174±60	nd	441±178	Odhiambo and others, 1996
Kitsault mine, British Columbia, Canada	Tailings (n=3)	nd	nd	10.8±2.7	nd	65±20	28,000±3,500	nd	998±280	nd	nd	371±230	nd	385±59	Odhiambo and others, 1996
White Cloud, Idaho	Mine waste[2]	<2	310	<2	61	31	73,000	2.6	910	1,500	21	250	4.1	430	Giles and others, 2009
Thompson Creek, Idaho	Tailings	nd	nd	nd	nd	20	nd	nd	nd	90	nd	nd	nd	nd	U.S. Environmental Protection Agency, 1992
Human health guideline	Residential soil	390	23	70	280	31,00	55,000	6.7	1,800	390	1,600	400	390	23,000	U.S. Environmental Protection Agency, 2008
Human health guideline	Industrial soil	5,100	160	810	1,400	41,000	7,200,000	28	23,000	5,100	20,000	800	5,100	310,000	U.S. Environmental Protection Agency, 2008
Continental crust	Average composition	0.08	1	0.098	185	75	70,600	nd	1,400	1	105	8	0.05	80	Taylor and McLennan, 1985

[1]Average of multiple samples.

[2]Orange to reddish to bright orange mine waste; collected fine (<2 mm) fraction from uppper 0.5 inch in surface layer; calcite and sulfides observed in mine waste.

rocks had NP/AP greater than 31:1 and samples of metasedimentary rocks were considered non-acid-forming (NP/AP greater than 3:1). The average NP/AP value for all tailings reported in 1991 was 0.84:1. For the proposed mining of the Quartz Hill deposit, acid producing waste rocks would be blended with waste materials that are acid consuming to prevent the formation of acid drainage from mine dumps (if not disposed of by submarine methods) (Hesse and Ellis, 1995).

Metal Mobility Related to Mining in Groundwater, Surface Water, and Soil

Molybdenum is more mobile in alkaline environments than in acidic environments, in contrast to the behavior of copper and other metals, which are precipitated as, or sorbed onto, hydroxides at high pH. The soluble molybdate anion, MoO_4^{2-}, is stable at neutral and moderately alkaline pH, and is readily transported in near-neutral surface and groundwaters. Molybdate is the principal stable species in most natural water conditions.

The average molybdenum concentration in surface waters of North America is about 1 µg/L (Hem, 1985). Molybdenum concentrations in Canadian natural freshwaters range from less than 0.1 µg/L to 500 µg/L (MEND, 2008). Groundwater molybdenum concentrations in Canada range from less than 0.1 µg/L to greater than 1,000 µg/L, depending on location and geology (MEND, 2008). Groundwaters near molybdenum mines in Canada and the United States may have elevated molybdenum concentrations (greater than 2,000 µg/L). For example, mine-impacted surface waters near the Endako mine contain between 1,460 and 24,600 µg/L molybdenum (Mathieu, 1995) (appendix 2).

Surface waters in tailings ponds and main drainages at the Thompson Creek mine had pH values ranging from 5.2 to 8.7, with maximum concentrations of 14 µg/L cadmium, 160 µg/L lead, 1.00 µg/L mercury, 9.0 µg/L selenium, 9,400 µg/L iron, 124 µg/L zinc, and 1,220 µg/L aluminum. For 10 years after the shutdown of the Boss Mountain mine, waters draining the site contained concentrations of metals that were within permitted levels (Macdonald and others, 1995). Waste-rock seepage at the Kitsault porphyry molybdenum deposit in British Columbia, Canada has pH ranging from 3 to 8, sulfate concentrations between 1 and 1,000 milligrams per liter (mg/L), aluminum concentrations between 0.01 and 2 mg/L, manganese concentrations between 0.01 and 1 mg/L, iron concentrations between 0.02 and 5 mg/L, and zinc concentrations between 0.005 and 0.2 mg/L (Day and Rees, 2006).

Mine-impacted soils near the Endako mine contain between 2.3 and 258 ppm molybdenum (appendix 2). Molybdenum concentrations decreased in soils with increasing distance from streams that receive drainage from the mine; the highest molybdenum concentration (258 ppm) was found within 5 meters, whereas the lowest molybdenum concentrations (2.3 ppm) was found 10 to 15 meters from a mine-impacted stream. Molybdenum concentrations also decrease with increasing distance from the mine site (Mathieu, 1995).

Pit Lakes

Limited data are available on flooded pits from mining arc-related porphyry molybdenum deposits. The pH of pit water is generally near-neutral to alkaline (appendix 2). The Denak East Pit at the Endako mine contains low concentrations of copper (2 to 5 µg/L), but substantial molybdenum concentrations (16.4 to 49 mg/L) (Mathieu, 1995).

Ecosystem Issues

Aquatic ecosystem threats are presented mainly by the acid-generating potential of the mine waste, which also relates to the potential mobility of trace metals. The oxidative weathering of pyrite (FeS_2) is described by reactions 1 to 4 in the Weathering/Supergene Processes section. The lower pH values generated by the oxidation of pyrite enhance the solubility of base metals, such as cadmium, cobalt, copper, lead, nickel, and zinc, and the ability for waters to attack silicate-gangue minerals, thus liberating aluminum, iron, and manganese. Most metals have greater solubility at lower pH values; however, aluminum and ferric iron have solubility minimums at near-neutral pH values, with greater solubility at lower and higher pH. Once liberated, the metals and acidity can affect downstream aquatic ecosystems. Metal contamination also can be dispersed downstream by the erosion and transport of tailings, which subsequently release metals to the water column.

The toxicity of cadmium, chromium, copper, lead, nickel, silver, and zinc to aquatic ecosystems is dependent on water hardness; higher concentrations of metals are needed to exceed toxicity limits at higher hardness values (U.S. Environmental Protection Agency, 2006). Hardness is a measure of the concentrations of calcium and magnesium. The concentration of hardness is expressed in terms of an equivalent concentration of $CaCO_3$, typically in mg/L. The USEPA provides hardness-dependent levels for acute (1-hour exposure) and chronic (4-day exposure) toxicity, and toxicity limits independent of hardness for cyanide, aluminum, antimony, arsenic, iron, mercury, selenium, and thallium (U.S. Environmental Protection Agency, 2006; table 9).

There are no National water-quality criteria for molybdenum. Nevada uses a water-quality standard of 19 µg/L for protection of aquatic life, based on toxicity data from around 1980 on long-term effects on rainbow trout, narrow-mouthed toad, *Daphnia magna* (an aquatic macroinvertebrate), and the ambient national background level of molybdenum in surface waters of the United States (Nevada Division of Environmental Protection, 2008). Canada freshwater criterion for the protection of aquatic life is 73 µg/L molybdenum and is based on chronic toxicity for rainbow trout with an order of magnitude scale factor (MEND, 2008). This criterion is based on 28-day bioassay tests on fertilized rainbow trout eggs by Birge (1978) and Birge and others (1980), who documented effective concentrations of 0.73 and 0.79 mg/L, respectively. However, numerous subsequent studies (Davies and others,

Table 9. Environmental guidelines relevant to mineral deposits.

[Elemental abbreviations: Al, aluminum; As, arsenic; Cd, cadmium; Cr, chromium; Cu, copper; Fe, iron; Hg, mercury; Mn, manganese; Mo, molybdenum; Ni, nickel; Pb, lead; Se, selenium; U, uranium; Zn, zinc. ppm, parts per million; mg/L, milligrams per liter; µg/L, micrograms per liter; USEPA, U.S. Environmental Protection Agency; WHO, World Health Organization; nd, no data; $CaCO_3$, calcium carbonate]

Element	Human health				Aquatic ecosystem	
Media	Residential soil	Industrial soil	Drinking water	Drinking water	Acute toxicity	Chronic toxicity
Units	ppm	ppm	mg/L	mg/L	µg/L	µg/L
Source	USEPA	USEPA	USEPA	WHO	USEPA	USEPA
Al	77,000	990,000	200	nd	750	87
As	23	160	10	10	340	150
Cd	70	810	5	3	2*	0.25*
Cr	280	1,400	100	50	570*	74*
Cu	3,100	41,000	1,300	2,000	13*	11*
Fe	55,000	720,000	300	nd	nd	1,000
Hg	6.7	28	2	6	1.4	0.77
Mn	1,800	23,000	50	400	nd	nd
Mo	390	5,100	nd	70	nd	nd
Ni	1,600	20,000	nd	70	470*	52*
Pb	400	800	15	10	65*	2.5*
Se	390	5,100	50	10	nd	5
U	230	3,100	nd	15	nd	nd
Zn	23,000	310,000	5,000	nd	120*	120*

*Hardness-dependent water-quality standards; value is based on a hardness of 100 mg/L $CaCO_3$.

2005) failed to document such low effective concentrations, but instead documented effective concentrations on fertilized eggs greater than or equal to 90 mg/L. Furthermore, acute lethal effective concentrations for a variety of fish species are high, ranging from 70 to greater than 2,000 mg/L molybdenum (Davies and others, 2005). Likewise, Schamphelaere and others (2010) proposed a median hazardous concentration affecting 5 percent of the test organisms at 38.2 mg/L molybdenum, based on chronic bioassay tests on several organisms including aquatic invertebrates, fish, and plants.

Terrestrial Ecosystems

Plants are capable of tolerating high concentrations of molybdenum in their tissues and toxicity from high molybdenum has not been reported for field-grown plants (Gupta and Lipsett, 1981). Molybdenum is an essential trace element for plants; tissue concentrations of about 0.03 to 0.15 ppm are generally needed to meet physiological requirements (Jarrell and others, 1980). Plants growing in near-neutral to alkaline (pH greater than 6.5) soils typically are enriched in molybdenum relative to plants growing in acidic (pH less than 5.5) soils (Hansuld, 1966; McGrath and others, 2010a). Yields of crops can be affected by high molybdenum concentrations; however, soil-water molybdenum concentrations appear to be a better predictor of reduced yields, suggesting that the relation of soil chemistry to molybdenum mobility is a primary factor controlling toxicity to plants (McGrath and others, 2010b). Molybdate in solution may be released as part of high-pH flotation mill effluent (Le Gendre and Runnells, 1975). In contact with weathering pyrite-bearing tailings, however, water pH decreases may result in molybdenum coprecipitation or sorption on iron oxyhydroxide (Ludington and others, 1995). A study of the algal community in surface waters affected by drainage from the Endako mine suggests that the community was not affected by mine water discharge or tailings seepages, and the high molybdate did not affect the algal growth (Mathieu, 1995).

Although not substantially toxic to plants, high molybdenum concentrations can cause molybdenosis in ruminant animals, a type of molybdenum toxicity that results in a copper deficiency, particularly in cattle and sheep, when they consume molybdenum-rich forage. Molybdenum reacts with sulfur in the rumen to form thiomolybdate complexes that render copper biologically unavailable (Gould and Kendall, 2011). Wildlife, particularly moose, and domestic animals feeding on plants growing on lands with elevated molybdenum may be at risk for molybdenosis where waste rock has been treated with alkaline material such as lime, which can exacerbate molybdenum mobility (Ward, 1978; Gardner and others, 1996; Majak and others, 2004; MEND, 2008). The overall Cu:Mo ratio in vegetation may be more indicative of potential nutritional problems in animals than total molybdenum concentrations. Mathieu (1995) stated that Cu:Mo ratios of below 2:1 may be problematic. Background and mine-impacted vegetation in the Endako mine region all have Cu:Mo ratios below 2:1 (Mathieu, 1995). Despite the low Cu:Mo ratios, no field evidence of molybdenosis in small mammals or larger wildlife, such as moose or deer, has been noted at the Endako mine (Mathieu, 1995; Riordan, 2003).

Aquatic Ecosystems

Many studies indicate that there is little to no risk to aquatic organisms from elevated molybdenum in water, even for concentrations on the order of several tens to hundreds of mg/L (MEND, 2008). For example, trout released into a pit lake at the Endako mine and recaptured after 3 and 14 months

(see appendix table 2 for pit lake chemistry) indicated that concentrations averaging 33 mg/L molybdenum did not have chronic toxicity effects (Mathieu, 1995). In contrast to trout, the stream macroinvertebrate community was affected by tailings seepage in surface waters near the Endako mine, with communities shifting toward more pollution-tolerant organisms compared to background sites (Mathieu, 1995). Overall, there is some variability in estimates of molybdenum toxicity to the aquatic ecosystem and, therefore, this is best evaluated on a site-specific basis (MEND, 2008).

Ecosystem issues also can arise from submarine tailings disposal. This was the method of tailings disposal at the Kitsault mine in British Columbia and has been proposed for the Quartz Hill deposit in Alaska. Potential ecosystem issues concerning submarine disposal of tailings at these types of sites include (1) effects to the spawning and rearing habitat for salmon, trout, and other fish; (2) changes to the habitat of Dungeness and tanner crabs, shrimp, and other marine invertebrates; and (3) effects on marine plants that are the food source for higher animals in the food chain (Goerold and Mehrkens, 1992). The postmining ecological effect of depositing tailings from the Kitsault mine into the Alice Arm was evaluated from 1982 to 1990. No bioaccumulation of metals occurred in the monitored benthic marine species (Hodgson, 1995). Postmining studies determined no effect to the water column community (Anderson, 1986; Mackas and Anderson, 1986) or the crab fishery (Jewett and others, 1985; Sloan, 1985; Sloan and Robinson, 1985). Minor trace metal bioaccumulation was documented in mussels and clams.

The Quartz Hill site is surrounded by wilderness lands of the Misty Fiords National Monument, where commercial and sport fishing is the predominant activity. Pilot test tailings were produced from Quartz Hill ore and used for toxicity testing. Sublethal tailings concentrations did not affect the growth and development of crab zoea within a 30-day exposure period. Also, the tailings had no demonstrable effect on clam burrowing behavior during a 16-week period and metals were not bioaccumulated by fish, clams, or crabs within a 4-month exposure period (Mitchell and others, 1984). A low-level of acute lethal toxicity was observed based on mussel larvae; the toxicity was because of an interaction of a number of constituents and could not be accounted for by manganese and molybdenum alone. Overall, the study indicated that the tailings had a relatively low toxicity (Mitchell and others, 1984).

Despite the low toxicity of the tailings based on pilot tests at Quartz Hill and ecosystem monitoring at the Kitsault mine, other potential effects from the submarine deposition of the tailings include changes in circulation and in bottom habitat because of the escape of fine sediments, changes to productivity from suspended sediments in the upper water column, and smothering effects to marine life from reduced dissolved oxygen (Hesse and Ellis, 1995). Postclosure monitoring at the Kitsault mine submarine disposal site did indicate recovery of the benthos after closure and thereafter parallel changes in benthos in tailings areas and areas without tailings (Pedersen and others, 1995). The maximum concentrations found in surface-water quality of seepage from waste-rock piles at Kitsault described above (Day and Rees, 2006) exceed acute criteria for aquatic organisms for aluminum, cadmium, lead, and zinc and the chronic criterion for iron (table 9).

Human Health Issues

Insoluble molybdenum compounds, such as MoS_2 (molybdenite), are nontoxic. Molybdenum is an essential element with relatively low toxicity (Barceloux, 1999). The tolerable daily intake level of 0.009 mg Mo/kg/day for humans, based on toxicological risk analysis, is more than twice the upper limit of adequate dietary intake in the United States (Vyskocil and Viau, 1999). Industrial occupational exposure to dust and fumes of soluble molybdenum trioxide and molybdates constitute greater hazards to human health than exposure to MoS_2, although no accidental deaths because of industrial molybdenum poisoning have been reported. Cattle and sheep are more susceptible than humans to molybdenum poisoning because of chronic exposure. Occupational standards for molybdenum exposure for the United States, as set by the Occupational Safety and Health Administration (OSHA), are 5 milligrams per cubic meter (mg/m^3) for soluble molybdenum compounds and 15 mg/m^3 for insoluble molybdenum compounds (www.osha.gov/index.html). Regulatory limits for industrial and environmental human exposure to molybdenum compounds are variable from country to country. The International Molybdenum Association website (2009) provides a list of regulatory limits, summaries of toxicological studies, and references on molybdenum in human health.

The maximum concentrations found in surface-water quality of seepage from waste-rock piles at Kitsault described above (Day and Rees, 2006) exceed several drinking water standards. Primary maximum contaminant limits (MCLs), which protect human health, are locally exceeded for cadmium and lead (table 9). Secondary drinking water standards, which address the aesthetic qualities of water (color, odor, taste) are locally exceeded for pH, sulfate, aluminum, iron, and manganese.

Climate Effects on Geoenvironmental Signatures

The release of metals from minerals to the environment is a function of weathering. Climate controls physical and chemical weathering. Chemical weathering is rapid in warm, humid climates. Weathering rates are lowest in desert and cold climates. Variations in the amount of precipitation and rates of evapotranspiration are important controls on weathering. The environmental effects associated with sulfide-rich mineral deposits typically are greater in wet climates than in dry climates because pyrite oxidizes more rapidly in humid climates. Evaporative concentration of metals and acidity in mine effluents can store metals and acidity in highly soluble sulfate minerals, which can be released to local watersheds during rainstorms or snowmelt following a dry spell. However,

minimal surface-water flow in dry climates inhibits generation of substantial volumes of acid-rock drainage (Ludington, 1995). Climate plays an important role in groundwater discharge to and recharge from streams and water table levels. Alternating wet and dry seasons provide intermittent flushing and removal of soluble weathering products; aridity promotes preservation of supergene products.

Knowledge Gaps and Future Research Directions

A major question remains as to what factors create productive intrusions and how this differs from barren systems. Do arc-related porphyry molybdenum deposits require specialized magma genesis beyond what is common above subduction zones? If so, are there favorable tectonic scenarios, such as slab gaps or slab windows, or favorable subduction angles? Do the cogenetic intrusions have inherently high concentrations of metals and volatiles, or do they have unique crystallization and degassing processes? Are specific regional structures required in controlling the emplacement of productive intrusions? Is interaction with continental crust necessary, or does a thick overburden simply help the primitive magma stall in the crust where it can evolve to the necessary chemical composition? Detailed geochemical, geophysical, fluid inclusion, and alteration studies are lacking, which inhibits detailed discussion on genetic differences between porphyry copper deposits, barren intrusions, and arc-related porphyry molybdenum deposits.

Numerous molybdenum deposits exist throughout the world, but are not classified into either of the molybdenum porphyry deposit models. Improved geological, geochemical, and tectonic information is needed to classify these deposits. Future classification will add to our understanding of the characteristics and genesis of arc-related porphyry molybdenum deposits, and may alter our ideas of grade and tonnage features.

Improving our knowledge of physical and chemical gradients within and adjacent to the deposits are of importance. This will help exploration geologists to vector in toward mineralization and aid in the discovery of more deposits.

One of the most important questions regarding molybdenum deposits, which still remains to be answered, is why are they so concentrated in the western cordillera of North America? If porphyry molybdenum deposits are emplaced at slightly greater depths than porphyry copper deposits, can future geologists expect to find molybdenum deposits through progressive erosion of the Andes in South America? Why are subduction-related porphyry copper deposits so prevalent throughout the world, but arc-related porphyry molybdenum deposits that form in the same tectonic environment so much more spatially restricted?

Acknowledgments

The first author would like to thank Jim Bliss (U.S. Geological Survey) and Bob Kamilli (U.S. Geological Survey) for their informative discussions on porphyry molybdenum deposits. Jim has worked tirelessly on creating deposit worksheets that include grades and tonnages for molybdenum deposits throughout the world, whereas Bob has worked on the alkali-feldspar rhyolite-granite porphyry molybdenum model. Eric Anderson (U.S. Geological Survey) offered insight and advice on the geophysics section of this model. Discussions with Cliff Taylor (U.S. Geological Survey) regarding deposits within the United States were useful. Dave Sinclair (Geological Survey of Canada–retired), Steve Ludington (U.S. Geological Survey), and Rich Goldfarb (U.S. Geological Survey) all provided helpful reviews that improved the manuscript in many ways.

References Cited

Anderson, E.P., 1986, Lethal and sublethal effects of a molybdenum mine tailings on marine zooplankton—Mortality, respiration, feeding, and swimming behavior in *Calanu marshallae, Metridia pacifica* and *Euphausia pacifica*: Marine Environment and Resources, v. 19, p. 131–155.

Arehart, G.B., Smith, J.L., and Pinsent, R., 2006, New models for mineral exploration in British Columbia—Is there a continuum between porphyry molybdenum deposits and intrusion-hosted gold deposits?: British Columbia Ministry of Energy, Mines, and Petroleum Resources, Geological Fieldwork paper 2007–1, 4 p.

Armstrong, R.L., Hollister, V.F., and Harakal, J.E., 1978, K-Ar dates for mineralization in the White Cloud-Cannivan porphyry molybdenum belt of Idaho and Montana: Economic Geology, v. 73, p. 94–96.

Ashleman, J.C., Taylor, C.D., and Smith, P.R., 1997, Porphyry molybdenum deposits of Alaska, with emphasis on the geology of the Quartz Hill deposit, southeastern Alaska: Economic Geology Monograph 9, p. 334–354.

Atkinson, D., 1995, The Glacier Gulch (Hudson Bay Mountain or Yorke-Hardy) porphyry molybdenum-tungsten deposit, west-central British Columbia, *in* Schroeter, T.G., ed., Porphyry deposits of the northwestern cordillera of North America: Special Volume 46, Canadian Institute of Mining, Metallurgy, and Petroleum, p. 704–707.

Ayres, L.D., Averill, S.A., and Wolfe, W.J., 1982, An Archean molybdenite occurrence of possible porphyry type at Setting Net Lake, northwestern Ontario, Canada: Economic Geology, v. 77, p. 1,105–1,119.

Barceloux, D.G., 1999, Molybdenum: Clinical Toxicology, v. 37, no. 2, p. 231–237.

Bard Ventures news release, 2009, Lone Pine Molybdenum 43–101 Resource Estimate Completed Measured + Indicated 110,340,000 tonnes Grading 0.083% Mo, news release January 13, 2009: *http://www.bardventures.com/s/NewsReleases.asp?ReportID=334201*, accessed February 2011.

Beane, R.E., 1983, The magmatic-hydrothermal transition: Geothermal Resources Council Special Report 13, p. 245–253.

Berger, B.R., Breit, G.N., Siems, D.F., Welsch, E.P., and Speckman, W.S., 1979, A geochemical survey of mineral deposits and stream deposits in the Eastern Pioneer wilderness study area, Beaverhead County, Montana: U.S. Geological Survey Open-File Report 79–1079, 128 p.

Birge, W.J., 1978, Aquatic toxicology of trace elements of coal and fly ash, *in* Thorp, J.H., and Gibbons, J.W., eds., Energy and environmental stress in aquatic systems: Department of Energy Symposium Series, CONF 771114.

Birge, W.J., Black, J.A., Westerman, A.G., and Hudson, J.E., 1980, Aquatic toxicity tests on inorganic elements occurring in oil shale, *in* Gale, C., ed., Oil shale symposium—Sampling, analysis and quality assurance: National Technical Information Service, Springfield, Virginia, EPA–600/9–80–022, p. 519–534.

Bloom, M.S., 1981, Chemistry of inclusion fluids—Stockwork molybdenum deposits from Questa, New Mexico, and Hudson Bay Mountain and Endako, British Columbia: Economic Geology, v. 76, p. 1,906–1,920.

Bodnar, R.J., 1995, Fluid-inclusion evidence for a magmatic source for metals in porphyry copper deposits, *in* Thompson, J.F.H., ed., Magmas, fluids, and ore deposits: Mineralogical Association of Canada short course series, v. 23, p. 139–152.

Bookstrom, A.A., Carten, R.B., Shannon, J.R., and Smith, R.P., 1988, Origins of bimodal leucogranite-lamprophyre suites, Climax and Red Mountain porphyry molybdenum systems, Colorado—Petrologic and strontium isotopic evidence: Colorado School of Mines Quarterly, v. 83, no. 2, p. 1–24.

Boyle, H.C., and Leitch, C.M.B., 1983, Geology of the Trout Lake molybdenum deposit: Canadian Mining and Metallurgical Bulletin, v. 76, no. 849, p. 115–124.

Brew, D.A., Johnson, B.R., Grybeck, D., Griscom, A., Barnes, D.F., Kimball, A.L., Still, J.C., and Rataj, J.L., 1978, Mineral Resources of Glacier Bay National Monument wilderness study area, Alaska: U.S. Geological Survey Open File Report 78–494, 670 p.

Bright, M.J., and Jonson, D.C., 1976, Glacier Gulch (Yorke-Hardy), *in* Sutherland Brown, A., ed., Porphyry deposits of the Canadian cordillera: Special Volume 15, Canadian Institute of Mining, Metallurgy, and Petroleum, p. 455–461.

British Columbia Geological Survey, minfile 082KNW087: Ministry of Energy, Mines and Petroleum Resources, 5 p., accessed February 2012.

British Columbia Geological Survey, minfile 082JW 005: Ministry of Energy, Mines and Petroleum Resources, 3 p., accessed February 2012.

British Columbia Geological Survey, minfile 093K 006: Ministry of Energy, Mines and Petroleum Resources, 5 p., accessed February 2012.

British Columbia Geological Survey, minfile 103P 120: Ministry of Energy, Mines and Petroleum Resources, 4 p., accessed February 2012.

British Columbia Geological Survey, minfile 103P 234: Ministry of Energy, Mines and Petroleum Resources, 3 p., accessed February 2012.

Brown, P., and Kahlert, B., 1995, Geology and mineralization of the Red Mountain porphyry molybdenum deposit, south-central Yukon, *in* Schroeter, T.G., ed., Porphyry deposits of the northwestern cordillera of North America: Special Volume 46, Canadian Institute of Mining, Metallurgy, and Petroleum, p. 747–756.

Burmistrov, A.A., Ivanov, V.N., and Frolov, A.A., 1990, Structural and mineralogical types of molybdenum-tungsten deposits of central Kazakhstan: International Geology Review, v. 32, p. 92–99.

Burnham, C.W., 1997, Magmas and hydrothermal fluids, *in* Barnes, H.L., ed., Geochemistry of hydrothermal ore deposits—3rd ed.: New York, N.Y., John Wiley & Sons, p. 63–123.

Burnham, C.W., and Ohmoto, H., 1980, Late-stage processes of felsic magmatism: Mining Geology Special Issue, no. 8, p. 1–11.

Bysouth, G.D., and Wong, G.Y., 1995, The Endako molybdenum mine, central British Columbia—An update, *in* Schroeter, T.G., ed., Porphyry deposits of the northwestern cordillera of North America: Special Volume 46, Canadian Institute of Mining, Metallurgy, and Petroleum, p. 697–703.

Candela, P.A., 1989, Magmatic ore-forming fluids—Thermodynamic and mass-transfer calculations of metal concentrations, *in* Whitney, J.A., and Naldrett, A.J., eds., Ore deposition associated with magmas: Reviews in Economic Geology, v. 4, p. 203–221.

Candela, P.A., 1992, Controls on ore metal ratios in granite-related ore systems—An experimental and computational approach: Transactions of the Royal Society of Edinburgh, Earth Sciences, v. 83, p. 317–326.

Candela, P.A., and Holland, H.D., 1986, A mass transfer model for copper and molybdenum in magmatic hydrothermal systems—the origin of porphyry-type ore deposits: Economic Geology, v. 81, p. 1–19.

Carten, R.B., Geraghty, E.P., Walker, B.M., and Shannon, J.R., 1988, Cyclic development of igneous features and their relation to high-temperature hydrothermal features in the Henderson porphyry molybdenum deposit, Colorado: Economic Geology, v. 83, p. 266–296.

Cathles, L.M., Erendi, A.H.J., and Barrie, T., 1997, How long can a hydrothermal system be sustained by a single intrusive event?: Economic Geology, v. 92, p. 766–771.

Changming, W., Qiuming, C., Shouting, Z., Jun, D., and Shuyun, X., 2008, Magmatic-hydrothermal superlarge metallogenic systems—A case study of the Nannihu ore field: Journal of China University of Geoscineces, v. 19, p. 391–403.

Chappell, W.R., Meglen, R.R., Moure-Eraso, R., Solomons, C.C., Tsonges, T.A., Walravens, P.A., and Winston, P.W., 1979, Human health effects of molybdenum in drinking water: Report number EPA–600/1–79–006, 101 p.

Chen, X., Qu, W., Han, S., Eleonora, S., Yang, N., Chen, Z., Zeng, F., Du, A., and Wang, Z., 2010, Re-Os geochronology of Cu and W-Mo deposits in the Balkhash metallogenic belt, Kazakhstan and its geological significance: Geoscience Frontiers, v. 1, p. 115–124.

Christiansen, E.H., and Wilson, R.T., 1982, Classification and genesis of stockwork molybdenum deposits—A discussion: Economic Geology, v. 77, p. 1,250–1,252.

Christie, Tony, and Brathwaite, Bob, 1995, Mineral commodity report 9—Molybdenum: New Zealand Mining, v. 18, p. 22–32.

Christopher, P.A., and Carter, N.C., 1976, Metallogeny and metallogenic epochs for porphyry mineral deposits, *in* Sutherland Brown, A., ed., Porphyry deposits of the Canadian cordillera: Canadian Institute of Mining, Metallurgy, and Petroleum, Special Volume 15, p. 64–71.

Clark, K.F., 1972, Stockwork molybdenum deposits in the western Cordillera of North America: Economic Geology, v. 67, p. 731–758.

Clark, J., and Baudry, P., 2011, Zuun Mod porphyry molybdenum-copper project, south-western Mongolia, Technical Report: Prepared for Erdene Resource Development Corp., 64 p. (Also available at *http://www.erdene.com/assets/pdf/ZuunMod43-101TechnicalReport_MinarcoJune2011.pdf*.)

Cobb, E.H., 1981, Summaries of data on and lists of references to metallic and selected nonmetallic mineral occurrences in the Mount Fairweather quadrangle, Alaska: Supplement to Open-File Report 78–316—part A–Summaries of data to January 1, 1980: U.S. Geological Survey Open-File Report 81–249A, 21p.

Cobb, E.H., and Elliot, R.L., 1980, Summaries of data on and lists of references to metallic and selected nonmetallic mineral deposits in the Ketchikan and Prince Rupert quadrangles, Alaska: U.S. Geological Survey Open-File Report 80–1053, 157 p.

Cook, S.J., 2000, Distribution and dispersion of molybdenum in lake sediments adjacent to porphyry molybdenum mineralization, central British Columbia: Journal of Geochemical Exploration, v. 71, p. 13–50.

Cope, G.R., and Spence, C.D., 1995, Mac porphyry molybdenum prospect, north-central British Columbia, *in* Schroeter, T.G., ed., Porphyry deposits of the northwestern cordillera of North America: Special Volume 46, Canadian Institute of Mining, Metallurgy, and Petroleum, p. 757–763.

Cox, D.P., and Singer, D.A., 1986, Mineral deposit models: U.S. Geological Survey Bulletin 1693, 379 p.

Darling, R.S., 1994, Fluid inclusion and phase equilibrium studies at the Cannivan Gulch molybdenum deposit, Montana, USA—Effect of CO_2 on molybdenite-powellite stability: Geochimica et Cosmochimica Acta, v. 58, p. 749–760.

Davies, T.D., Pickard, J., and Hall, K.J., 2005, Acute molybdenum toxicity to rainbow trout and other fish: Journal of Environmental Engineering and Science, v. 4, p. 481–485.

Day, S., and Rees, B., 2006, Geochemical controls on waste-rock dump seepage chemistry at several porphyry mines in the Canadian Cordillera, *in* Seventh International Conference on Acid Rock Drainage (ICARD) Proceedings, St. Louis, Mo., Lexington, Ky., American Society of Mining and Reclamation, p. 439–456.

Doebrich, J.L., Garside, L.J., and Shawe, D.R., 1996, Characterization of mineral deposits in rocks of the Triassic to Jurassic magmatic arc of western Nevada and eastern California: U.S. Geological Survey, Open-File Report 96–9, 107 p.

Downie, C.C., Pighin, David, and Price, Barry, 2006, Technical report for the Sphinx property: Accessed February 2011 at *http://www.eagleplains.ca/projects/bc/sphinx/2005_sphinx_43_101_may2006.pdf*.

Duke, C.P., 2007, Pidgeon Molybdenum project: Toronto, Ontario, Wardrop Engineering Inc., NI 34–101 Compliant Report for MPH Ventures Corporation, October 19, 2007, 92 p.

Eakins, G.R., Bundtzen, T.K., Robinson, M.S., Clough, J.G., Green, C.B., Clautice, K.H., and Albanese, M.D., 1983, Alaska's mineral industry 1982: Alaska Division of Geological and Geophysical Surveys Special Report 31, 68 p.

Elliot, R.L., Smith, J.G., and Hudson, Travis, 1976, Upper Tertiary high-level plutons of the Smeaton Bay area, southeastern Alaska: U.S. Geological Survey, Open-File Report 76–507, 15 p.

Fisher, Derek, 2009, Updated technical report Spinifex Ridge Mo-Cu deposit August 2009: Moly Mines Limited, 404 p., accessed February, 2011, at *http://www1.molymines.com/public/documents/4/5/NI43-101_MolyTechReport_FINAL_20090826.pdf*.

Ford, Ken, Keating, P., and Thomas, M.D., 2007, Overview of geophysical signatures associated with Canadian ore deposits, *in* Goodfellow, W.D., ed., Mineral deposits of Canada—A synthesis of major deposit-types, district metallogeny, the evolution of geological provinces, and exploration methods: Special Publication 5, Mineral Deposits Division, Geological Association of Canada, no. 5, p. 939–970.

Gardner, W.C., Popp, J.D., Quinton, D.A., Mir, Z., Mir, P.S., and Buckley, W.T., 1996, Animal response to grazing on reclaimed mine tailings, *in* Proceedings of the 20th Annual British Columbia Mine Reclamation Symposium, Kamloops, British Columbia, p. 23–31.

Giles, D.L., and Livingston, D.E., 1975, Geology and isotope geochemistry of the MoS_2 orebody of the Lime Creek stock, Alice Arm, British Columbia [abs.]: Economic Geology, v. 70, p. 245.

Giles, S.A., Granitto, M., and Eppinger, R.G., 2009, Selected geochemical data for modeling near-surface processes in mineral systems: U.S. Geological Survey Data Series 433, CD–ROM.

Giroux, G.H., 2008, 2007 update resource estimation on the Red Bird porphyry Mo/Cu deposit: 56 p., accessed October 3, 2011, at *http://www.torchriver.ca/techrepjan1508.pdf*.

Goerold, W.T., and Mehrkens, J., 1992, Quartz Hill Molybdenum Mine—Would environmental protection price it out of the market?: Proceedings of the First Annual Mineral Economics and Management Society (MEMS), annual meeting in Washington, D.C., March 19–21, 1992.

Goldrea Resources, 2009, accessed October 3, 2011, at *http://www.goldrea.com/images/financial/FinStat-2009-2nd-MD&A.pdf*.

Gorelov, V.A., Larin, A.M., and Turchenko, S.I., 1997, Karelia Terrain, *in* Rundqvist, D.V., and Gillen, C., eds., Precambrian Ore Deposits of the East European and Siberian Cratons: Elsevier Science, p. 51–76.

Gould, L., and Kendall, N.R., 2011, Role of the rumen in copper and thiomolybdate absorption: Nutrition Research Reviews, v. 24, p. 176–182.

Gupta, U.C., and Lipsett, J., 1981, Molybdenum in soils, plants, and animals: Advances in Agronomy, v. 34, p. 73–115.

Hansuld, J.A., 1966, Behavior of molybdenum in secondary dispersion media—A new look at an old geochemical puzzle: Mining Engineering, v. 18, no. 3, p. 410

Hall, W.E., 1995, Cretaceous molybdenum stockworks, *in* Fisher, F.S., and Johnson, K.M., eds., Geology and Mineral Resource Assessment of the Challis 1E × 2E Quadrangle, Idaho: U.S. Geological Survey Professional Paper 1525, p. 127–130.

Hall, W.E., Schmidt, E.A., Howe, S.S., and Broch, M.J., 1984, The Thompson Creek, Idaho, porphyry molybdenum deposit—An example of a fluorine-deficient molybdenum granodiorite system, *in* Janelidze, T.V., and Tvalchrelidze, A.G., eds., Proceedings of the Sixth Quadrennial Symposium of the International Association on the Genesis of Ore Deposits, Tbilisi, USSR, 6–12 September 1982, Stuttgart, W. Schweizerbar'sche, p. 349–357.

Hammitt, R.W., and Schmidt, E.A., 1982, Geology and mineralization of the Cannivan Gulch deposit, Beaverhead County, Montana, *in* Beaver, P., ed., The overthrust province in the vicinity of Dillon, Montana and how this structural framework has influenced mineral and energy resource accumulation: Guidebook of the Seventh Annual Tobacco Root Geological Society Conference, p. 15–20.

Hansuld, J.A., 1966, Behavior of molybdenum in secondary dispersion media—A new look at an old geochemical puzzle: Mining Engineering, v. 18, no. 3, p. 410.

Heinhorst, J., Lehmann, B., Ermolov, P., Serykh, V., and Zhurutin, S., 2000, Paleozoic crustal growth and metallogeny of Central Asia—Evidence from magmatic-hydrothermal ore systems of central Kazakhstan: Tectonophysics, v. 328, p. 69–87.

Heintze, Ludwig, 1985, Geology and geochemistry of the porphyry stockwork molybdenum deposit at Tamboras, La Negra Zone (Peru): Economic Geology, v. 80, p. 2,019–2,027.

Hem, J.D., 1985, Study and interpretation of the chemical characteristics of natural waters, 3rd ed.: U.S. Geological Survey Water Supply Paper 2254, 264 p.

Hemley, J.J., and Jones, W.R., 1964, Chemical aspects of hydrothermal alteration with emphasis on hydrogen metasomatism: Economic Geology, v. 59, p. 538–569.

Hesse, C.A., and Ellis, D.V., 1995, Quartz Hill, Alaska—A case history of engineering and environmental requirements for STD in the USA, *in* Ellis, D.V., and Poling, G.W., eds., Submarine Tailings Disposal Special Issue: Marine Georesources and Geotechnology, v. 13, no. 1–2, p. 135–182.

Hesse Associates, 1993, Regulatory aspects of submarine tailings disposal—The Quartz Hill case study: U.S. Bureau of Mines Open File Report 66–93, 141 p. (available at *http://www.blm.gov/pgdata/etc/medialib/blm/ak/jrmic/usbm_rpts.Par.34820.File.tmp/OFR_66-93.pdf*)

Hildenbrand, T.G., Berger, Byron, Jachens, R.C., and Ludington, Steve, 2000, Regional crustal structures and their relationship to the distribution of ore deposits in the western United States, based on magnetic and gravity data: Economic Geology, v. 95, p. 1,583–1,603.

Hildreth, Wes, and Moorbath, S., 1988, Crustal contributions to arc magmatism in the Andes of Central Chile: Contributions to Mineralogy and Petrology, v. 98, p. 455–489.

Hodgson, C.J., 1995, Kitsault (Lime Creek) molybdenum mine, northwestern British Columbia, *in* Schroeter, T.G., ed., Porphyry deposits of the northwestern cordillera of North America: Special Volume 46, Canadian Institute of Mining, Metallurgy, and Petroleum, p. 708–711.

Hollister, V.F., 1975, The porphyry molybdenum deposit of Compaccha, Peru, and its geological setting: Mineralium Deposita, v. 10, p. 141–151.

Hollister, V.F., 1978, Porphyry molybdenum deposits, *in* Sutulov, A., ed., International molybdenum encyclopedia: Santiago, Chile, Internet Publications, v. 1., p. 270–283.

Horton, D.J., 1978, Porphyry-type copper-molybdenum mineralization belts in eastern Queensland, Australia: Economic Geology, v. 73, no. 5, p. 904–921.

Hudson, T., Smith, J.G., and Elliott, R.L., 1979, Petrology, composition, and age of intrusive rocks associated with the Quartz Hill molybdenite deposit, southeastern Alaska: Canadian Journal of Earth Sciences, v. 16, p. 1,805–1,822.

Hudson, T., Arth, J.G., and Muth, K.G., 1981, Geochemistry of intrusive rocks associated with molybdenite deposits, Ketchikan Quadrangle, southeastern Alaska: Economic Geology, v. 76, p. 1,225–1,232.

Hunt, P.A., and Roddick, J.C., 1987, A compilation of K-Ar ages, Report 17, *in* Radiogenic and Isotopic Studies—Report 1: Geological Survey of Canada, Paper 87–2, p. 143–210.

Hyndman, R.D., Riddihough, R.P., and Herzer, R., 1979, The Nootka fault zone—A new plate boundary off western Canada: Geophysical Journal of the Royal Astronomical Society, v. 58, p. 667–683.

International Molybdenum Association website, 2009, at *http://www.imoa.info/HSE/environmental_data/human_health/molybdenum_levels_humans.htm*.

Jambor, J.L., Dutrizac, J.E., Groat, L.A., and Raudsepp, M., 2002, Static tests of neutralization potentials of silicate and aluminosilicate minerals: Environmental Geology, v. 43, p. 1–17.

Janković, S., 1982, Yugoslavia, *in* Dunning, F.W., Mykura, W., and Slater, D., eds., Mineral deposits of Europe, v. 2, Southeast Europe: Institution of Mining and Metallurgy-Mineralogical Society, London, p. 143–202.

Jarrell, W.M., Page, A.L., and Elseewi, A.A., 1980, Molybdenum in the environment: Residue Reviews, v. 74, p. 1–43.

Jewett, S.C., Sloan, N.A., and Somerton, D.A., 1985, Size at sexual maturity and fecundity of the fjord-dwelling golden king crab *Lithodes aequispina* Benedict from northern British Columbia: Journal of Crustacean Biology, v. 5, no. 3, p. 377–385.

John, D.A., Ayuso, R.A., Barton, M.D., Blakely, R.J., Bodnar, R.J., Dilles, J.H., Gray, Floyd, Graybeal, F.T., Mars, J.C., McPhee, D.K., Seal, R.R., Taylor, R.D., and Vikre, P.G., 2010, Porphyry copper deposit model, chap. B *of* Mineral deposit models for resource assessment: U.S. Geological Survey Scientific Investigations Report 2010–5070–B, 169 p.

Kay, R.W., 1978, Aleutian magnesian andesite—Melts from subducted Pacific Ocean crust: Journal of Volcanological and Geothermal Research, v. 4, p. 117–132.

Keith, J.D., Christiansen, E.H., and Carten, R.B., 1993, The genesis of giant porphyry molybdenum deposits, *in* Whiting, B.H., Hodgson, C.J., and Mason, R., eds., Giant ore deposits: Society of Economic Geologists Special Publication 2, p. 285–317.

Kelly, J.A., 2008, Technical report on the resource assessment of the Gamma and Delta Zones mineral tenure 515427 Nithi Mountain molybdenum property: Accessed February 2011 at *http://www.leewardcapital.com/UserFiles/NithiReport_JKelly.pdf*.

Kerr, A., van Nostrand, T.S., Dickson, W.L., and Lynch, E.P., 2009, Molybdenum and tungsten in Newfoundland—A geological overview and a summary of recent exploration developments: Newfoundland and Labrador Department of Natural Resources Geological Survey, Report 09–1, p. 43–80.

Kimball, A.L., Still, J.C., and Rataj, J.L., 1978, Mineral resources, *in* Brew, D.A., and others, Mineral resources of the Glacier Bay National Monument wilderness study area, Alaska: U.S. Geological Survey Open-File Report 78–494, p. C1–C375.

Kimura, E.T., Bysouth, G.D., and Drummond, A.D., 1976, Endako, *in* Sutherland Brown, A., ed., Porphyry deposits of the Canadian cordillera: Canadian Institute of Mining, Metallurgy, and Petroleum, Special Volume 15, p. 444–454.

Kingsman Resources Corporation, 2009, Luxor Molybdenum Property—Ground truthing of soil geochemical anomaly suggests exploration potential: News Release dated January 8, 2009, accessed May 24, 2011, at *http://www.kingsmanresources.com/s/NewsReleases.asp?ReportID=333526&_Type=News-Releases&_Title=Luxor-Molybdenum-Property-Ground-Truthing-of-Soil-Geochemical-Anomaly-Sugge.*

Kirkemo, Harold, Anderson, C.A., and Creasey, S.C., 1965, Investigations of molybdenum deposits in the conterminous United States 1942–1960: Contributions to Economic Geology, Geological Survey Bulletin 1182–E, 90 p.

Kirkham, R.V., 1998, Tectonic and structural features of arc deposits, *in* Lefebure, D.V., coordinator, ed., Metallogeny of volcanic arcs: British Columbia Geological Survey, Short Course Notes, Open File 1998–8, Section B, 44 p.

Knittel, U., and Burton, C.K., 1985, Polillo Island (Philippines)—Molybdenum mineralization in an island arc: Economic Geology, v. 80, p. 2,013–2,018.

Kubota, J., 1977, Molybdenum status of United States soils and plants, *in* Chappell, W.R., and Petersen, K.K., Molybdenum in the environment, v. 2, The geochemistry, cycling, and industrial uses of molybdenum: Proceedings of an International Symposium on Molybdenum in the Environment, Denver, Colo., U.S.A., June 16–19, 1975, p. 555–581.

Kuehnbaum, R.M., MacFarlane, G.R., and Roberts, S.A., 2009, Technical report on the Storie molybdenum deposit, Liard Mining Division, British Columbia for Columbia Yukon Explorations Inc.: Watss, Griffis and McOuat Limited and Mintec, Inc., NI43–101 compliant report, 118 p.

Lawley, C.J.M., 2009, Age, geochemistry, and fluid characteristics of the MAX porphyry Mo deposit, southeast British Columbia: Unpublished M.Sc. thesis, Edmonton, Canada, University of Alberta, 166 p.

Lawley, C.J.M., Richards, J.P., Anderson, R.G., Creaser, R.A., and Heaman, L.M., 2010, Geochronology and geochemistry of the MAX porphyry Mo deposit and its relationship to Pb-Zn-Ag mineralization, Kootenay Arc, southeastern British Columbia, Canada: Economic Geology, v. 105, p. 1,113–1,142.

Laznicka, P., 1976, Porphyry copper and molybdenum deposits of the U.S.S.R. and their plate tectonic settings: Transactions of the Institution of Mining and Metallurgy, v. 85, p. B14–B32.

Le Gendre, G.R., and Runnells, D.D., 1975, Removal of dissolved molybdenum from wastewaters by precipitates of ferric iron: Environmental Science and Technology, v. 9, p. 744.

Lewis, R.S., Kilsgaard, T.H., Bennett, E.H., and Hall, W.E., 1987, Lithologic and chemical characteristics of the central and southeastern part of the southern lobe of the Idaho batholith, *in* Vallier, T.L., and Brooks, H.C., eds., Geology of the Blue Mountains region of Oregon, Idaho, and Washington—The Idaho batholith and its border zone: U.S. Geological Survey Professional Paper 1436, p. 171–196.

Leybourne, M.I., 2007, Aqueous geochemistry in mineral exploration, *in* Goodfellow, W.D., ed., Mineral deposits of Canada—A synthesis of major deposit-types, district metallogeny, the evolution of geological provinces, and exploration methods: Geological Association of Canada, Mineral Deposits Division, Special Publication no. 5, p. 1,007–1,033.

Li, X., Feng, Z., Wang, C., Li, R., and Tang, Z., 2010, Molybdenite Re-Os and zircon SHRIMP U-Pb dating at the Baishiding deposit, Guposhan district—New evidence for Silurian Mo mineralization in south China: Resource Geology, v. 60, p. 260–270.

Linnen, R.L., and Williams-Jones, A.E., 1990, Evolution of aqueous-carbonic fluids during contact metamorphism, wall-rock alteration and molybdenite deposition at Trout Lake, British Columbia: Economic Geology, v. 85, p. 1,840–1,856.

Linnen, R.L., Williams-Jones, A.E., Leitch, C.H.B., and Macauley, T.N., 1995, Molybdenum mineralization in a fluorine-poor system—The Trout Lake stockwork deposit, southeastern British Columbia, *in* Schroeter, T.G., ed., Porphyry deposits of the northwestern cordillera of North America: Special Volume 46, Canadian Institute of Mining, Metallurgy, and Petroleum, p. 771–780.

Long, K.R., 1992, Reserves and production data for selected deposits in the United States found in the files of the Anaconda Copper Company: U.S. Geological Survey Open-File Report 92–002, 21 p.

Ludington, Steve, and Plumlee, G.S., 2009, Climax-type porphyry molybdenum deposits: U.S. Geological Survey Open-File Report 2009–1215, 16 p.

Ludington, Steve, Bookstrom, A.A., Kamilli, R.J., Walker, B.M., and Jlein, D.P., 1995, Climax Mo deposits, *in* du Bray, E.A., ed., Preliminary compilation of descriptive geoenvironmental mineral deposit models: U.S. Geological Survey Open-File Report 95–821, p.70–74.

Ludington, Steve, Hammarstrom, Jane, and Piatak, Nadine, 2009, Low-fluorine stockwork molybdenite deposits: U.S. Geological Survey Open-File Report 2009–1211, 9 p.

Macauley, T.N., 2004, Technical report on the Trout Lake molybdenum project REvelstoke Mining Division British Columbia Canada, 16 p., accessed October 3, 2011. (Also available at *http://www.rocamines.com/i/pdf/Max_43-101_Report.pdf*.)

Macdonald, A.J., 1983, Boss Mountain molybdenite deposit—Fluid geochemistry and hydrodynamic considerations: University of Toronto, unpublished Ph.D. dissertation, 410 p.

Macdonald, A.J., Spooner, E.T.C., and Lee, G., 1995, The Boss Mountain molybdenum deposit, central British Columbia, *in* Schroeter, T.G., ed., Porphyry deposits of the northwestern cordillera of North America: Special Volume 46, Canadian Institute of Mining, Metallurgy, and Petroleum, p. 691–696.

MacDonald, D.D., Ingersoll, C.G., and Berger, T.A., 2000, Development and evaluation of consensus-based sediment quality guidelines for freshwater ecosystems: Archives of Environmental Contamination and Toxicology, v. 39, no. 1, p. 20–31.

Mackas, D.L., and Anderson, E.P., 1986, Small-scale zooplankton community variability in a northern British Columbia fjord system: Estuarine and Coastal Shelf Sciences, v. 22, p. 115–142.

Majak, W., Steinke, D., McCillivray, J., and Lysyk, T., 2004, Clinical signs in cattle grazing high molybdenum forage: Journal of Range Management, v. 57, p. 269–274.

Mao, J.W., Xie, G.Q., Bierlein, F., Qü, W.J., Du, A.D., Ye, H.S., Pirajno, F., Li, H.M., Guo, B.J., Li, Y.F., and Yang, Z.Q., 2008, Tectonic implications from Re-Os dating of Mesozoic molybdenum deposits in the East Qinling-Dabie orogenic belt: Geochimica et Cosmichimica Acta, v. 72, p. 4,607–4,626.

Mathieu, S., 1995, Molybdenum compilation—Summary of environmental research conducted at Placer Dome Canada, Ltd., Endako Mines Division from 1989 to 1994: Endako, B.C., p. 82.

McGrath, S.P., Micó, C., Curdy, R., and Zhao, F.J., 2010a, Predicting molybdenum toxicity to higher plants—Influence of soil properties: Environmental Pollution, v. 158, p. 3,095–3,102.

McGrath, S.P., Micó, C., Zhao, F.J., Stroud, J.L., Zhang, H., and Fozard, S., 2010b, Predicting molybdenum toxicity to higher plants—Estimation of toxicity threshold values: Environmental Pollution, v. 158, p. 3,085–3,094.

McMillian, W.J., Thompson, J.F.H., Hart, C.J.R., and Johnston, S.T., 1996, Porphyry deposits of the Canadian Cordillera: Geoscience Canada, v. 23, p. 125–134.

Meinert, L.D., Dipple, G.M., and Nicolescu, S., 2005, World skarn deposits: Economic Geology 100th Anniversary volume, p. 299–336.

Mine Environment Neutral Drainage , 2008, A review of environmental management criteria for selenium and molybdenum: MEND Report 10.1.1.

Ministry of Energy, Mines and Petroleum Resources, 2010a, Exploration and mining in British Columbia 2009: Ministry of Energy, Mines and Petroleum Resources Mining and Minerals Division, British Columbia, Canada, 90 p.

Ministry of Energy, Mines and Petroleum Resources, 2010b, British Columbia mines and mineral exploration overview 2009: Ministry of Energy, Mines and Petroleum Resources Mining and Minerals Division, British Columbia, Canada, 36 p.

Misra, K.C., 2000, Understanding mineral deposits: Netherlands, Kluwer Academic Publishers, 845 p.

Mitchell, D.G., Vigers, G.A., Morgan, J.D., Nix, P.G., Chapman, P.M. and Deverall, R.W., 1984, Report on acute, chronic and sublethal bioassays and bioaccumulation studies for the Quartz Hill Project, Southeast Alaska: Prepared for U.S. Borax and Chemical Corp., by E.V.S. Consultants, Vancouver, B.C.

Mutschler, F.E., Wright, E.G., Ludington, S., and Abbott, J.T., 1981, Granite molybdenite systems: Economic Geology, v. 76, p. 874–897.

Nevada Division of Environmental Protection, 2008, Rationale for proposed revision to aquatic life water quality criteria for molybdenum: Bureau of Water Quality Planning, July 2008, Report NAC 445A.144.

Newsom, H.E., and Palme, H., 1984, The depletion of siderophile elements in the Earth's mantle—New evidence from molybdenum and tungsten: Earth and Planetary Science Letters, v. 69, p. 354–364.

Northcott, L., 1956, Molybdenum—Metallurgy of the rarer metals, 5: Butterworths Scientific Publications, London, 222 p.

Nunes, P.D., and Ayres, L.D., 1982, U-Pb zircon age of the Archean Setting Net Lake porphyry molybdenum occurrence, northwestern Ontario, Canada: Economic Geology, v. 77, p. 1,236–1,239.

Odhiambo, B.K., Macdonald, R.W., O'Brien, M.C., Harper, J.R., and Yunker, M.B., 1996, Transport and fate of mine tailings in a coastal fjord of British Columbia as inferred from the sediment record: Science and the Total Environment, v. 191, p. 77–94.

Pearson, R.C., Berger, B.R., Kaufmann, H.E., Hanna, W.F., and Zen, E-an, 1988, Mineral resources of the eastern Pioneer Mountains, Beaverhead County, Montana: U.S. Geological Survey Bulletin 1766, 34 p.

Pedersen, T.F., Ellis, D.V., Poling, G.W., and Pelletier, C., 1995, Effects of changing environmental rules—Kitsault Molybdenum Mine, Canada: Marine Georesources and Geotechnology, v. 13, p. 119–133.

Plumlee, G.S., 1999, The environmental geology of mineral deposits, *in* Plumlee, G.S., and Logsdon, M.J., eds., The environmental geochemistry of mineral deposits, Part A—Processes, techniques, and health issues: Reviews in Economic Geology, v. 6A, p. 71–116.

Price, W.A., 1989, An examination of factors affecting vegetation establishment at the Kitsault minesite: University of British Columbia, Vancouver, B.C., Canada, unpublished Ph.D. dissertation.

Ray, G.E., Webster, I.C.L., Ballantyne, S.B., Kilby, C.E., and Cornelius, S.B., 2000, The geochemistry of three tin-bearing skarns and their related plutonic rocks, Atlin, northern British Columbia: Economic Geology, v. 95, p. 1,349–1,365.

Richards, J.P., 2003, Tectono-magmatic precursors for porphyry Cu-(Mo-Au) deposit formation: Economic Geology, v. 98, p. 1,515–1,533.

Richards, J.P., 2009, Postsubduction porphyry Cu-Au and epithermal deposits—Products of remelting subduction-modified lithosphere: Geology, v. 37, p. 247–250.

Richards, J.P., and Kerrich, R., 2007, Adakite-like rocks—Their diverse origins and questionable role in metallogenesis: Economic Geology, v. 102, p. 537–576.

Riordan, B., 2003, A comparison of pre-development and present molybdenum concentrations in vegetation on the Endako mine site and implications to ungulate health: Presented at the 27th Annual British Columbia Mine Reclamation Symposium, Kamloops, September 15–18, 2003.

Roscoe, W.E., Postle, J.T., and Pelletier, P.C., 2007, Technical report on the mineral resources and mineral reserves of the Thompson Creek Molybdenum Mine, Central Idaho, U.S.A.: Report for NI43-101 prepared for Thompson Creek Metals Company, Inc., 97 p. (Also available at *http://www.thompsoncreekmetals.com/i/pdf/Reserve-Report-FINAL-Dec07.pdf*.)

Schamphelaere, K.A.C., Stubblefield, W., Rodriguez, P., Vleminckx, K., and Janssen, C.R., 2010, The chronic toxicity of molybdate to freshwater organisms. I. Generating reliable effects data: Science of the Total Environment, v. 408, p. 5,362–5,371.

Schmidt, E.A., Broch, M., and White, R., 1983, Geology of the Thompson Creek molybdenum deposit, Custer County, Idaho, *in* Proceedings of the Denver Region Exploration Geologists Society symposium, The genesis of Rocky Mountain ore deposits; changes with time and tectonics: p. 79–84.

Schroeter, Tom, and Fulford, Alya, 2005, Table of significant British Columbia porphyry molybdenum resources: British Columbia Ministry of Energy and Mines, Geofile 2005–23, 6 p.

Seedorff, E., Dilles, J.H., Proffett, J.M. Jr., Einaudi, M.T., Zurcher, L., Stavast, W.J.A., Johnson, D.A., and Barton, M.D., 2005, Porphyry deposits—Characteristics and origin of hypogene features: Economic Geology 100th Anniversary Volume, p. 251–298.

Selby, D., Nesbitt, B.E., Muehlenbachs, K., and Prochaska, W., 2000, Hydrothermal alteration and fluid chemistry of the Endako porphyry molybdenum deposit, British Columbia: Economic Geology, v. 95, p. 183–202.

Seraphim, R.H., and Hollister, V.F., 1976, Structural settings, *in* Sutherland Brown, A., ed., Porphyry deposits of the Canadian cordillera: Canadian Institute of Mining, Metallurgy, and Petroleum, Special Volume 15, p. 30–43.

Shinohara, H., Kazahaya, K., and Lowenstern, J.B., 1995, Volatile transport in a convecting magma column—Implications for porphyry Mo mineralization: Geology, v. 23., p. 1091–1094.

Sillitoe, R.H., 1980, Types of porphyry molybdenum deposits: Mining Magazine, v. 142, p. 550–553.

Sillitoe, R.H., 2010, Porphyry copper deposits: Economic Geology, v. 105, p. 3–41.

Simic, M., 2001, Metallogenic features of the Mackatica ore field—Bratislava, Slovakia; September 1–4, 2002, XVII Congress of Carpatian-Balkan Geological Association, Proceedings, 4 p. (Also available at *www.geologicacarpathica.sk/special/S/Simic.pdf*.)

Simpson, R.G., 2009, Resource estimate, Lone Pine Molybdenum Project, Omineca Mining Division, British Columbia: Vancouver, Canada, GeoSim Services, Inc., Technical Report for Bard Ventures Ltd., 70 p.

Sinclair, W.D., 1995, Porphyry Mo (low-F type), *in* Lefebure, D.V., and Ray, G.E., eds., Selected British Columbia mineral deposit profiles—Vol. 1, Metallics and coal: British Columbia Ministry of Energy, Mines, and Petroleum Resources, Open File 1995–20, p. 93–96.

Sinclair, W.D., 2007, Porphyry deposits, *in* Goodfellow, W.D., ed., Mineral Deposits of Canada—A synthesis of major deposit-types, district metallogeny, the evolution of Geological provinces, and exploration methods: Geological Association of Canada, Mineral Deposits Division, Special Publication No. 5, p. 223–243.

Sinclair, W.D., Jonasson, L.R., Kirkham, R.V., and Soregaroli, A.E., 2009, Rhenium and other platinum-group metals in porphyry deposits: Geological Survey of Canada, Open File 6181, 1 sheet.

Singer, P.C., and Stumm, W., 1970, Acidic mine drainage—The rate-determining step: Science, v. 167, no. 3921, p. 1,121–1,123.

Situmorang, B., 1982, The formation of the Makassar Basin as determined from subsidence curves: Proceedings of the of the 11th annual Indonesian Petroleum Association Convention, p. 82–107.

Sloan, N.A., 1985, Life history characteristics of fjord-dwelling golden king crab *Lithodes aequispina*: Marine Ecology Progress Series, v. 22, p. 219–228.

Sloan, N.A., and Robinson, S.M.C., 1985, The effect of trap soak time on yields of the deep-water golden king crab (*Lithodes aequispina* Benedict) in northern British Columbia fjord: Journal of Shellfish Research, v. 5, no. 1, p. 21–23.

Smith, J.L., 2009, A study of the Adanac porphyry molybdenum deposit and surrounding placer gold mineralization in Northwest British Columbia with a comparison to porphyry molybdenum deposits in the North American cordillera and igneous geochemistry of the Western United States: University of Nevada, Reno, UMI dissertation publishing, unpublished M.S. thesis, 186 p.

Smith, R.W., Norman, D.I., and Popp, C.J., 1980, Calculated solubility of molybdenite in hydrothermal solutions [abs.]: Geological Society of America, Abstracts with Programs, v. 12, no. 7, p. 525.

Soeria-Atmadja, R., Priadi, B., van Leeuwen, T.M., and Kavalieris, I., 1999, Tectonic setting of porphyry Cu-Au, Mo and related mineralization associated with contrasted Neogene magmatism in the western Sulawesi arc: The Island Arc, v. 8, p. 47–55.

Soregaroli, A.E., and Nelson, W.I., 1976, Boss Mountain, *in* Sutherland Brown, A., ed., Porphyry deposits of the Canadian cordillera: Canadian Institute of Mining, Metallurgy, and Petroleum, Special Volume 15, p. 432–443.

Soregaroli, A.E., and Sutherland Brown, A., 1976, Characteristics of Canadian Cordilleran molybdenum deposits, *in* Sutherland Brown, A., ed., Porphyry deposits of the Canadian cordillera: Canadian Institute of Mining, Metallurgy, and Petroleum, Special Volume 15, p. 417–431.

Stein, H.J., and Hannah, J.L., 1985, Movement and origin of ore fluids in Climax-type systems: Geology, v. 13, p. 469–474.

Stein, H.J., Markey, R.J., Morgan, J.W., Du, A., and Sun, Y., 1997, Highly precise and accurate Re-Os ages for molybdenite from the East Qinling molybdenum belt, Shaanxi Province, China: Economic Geology, v. 92, p. 827–835.

Steininger, R.C., 1985, Geology of the Kitsault molybdenum deposit, British Columbia: Economic Geology, v. 80, p. 57–71.

Stevens, R.D., Delabio, R.N., and Lachance, G.R., 1982, Age determinations and geological studies, K-Ar isotopic ages, report 16: Geological Survey of Canada, Paper 82–2, 56 p.

Sutulov, Alexander, 1973, Mineral resources and the economy of the USSR: New York, Engineering and Mining Journal, 192 p.

Sutulov, A., 1978, Resources—World survey, *in* Sutulov, A., ed., International Molybdenum Encyclopedia 1778–1978, Volume 1: Santiago, Chile, Resources and Production, Internet Publications, 402 p.

Taylor, S.R., and McClennan, S.M., 1985, The continental crust—its composition and evolution: Oxford, Blackwell Scientific Publications, 312 p.

Theodore, T.G., 1986, Descriptive model of porphyry Mo, Low-F, *in* Cox, D.P., and Singer, D.A., eds., Mineral deposit models: U.S. Geological Survey Bulletin 1693, p. 120–122.

Theodore, T.G., and W.D. Menzie, 1984, Fluorine deficient porphyry molybdenum deposits in the western North American Cordillera, *in* Janelidge, T.V., and Tvalehredidge, A.G., Proceedings of the Sixth Quadrennial IAGOD Symposium: Stuttgart, Germany, p. 463–470.

Theodore, T.G., Blake, D.W., Loucks, T.A., and Johnson, C.A., 1992, Geology of the Buckingham stockwork molybdenum deposit and surrounding area, Lander County, Nevada: U.S. Geological Survey Professional Paper 798–D, 307 p.

Tulloch, A.J., and Rabone, S.D.C., 1993, Mo-bearing granodiorite porphyry plutons of the Early Cretaceous Separation Point Suite, west Nelson, New Zealand: New Zealand Journal of Geology and Geophysics, v. 36, p. 401–408.

Tuttle, M.L., Wanty, R.B., and Berger, B.R., 2002, Environmental behavior of two molybdenum porphyry systems, *in* Seal, R.R., II, and Foley, N.K., eds., Progress on geoenvironmental models for selected mineral deposit types: U.S Geological Survey Open-File Report 02–0195, p. 65–86. (Also available at *http://pubs.usgs.gov/of/2002/of02-195/OF02-195D.pdf*.)

Ulrich, Thomas, and Mavrogenes, John, 2008, An experimental study of the solubility of molybdenum in H_2O and KCl-H_2O solutions from 500 degrees C to 800 degrees C, and 150 to 300 MPa: Geochimica et Cosmochimica Acta, v. 72, p. 2,316–2,330.

United States Borax & Chemical Corporation and Bechtel Civil and Minerals, Inc. (U.S. Borax), 1982, Comments on ore mining and dressing point source category—Proposed effluent limitation guidelines and new source performance standards: Federal Register, June 14, 1982; August 24, 1982.

U.S. Environmental Protection Agency, 1992, Mine site visit—Cyprus Thompson Creek: U.S. Environmental Protection Agency, Office of Solid Waste, Technical Resources Document, 31 p.

U.S. Environmental Protection Agency, 2006, National Recommended Water Quality Criteria. (Also available at *http://www.epa.gov/waterscience/criteria/nrwqc-2006.pdf*.)

U.S. Environmental Protection Agency, 2008, Regional Screening Levels (RSL) for Chemical Contaminants at Superfund Sites, RSL Table Update Sept. 2008. (Available at *http://www.epa.gov/region09/superfund/prg/*.)

U.S. Environmental Protection Agency, 2009, National Primary Drinking Water Regulations: EPA 816–F–09–004, accessed July 9, 2009, at *http://www.epa.gov/safewater/consumer/pdf/mcl.pdf*.

U.S. Forest Service, 1988, Final environmental impact statement for Quartz Hill molybdenum project mine development, vols. 1–2, Tongass National Forest R10–MB041a.

U.S. Geological Survey Headwaters Province Project Team (Karen Lund, scientific ed.), 2007, Earth science studies in support of public policy development and land stewardship—Headwaters province, Idaho and Montana: U.S. Geological Survey Circular 1305, 92 p.

van Leeuwen, T.M., Taylor, R., Coote, A., and Longstaffe, F.J., 1994, Porphyry molybdenum mineralization in a continental collision setting at Malala, northwest Sulawesi, Indonesia: Journal of Geochemical Exploration, v. 50, p. 279–315.

Villeneuve, Mike, Whalen, J.B., Anderson, R.G., and Struik, L.C., 2001, The Endako batholith—Episodic plutonism culminating in formation of the Endako porphyry molybdenite deposit, north-central British Columbia: Economic Geology, v. 96, p. 171–196.

Voegeli, P.T., Sr., and King, R.U., 1969, Occurrence and distribution of molybdenum in surface waters of Colorado: U.S. Geological Survey Water-Supply Paper, W 1535–N, p. N1–N32.

Vyskocil, A., and Viau, C., 1999, Assessment of molybdenum toxicity in humans: Journal of Applied Toxicology, v. 19, p. 185–192.

Wallace, S.R., 1995, The Climax-type molybdenite deposits—What they are, where they are, and why they are: Economic Geology, v. 90, p. 1,359–1,380.

Wanty, R.B., Tuttle, M.L., Berger, B.R., Bove, D., Eppinger, R., 2003, Environmental behavior of several porphyry molybdenum and copper deposits in the western U.S.: 4th European Congress on Geoscientific Cartography, Bologna, Italy, June 16–20, 2003. (Also available at *http://www.regione.emilia-romagna.it/geologia/convegni/download/4th_congress/abs_poster/13_wanty.pdf*.)

Ward, G.M., 1978, Molybdenum toxicity and hypocuprosis in ruminants—A review: Journal of Animal Science, v. 46, p. 1,078–1,085.

Westra, G., and Keith, S.B., 1981, Classification and genesis of stockwork molybdenum deposits: Economic Geology, v. 76, p. 844–873.

Whalen, J.B., Anderson, R.G., Struik, L.C., and Villeneuve, M.E., 2001, Geochemistry and Nd isotopes of the François Lake plutonic suite, Endako batholith—Host and progenitor to the Endako molybdenum camp, central British Columbia: Canadian Journal of Earth Science, v. 38, p. 603–618.

Williamson, M.A., Kirby, C.S., and Rimstidt, J.D., 2006, Iron dynamics in acid mine drainage, *in* Barnhisel, R.I., ed., The 7th International Conference on Acid Rock Drainage, St. Louis, Missouri, USA, p. 2,411–2,423.

Winick, J.A., aylor, C.D., Kunk, M.J., and Unruh, D., 2002, Revised $^{40}Ar/^{39}Ar$ ages of the White Cloud molybdenum deposit, Custer County, Idaho: Geological Society of America, Abstracts with Programs, v. 34, no. 6, p. 337.

Winter, J.D., 2001, An introduction to igneous and metamorphic petrology: New Jersey, Prentice Hall, Upper Saddle River, 697 p.

Witcher, I.G., 1975, Anduramba molybdenum prospect, *in* Knight, C.L., ed., Economic geology of Australia and Papau New Guinea, 1, metals: Australasian Institute of Mining and Metallurgy, 5, p. 793–794.

Wolfe, W.J., 1995, Exploration and geology of the Quartz Hill molybdenum deposit, southeast Alaska, *in* Schroeter, T.G., ed., Porphyry deposits of the northwestern cordillera of North America: Special Volume 46, Canadian Institute of Mining, Metallurgy, and Petroleum, p. 764–770.

Woodcock, J.R., and Carter, N.C., 1976, Geology and geochemistry of the Alice Arm molybdenum deposits, *in* Sutherland Brown, A., ed., Porphyry deposits of the Canadian cordillera: Canadian Institute of Mining, Metallurgy, and Petroleum, Special Volume 15, p. 462–475.

World Health Organization, 2008, Guidelines for drinking-water quality, 3rd. Electron version for the web. WHO Press, Geneva, Switzerland. available online at *http://www.who.int/water_sanitation_health/dwq/gdwq3rev/en/index.html*

Worthington, J.E., 2007, Porphyry and other molybdenum deposits of Idaho and Montana: Idaho Geological Survey, Technical Report 07–3, 22 p.

www.thompsoncreek metals.com; accessed February 2011.

www.osha.gov/index.html; accessed March 2012.

Young, M.J., and Aird, C., 1969, Geology of Gem molybdenum deposit: CIM Bulletin, v. 62, p. 41–45.

Yukon Geological Survey, Yukon MINFILE No. 105C 009

Zeng, Q., Liu, J., Zhang, Z., Chen, W., Zhang, W., 2011, Geology and geochronology of the Xilamulun molybdenum metallogenic belt in eastern Inner Mongolia, China: International Journal of Earth Science, v. 100, p. 171–185.

Zhang, L., Xiao, W., Qin, K., Qu, W., and Du, A., 2005, Re-Os isotopic dating of molybdenite and pyrite in the Baishan Mo-Re deposit, eastern Tianshan, NW China, and its geological significance: Mineralium Deposita, v. 39, p. 960–969.

Zhu, L., Zhang, G., Guo, B., Lee, B., Gong, H., and Wang, F., 2010, Geochemistry of the Jinduicheng Mo-bearing porphyry and deposit, and its implications for the geodynamic setting in East Qinling, P.R. China; Chemie der Erde, v. 70, p. 159–174.

Appendix 1.

Grade and Tonnage

Table A1 lists the 40 known arc-related porphyry molybdenum deposits of the world with greater than 1 Mt of ore. Listed latitude and longitude coordinates are utilized in figure 1, and the grade and tonnage statistics are graphically represented in figure A1. Select alkali-feldspar rhyolite-granite porphyry molybdenum deposits are also shown in figure A1 for comparison.

Many other porphyry molybdenum deposits exist throughout the world, but classification is unreliable due to a lack of published information. Because of this, deposits that may be classified as arc-related porphyry molybdenum deposits with additional research in the future are currently excluded from this list.

In addition, many of the listed deposits are currently subeconomic and have yet to be thoroughly drilled and characterized for more precise grade and tonnage values. Any possible increases in molybdenum price may in the future alter the grades and tonnages listed in table A1 by increasing interest in them, and therefore directing mining companies to better characterize the deposit. This may also help in concretely classifying many other molybdenum deposits.

The largest known arc-related porphyry molybdenum deposit is Quartz Hill, Alaska which contains 1,600 Mt of ore at a grade of 0.076% Mo. Molybdenum grades for all arc-related porphyry molybdenum deposits with over 1 Mt of ore ranges from 0.027 to 0.200% Mo with a median value of 0.071% Mo. The median size is 62 Mt of ore. Figure A2 displays the top 30 deposits in contained molybdenum.

Table A1. Molybdenum grade, tonnage, and location for known arc-related porphyry molybdenum deposits containing over 1 million tonnes of ore.

[B.C., British Columbia, Canada; Mt, million tonnes; Mo %, molybdenum percent grade of ore; Mo, molybdenum; nd, no data]

Deposit	Location	Size (Mt)	Mo %	Contained Mo (tonnes)	Resource reference	Latitude	Longitude	Figure 1 location number
Ajax	B.C.	174.14	0.074	128,866.56	Schroeter and Fulford, 2005	55.5900	–129.4014	1
Bell Moly	B.C.	32.53	0.060	19,518.00	British Columbia Geological Survey, minfile 103P 234	55.4622	–129.3350	2
Boss Mountain	B.C.	63.00	0.074	46,620.00	Sinclair, 2007	52.0967	–120.9075	3
Burroughs Bay	Alaska	nd	0.036	n/a	Eakins and others, 1983	56.0000	–131.3000	4
Canicanian	Philippines	16.50	0.051	8,415.00	Knittel and Burton, 1985	14.7500	121.9920	n/a
Cannivan Gulch	Montana	324.30	0.060	194,580.00	Darling, 1994	45.6547	–112.9556	5
Carmi	B.C.	20.70	0.060	12,420.00	Schroeter and Fulford, 2005	49.5181	–119.1678	6
Compaccha	Peru	4.60	0.072	3,312.00	Jim Bliss, written commun., 2011	–8.0333	–77.9833	n/a
Cucomungo	Nevada	35.20	0.076	26,752.00	Jim Bliss, written commun., 2011	37.3591	–117.6326	7
Davidson	B.C.	75.28	0.177	133,245.60	Schroeter and Fulford, 2005	54.8167	–127.3000	8
Empress	B.C.	7.49	0.061	4,582.68	Goldrea Resources, 2009	49.6633	–120.0508	9
Endako	B.C.	777.26	0.053	411,949.39	British Columbia Geological Survey, minfile 093K 006	54.0361	–125.1100	10
Gem	B.C.	15.87	0.070	11,111.98	Schroeter and Fulford, 2005	49.7114	–121.7211	11
Joem	B.C.	12.25	0.080	9,796.68	Schroeter and Fulford, 2005	59.3469	–129.5142	12
Kitsault	B.C.	701.80	0.071	496,172.60	British Columbia Geological Survey, minfile 103P 120	55.4219	–129.4194	13
Little Boulder Creek	Idaho	181.00	0.120	217,200.00	Long, 1992	44.0530	–114.5570	14
Lone Pine	B.C.	152.00	0.070	106,400.00	Simpson, 2009	54.5200	–126.7300	15
Lucky Ship	B.C.	18.40	0.098	18,032.00	Schroeter and Fulford, 2005	54.0244	–127.4781	16
Luxor	B.C.	nd	nd	nd		51.3972	–119.8650	17
Mac	B.C.	100.00	0.072	72,000.00	Schroeter and Fulford, 2005	54.8600	–125.5772	18
Malala	Indonesia	100.00	0.084	84,000.00	Sinclair, 2007	0.6667	120.5000	n/a
MAX (Trout Lake)	B.C.	42.94	0.120	51,506.53	Macauley, 2004	50.6364	–117.6028	19
Mike	Alaska	25.00	0.200	50,000.00	Ashleman and others, 1997	57.0500	–157.2167	20
Mount Haskin	B.C.	12.25	0.090	11,021.27	Sinclair, 2007	59.3167	–129.4583	21
Mount Thomlinson	B.C.	40.82	0.071	28,982.20	Schroeter and Fulford, 2005	55.5872	–127.4903	22
Nithi Mountain	B.C.	241.10	0.027	65,579.20	Kelly, 2008	53.9667	–124.8333	23
Nunatak	Alaska	154.30	0.042	64,806.00	Kimball and others, 1978	58.9833	–136.1000	24
Pine Nut	Nevada	181.00	0.060	108,600.00	Sinclair, 2007	38.8702	–119.6250	25
Pitman	B.C.	3.40	0.080	2,720.00	Schroeter and Fulford, 2005	54.7303	–128.3336	26
Quartz Hill	Alaska	1,600.00	0.076	1,216,000.00	Sinclair, 2007	55.4028	–130.4828	27
Red Bird (Haven Lake)	B.C.	151.60	0.059	88,686.00	Giroux, 2008	53.2992	–127.0103	28
Red Mountain	Yukon	187.24	0.100	187,240.00	Sinclair, 2007	60.9892	–133.7494	29
Roundy Creek	B.C.	7.26	0.072	5,224.32	Schroeter and Fulford, 2005	55.4136	–129.4922	30
Salal Creek	B.C.	nd	nd	nd		50.7689	–123.4056	31
Serb Creek	B.C.	41.15	0.040	16,460.00	Schroeter and Fulford, 2005	54.6461	–127.7611	32
Sphinx	B.C.	62.00	0.035	21,700.00	Downie and others, 2006	49.6333	–116.6667	33
Storie	B.C.	140.00	0.064	89,600.00	Kuehnaum and others, 2009	59.2469	–129.8683	34
Thompson Creek	Idaho	326.40	0.068	221,952.00	www.thompsoncreekmetals.com	44.3169	–114.5358	35
Tidewater	B.C.	9.10	0.060	5,460.00	Sinclair, 2007	55.4681	–129.5472	36
Trapper Lake (Karen)	B.C.	54.40	0.096	52,224.00	Theodore and Menzie, 1984	58.2958	–132.6500	37

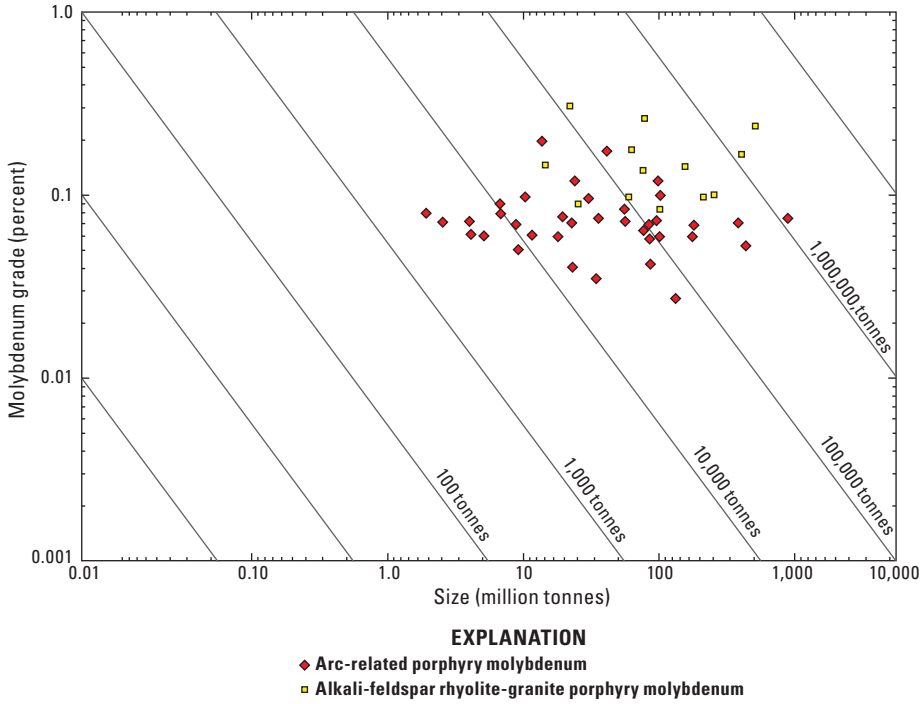

Figure A1. Grade-tonnage for 37 arc-related porphyry deposits with known molybdenum grade and tonnage. Data for arc-related calc-alkaline porphyry molybdenum deposits from Table A1. For comparison, data listed for select Climax-type molybdenum deposits from Climax, CO (Sinclair, 2007, and references within), Henderson-Urad, CO (Sinclair, 2007, and references within), Mount Emmons, CO (Sinclair, 2007, and references within), Redwell Basin, CO (Keith and others, 1993, and references within), Silver Creek, CO (Sinclair, 2007, and references within), Questa, NM (Sinclair, 2007, and references within), Log Cabin, NM (Keith and others, 1993, and references within), Pine Grove, UT (Sinclair, 2007, and references within), Mount Hope, NV (Sinclair, 2007, and references within), Big Ben, MT (Sinclair, 2007, and references within), Cave Creek, TX (Keith and others, 1993, and references within), Malmbjerg, Greenland (Keith and others, 1993, and references within), and Nordli, Norway (Keith and others, 1993, and references within).

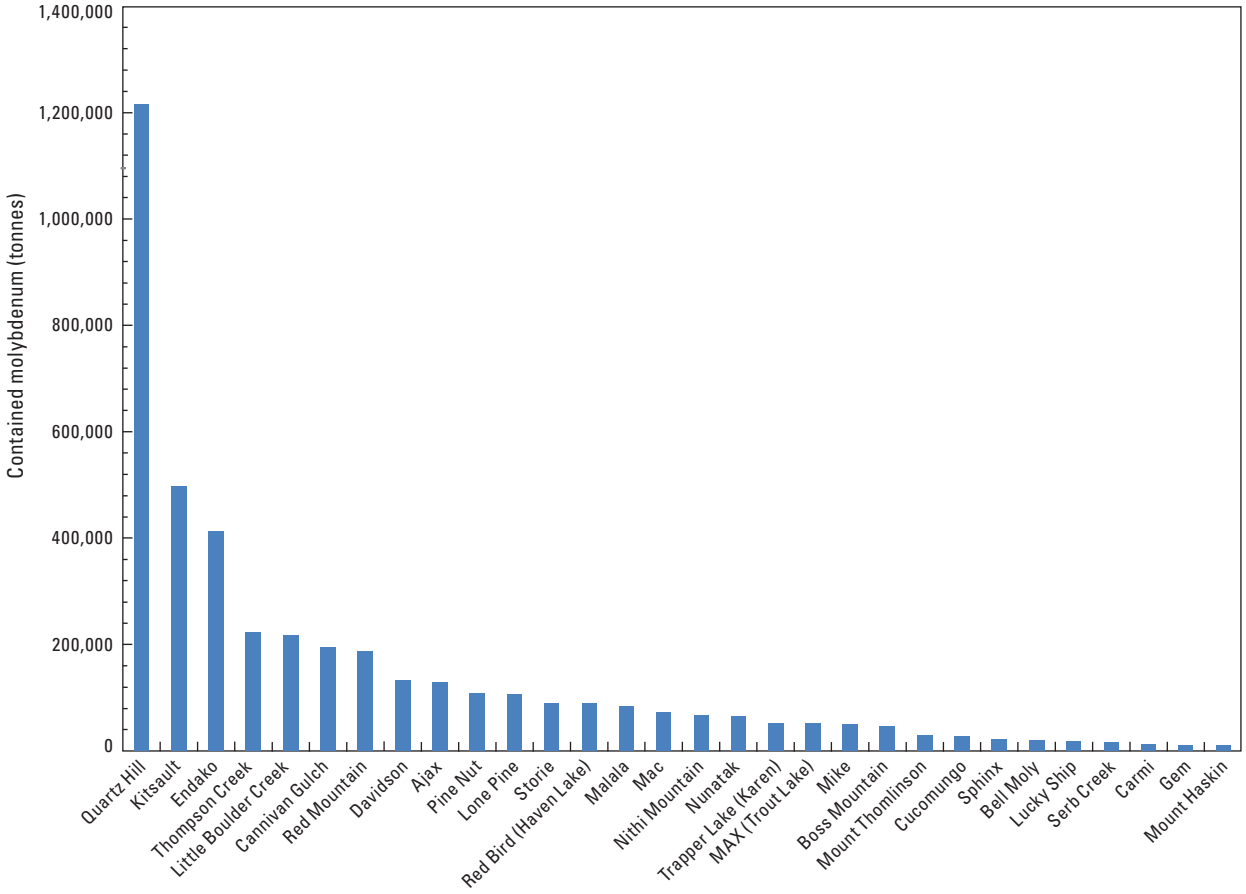

Figure A2. The top 30 largest arc-related porphyry molybdenum deposits in contained molybdenum (Mo). Data from table A1.

Appendix 2. pH and dissolved metal concentrations of waters associated with arc-related porphyry molybdenum deposits and the Buckingham, Nevada molybdenum-rich porphyry copper deposit for comparison.

[mg/L, milligrams per liter; $CaCO_3$, calcium carbonate; µg/L, micrograms per liter; -, not reported or not analyzed; <, less than. Elemental abbreviations: Al, aluminum; As, arsenic; Cd, cadmium; Co, cobalt, Cr, chromium; Cu, copper; Fe, iron; Hg, mercury; Mn, manganese; Mo, molybdenum; Ni, nickel; Pb, lead; Se, selenium; Zn, zinc]

Deposit	Water type	pH	Alkalinity (mg/L $CaCO_3$)	Al (µg/L)	As (µg/L)	Cd (µg/L)	Co (µg/L)	Cr (µg/L)	Cu (µg/L)
Endako, British Columbia	premining surface water	-	-	-	-	-	-	-	-
Endako, British Columbia	background of mining area, surface water	-	-	-	-	-	-	-	-
Endako, British Columbia	tailings seepage	-	-	-	-	-	-	-	-
Endako, British Columbia	open pit discharge	-	-	-	-	-	-	-	-
Endako, British Columbia	mine drainage and downstream mine-impacted waters	7.5–8.2	194–393.5	-	-	-	-	-	5–9
Endako, British Columbia	background surface waters upstream of mining	7.0–7.5	101–230	-	-	-	-	-	7–9
Endako, British Columbia	Denak East Pit-pit lake	7.37–8.13	-	-	-	-	-	-	2–5
White Cloud, Idaho	adit on hillside about 80 feet above Little Boulder Creek, as shown on USGS 7.5' topo quad	7.7	-	3.4	3.1	0.3	1.4	<1	0.6
White Cloud, Idaho	Little Boulder Creek about 0.5 mile downstream from the Baker adit	8	-	0.6	0.5	<0.02	<0.02	<1	<0.5
Cannivan Gulch, Montana	no known mining-related disturbances upgradient or upstream from the sampling site; creek that drains parallel to road near Queens Gulch	7.79	102	9.6	2	<0.02	0.08	<1	<0.5
Cannivan Gulch, Montana	no known mining-related disturbances upgradient or upstream from the sampling site; Queens Gulch(?)	7.84	58.6	19.8	2	<0.02	0.07	<1	0.52
Cannivan Gulch, Montana	no known mining-related disturbances upgradient or upstream from the sampling site; downstream from confluence of sites 2 and 3	7.79	92.1	13.7	2	0.02	0.1	<1	<0.5
Cannivan Gulch, Montana	no known mining-related disturbances upgradient or upstream from the sampling site; small creek that drains east side of park, 200 meters east of site 4	7.02	21.6	54.3	2	0.02	0.17	<1	1.3
Cannivan Gulch, Montana	potential mining-related disturbances upgradient or upstream from the sampling site; Queens Gulch at top of meadow	8.61	-	5.2	1	<0.02	0.03	<1	<0.5
Cannivan Gulch, Montana	definite mining-related disturbances upgradient or upstream from the sampling site; drainage from lower adit of Queen of the Hills mine	7.02	77.3	4.3	<1	0.26	0.02	<1	<0.5
Cannivan Gulch, Montana	definite mining-related disturbances upgradient or upstream from the sampling site; toe of dump; one of two springs	7.89	78.2	4.7	<1	0.17	0.02	<1	<0.5
Cannivan Gulch, Montana	definite mining-related disturbances upgradient or upstream from the sampling site; toe of dump; two of two springs	7.94	77	21.1	<1	0.17	0.03	<1	<0.5
Cannivan Gulch, Montana	definite mining-related disturbances upgradient or upstream from the sampling site; Queens Gulch due south of Queen of the Hills mine	-	-	6	1	<0.02	0.03	<1	<0.5
Cannivan Gulch, Montana	definite mining-related disturbances upgradient or upstream from the sampling site; drainage from exploration adit at head of Buffalo Gulch	7.63	-	4.4	1	0.87	0.03	<1	3.8
Cannivan Gulch, Montana	definite mining-related disturbances upgradient or upstream from the sampling site; spring issuing from base of mine dump	7.26	-	3.8	<1	0.43	0.05	<1	2.2

Appendix 2. pH and dissolved metal concentrations of waters associated with arc-related porphyry molybdenum deposits and the Buckingham, Nevada molybdenum-rich porphyry copper deposit for comparison.—Continued

[mg/L, milligrams per liter; $CaCO_3$, calcium carbonate; µg/L, micrograms per liter; -, not reported or not analyzed; <, less than. Elemental abbreviations: Al, aluminum; As, arsenic; Cd, cadmium; Co, cobalt, Cr, chromium; Cu, copper; Fe, iron; Hg, mercury; Mn, manganese; Mo, molybdenum; Ni, nickel; Pb, lead; Se, selenium; Zn, zinc]

Deposit	Fe (µg/L)	Hg (µg/L)	Mn (µg/L)	Mo (µg/L)	Ni (µg/L)	Pb (µg/L)	Se (µg/L)	Sulfate (mg/L)	Zn (µg/L)	Reference
Endako, British Columbia	-	-	-	0–32+	-	-	-	-	-	Mathieu, 1995
Endako, British Columbia	-	-	-	10–340	-	-	-	-	-	Mathieu, 1995
Endako, British Columbia	-	-	-	1,500–6,000	-	-	-	-	-	Mathieu, 1995
Endako, British Columbia	-	-	-	25,000	-	-	-	-	-	Mathieu, 1995
Endako, British Columbia	<30–54	-	-	213–16,800	-	<1	-	5.84–1,225	-	Mathieu, 1995
Endako, British Columbia	<30–48	-	-	9–217	-	<1	-	6.3–39.2	-	Mathieu, 1995
Endako, British Columbia	-	-	-	16,400–49,000	-	-	-	-	-	Mathieu, 1995
White Cloud, Idaho	290	<0.005	290	160	2.6	0.08	<0.4	63	57	Giles and others, 2009
White Cloud, Idaho	31	-	0.57	9.4	<0.1	<0.05	<0.4	4.1	<0.5	Giles and others, 2009
Cannivan Gulch, Montana	<50	-	10.5	<2	0.8	<0.05	<1	1.73	1.3	Wanty and others, 2003; Giles and others, 2009
Cannivan Gulch, Montana	<50	-	6.1	<2	0.9	<0.05	<1	0.7	2.8	Wanty and others, 2003; Giles and others, 2009
Cannivan Gulch, Montana	<50	-	14.7	4.1	0.9	<0.05	<1	1.48	9.3	Wanty and others, 2003; Giles and others, 2009
Cannivan Gulch, Montana	106	-	24.4	<2	1.4	0.1	<1	1.35	18.9	Wanty and others, 2003; Giles and others, 2009
Cannivan Gulch, Montana	<50	-	0.2	<2	0.8	0.82	<1	4.86	1.2	Wanty and others, 2003; Giles and others, 2009
Cannivan Gulch, Montana	<50	-	0.7	<2	0.6	0.09	<1	2.75	18.8	Wanty and others, 2003; Giles and others, 2009
Cannivan Gulch, Montana	<50	-	0.6	<2	0.6	0.07	<1	2.71	11	Wanty and others, 2003; Giles and others, 2009
Cannivan Gulch, Montana	<50	-	0.7	<2	0.6	0.07	<1	2.74	12.2	Wanty and others, 2003; Giles and others, 2009
Cannivan Gulch, Montana	<50	-	<0.2	<2	0.9	<0.05	<1	-	1.4	Wanty and others, 2003; Giles and others, 2009
Cannivan Gulch, Montana	<50	-	1.3	821	1	<0.05	1.6	36.1	33.2	Wanty and others, 2003; Giles and others, 2009
Cannivan Gulch, Montana	<50	-	1.6	273	1.7	<0.05	<1	34.5	51.1	Wanty and others, 2003; Giles and others, 2009

Appendix 2. pH and dissolved metal concentrations of waters associated with arc-related porphyry molybdenum deposits and the Buckingham, Nevada molybdenum-rich porphyry copper deposit for comparison.—Continued

[mg/L, milligrams per liter; $CaCO_3$, calcium carbonate; µg/L, micrograms per liter; -, not reported or not analyzed; <, less than. Elemental abbreviations: Al, aluminum; As, arsenic; Cd, cadmium; Co, cobalt, Cr, chromium; Cu, copper; Fe, iron; Hg, mercury; Mn, manganese; Mo, molybdenum; Ni, nickel; Pb, lead; Se, selenium; Zn, zinc]

Deposit	Water type	pH	Alkalinity (mg/L $CaCO_3$)	Al (µg/L)	As (µg/L)	Cd (µg/L)	Co (µg/L)	Cr (µg/L)	Cu (µg/L)
Cannivan Gulch, Montana	no known mining-related disturbances upgradient or upstream from the sampling site; headwater spring of Cannivan Gulch	7.59	178	5.2	<1	0.18	0.05	<1	1.2
Cannivan Gulch, Montana	no known mining-related disturbances upgradient or upstream from the sampling site; small rivulet that crosses Cannivan Gulch Road	7.21	184	5.3	<1	0.23	0.05	<1	1.4
Cannivan Gulch, Montana	potential mining-related disturbances upgradient or upstream from the sampling site; Cannivan Gulch at lowest flowing water	8.35	172	12.9	1	0.08	0.05	<1	1.2
Thompson Creek, Idaho[3]	surface-water pit sump concentrations (1989 and 1990) at active mine	3.6–7.3	-	570	<5.0–167	<5–68	-	-	<10–210
Thompson Creek, Idaho[3]	surface water monitoring stations along a creek downstream from tailings pond (1989–1990) at active mine	6.1–8.6	-	<100–270	<5.0	<5.0–12.0	-	-	<10–20
Thompson Creek, Idaho[3]	surface water monitoring for tailings pond and main drain (1989 and 1990)	5.2–8.7	-	<100–1,200	<5.0	<5.0–10	-	-	<10–60
Thompson Creek, Idaho[3]	ground water monitoring wells associated with tailings impoundment	5.8–8.0	-	<100–44,000	<5.0–23	<5.0–32	-	-	<10–120
Buckingham, Nevada	no known mining-related disturbances upgradient or upstream from the sampling site; spring at Long Canyon; field site 98NV001	7	167	< 10	7.22	71.7	0.04	0.24	1.94
Buckingham, Nevada	no known mining-related disturbances upgradient or upstream from the sampling site; stream at Long Canyon; field site 98NV002	8	71	35	41.2	21.8	0.04	0.09	<0.01
Buckingham, Nevada	no known mining-related disturbances upgradient or upstream from the sampling site; North Fork, Long Canyon; field site 98NV003	8	51	70	74.7	15.6	0.07	0.08	0.01
Buckingham, Nevada	no known mining-related disturbances upgradient or upstream from the sampling site; South Fork, Long Canyon; field site 98NV004	8	36	90	99.5	9.4	0.08	0.08	0.01
Buckingham, Nevada	no known mining-related disturbances upgradient or upstream from the sampling site; Licking Creek; field site 98NV005	8	50	21	24.7	17.1	0.03	0.08	0.02
Buckingham, Nevada	no known mining-related disturbances upgradient or upstream from the sampling site; Licking Creek; field site 98NV006	8	50	18	19.9	17.3	0.03	0.09	0.01
Buckingham, Nevada	no known mining-related disturbances upgradient or upstream from the sampling site; tributary to Licking Creek; field site 98NV007	5	-	3,100	3,190	114	11.1	20.2	0.05
Buckingham, Nevada	no known mining-related disturbances upgradient or upstream from the sampling site; springs at site 98NV-7; field site 98NV008	4	-	9,800	9,880	122	27.9	51.7	0.02
Buckingham, Nevada	no known mining-related disturbances upgradient or upstream from the sampling site; Licking Creek Below confluence with sample 98NV-007; field site 98NV009A	7	34	67	72.5	50.7	1.52	5.16	0.01
Buckingham, Nevada	no known mining-related disturbances upgradient or upstream from the sampling site; Licking Creek above confluence with site 98NV-007; field site 98NV010	8	51	13	17	19.9	0.02	0.1	<0.01

Appendix 2. pH and dissolved metal concentrations of waters associated with arc-related porphyry molybdenum deposits and the Buckingham, Nevada molybdenum-rich porphyry copper deposit for comparison.—Continued

[mg/L, milligrams per liter; $CaCO_3$, calcium carbonate; µg/L, micrograms per liter; -, not reported or not analyzed; <, less than. Elemental abbreviations: Al, aluminum; As, arsenic; Cd, cadmium; Co, cobalt, Cr, chromium; Cu, copper; Fe, iron; Hg, mercury; Mn, manganese; Mo, molybdenum; Ni, nickel; Pb, lead; Se, selenium; Zn, zinc]

Deposit	Fe (µg/L)	Hg (µg/L)	Mn (µg/L)	Mo (µg/L)	Ni (µg/L)	Pb (µg/L)	Se (µg/L)	Sulfate (mg/L)	Zn (µg/L)	Reference
Cannivan Gulch, Montana	<50	-	0.4	133	1.4	<0.05	<1	13.2	25.3	Wanty and others, 2003; Giles and others, 2009
Cannivan Gulch, Montana	<50	-	<0.2	173	1.4	<0.05	<1	16.3	27.2	Wanty and others, 2003; Giles and others, 2009
Cannivan Gulch, Montana	<50	-	1.4	49.3	1.3	<0.05	<1	5.2	5.6	Wanty and others, 2003; Giles and others, 2009
Thompson Creek, Idaho[3]	460–2,500	<0.50–50	1,300	-	-	<50–150		-	<5–1,080	U.S. Environmental Protection Agency, 1992
Thompson Creek, Idaho[3]	<10–190	<0.50–6.8	<10–50	-	-	<50–140	<5.0	-	<5–20	U.S. Environmental Protection Agency, 1992
Thompson Creek, Idaho[3]	170–9,400	-	270–9,600	-	-	<50–160	<2–9.0		<5–124	U.S. Environmental Protection Agency, 1992
Thompson Creek, Idaho[3]	210–14,000	-	<50–890	-	-					
Buckingham, Nevada	1,600	0.016	16.8	250	0.01	0.03	3.5	132	–0.005	Tuttle and others, 2002; Giles and others, 2009
Buckingham, Nevada	<50	0.006	7.59	1.7	0.02	0.03	3.1	45	–0.005	Tuttle and others, 2002; Giles and others, 2009
Buckingham, Nevada	52	0.006	5.9	1.2	0.03	0.02	2.8	34	0.005	Tuttle and others, 2002; Giles and others, 2009
Buckingham, Nevada	58	0.005	3.32	0.7	0.03	0.05	3.2	25	–0.005	Tuttle and others, 2002; Giles and others, 2009
Buckingham, Nevada	<50	0.008	5.86	0.8	0.02	0.06	3.3	51	–0.005	Tuttle and others, 2002; Giles and others, 2009
Buckingham, Nevada	<50	0.005	5.88	1.2	0.02	0.06	3.1	52	–0.005	Tuttle and others, 2002; Giles and others, 2009
Buckingham, Nevada	<50	0.007	40.3	749	10.7	0.01	6.2	0	1.15	Tuttle and others, 2002; Giles and others, 2009
Buckingham, Nevada	<50	0.007	42.3	2,000	29.4	0.05	7.6	0	3.15	Tuttle and others, 2002; Giles and others, 2009
Buckingham, Nevada	<50	0.006	17.7	211	1.27	0.01	4.4	201	0.08	Tuttle and others, 2002; Giles and others, 2009
Buckingham, Nevada	<50	0.006	6.64	1.7	0.02	0.06	3.3	61	–0.005	Tuttle and others, 2002; Giles and others, 2009

Appendix 2. pH and dissolved metal concentrations of waters associated with arc-related porphyry molybdenum deposits and the Buckingham, Nevada molybdenum-rich porphyry copper deposit for comparison.—Continued

[mg/L, milligrams per liter; $CaCO_3$, calcium carbonate; µg/L, micrograms per liter; -, not reported or not analyzed; <, less than. Elemental abbreviations: Al, aluminum; As, arsenic; Cd, cadmium; Co, cobalt, Cr, chromium; Cu, copper; Fe, iron; Hg, mercury; Mn, manganese; Mo, molybdenum; Ni, nickel; Pb, lead; Se, selenium; Zn, zinc]

Deposit	Water type	pH	Alkalinity (mg/L $CaCO_3$)	Al (µg/L)	As (µg/L)	Cd (µg/L)	Co (µg/L)	Cr (µg/L)	Cu (µg/L)
Buckingham, Nevada	no known mining-related disturbances upgradient or upstream from the sampling site; Licking Creek above confluence with Long Creek; field site 98NV011	8	34	95	109	49.1	0.23	3.82	0.01
Buckingham, Nevada	no known mining-related disturbances upgradient or upstream from the sampling site; Long Creek above confluence with Licking Creek; field site 98NV012	8	86	41	48.3	30.6	0.04	0.13	<0.01
Buckingham, Nevada	no known mining-related disturbances upgradient or upstream from the sampling site; confluence of sites 98NV-011 and 98NV-012; field site 98NV013	8	63	55	62.6	37.8	0.12	1.47	<0.01
Buckingham, Nevada	probable mining-related disturbances upgradient or upstream from the sampling site; Cow Creek below mine effluent; field site 98NV014	8	150	80	92.3	51.8	–0.01	0.91	0.31
Buckingham, Nevada	definite mining-related disturbances upgradient or upstream from the sampling site; mine effluent before it enters Cow Creek; field site 98NV015	5		2,900	3,170	59.4	5.47	18.8	5.94
Buckingham, Nevada	no known mining-related disturbances upgradient or upstream from the sampling site; Cow Creek above confluence with mine effluent; field site 98NV016	8	164	12	15.1	51.8	0.01	0.14	0.06
Buckingham, Nevada	definite mining-related disturbances upgradient or upstream from the sampling site; drainage from pyrite-rich dump; field site 98NV017	3		35,000	38,300	74.4	30.1	49.8	4.73
Buckingham, Nevada	no known mining-related disturbances upgradient or upstream from the sampling site; natural drainage above site 98NV-017; field site 98NV018	8	145	24	19.8	38.8	0.02	0.13	0.03
Buckingham, Nevada	no known mining-related disturbances upgradient or upstream from the sampling site; Duck Creek Headwaters above Galena townsite; field site 98NV019	8	86	53	55.8	23.5	0.06	0.15	0.03
Buckingham, Nevada	definite mining-related disturbances upgradient or upstream from the sampling site; caved adit; field site 98NV020	7	253	< 10	9.86	182	0.05	39.8	3.53
Buckingham, Nevada	probable mining-related disturbances upgradient or upstream from the sampling site; Duck Creek; field site 98NV021	8	129	76	90.1	78.4	0.08	0.96	0.02
Buckingham, Nevada	probable mining-related disturbances upgradient or upstream from the sampling site; Butte Canyon; field site 98NV023	3	-	68,000	73,100	298	144	720	<1
Buckingham, Nevada	probable mining-related disturbances upgradient or upstream from the sampling site; Iron Canyon; field site 98NV024	-	-	310,000	363,000	545	349	4790	<1
Buckingham, Nevada	potential mining-related disturbances upgradient or upstream from the sampling site; Duck Creek at old haulage road; field site 98NV025	8	124	230	75.7	178	0.07	68.7	0.01
Buckingham, Nevada	potential mining-related disturbances upgradient or upstream from the sampling site; Little Cottonwood Creek; field site 98NV026	8	89	51	21.9	30	0.02	0.12	<0.01

Appendix 2. pH and dissolved metal concentrations of waters associated with arc-related porphyry molybdenum deposits and the Buckingham, Nevada molybdenum-rich porphyry copper deposit for comparison.—Continued

[mg/L, milligrams per liter; $CaCO_3$, calcium carbonate; µg/L, micrograms per liter; -, not reported or not analyzed; <, less than. Elemental abbreviations: Al, aluminum; As, arsenic; Cd, cadmium; Co, cobalt, Cr, chromium; Cu, copper; Fe, iron; Hg, mercury; Mn, manganese; Mo, molybdenum; Ni, nickel; Pb, lead; Se, selenium; Zn, zinc]

Deposit	Fe (µg/L)	Hg (µg/L)	Mn (µg/L)	Mo (µg/L)	Ni (µg/L)	Pb (µg/L)	Se (µg/L)	Sulfate (mg/L)	Zn (µg/L)	Reference
Buckingham, Nevada	<50	0.006	17	155	0.21	0.02	4.3	203	0.02	Tuttle and others, 2002; Giles and others, 2009
Buckingham, Nevada	<50	0.01	9.5	3.1	0.02	0.04	3.3	59	–0.005	Tuttle and others, 2002; Giles and others, 2009
Buckingham, Nevada	<50	0.006	12.5	61.2	0.12	0.03	3.6	114	0.007	Tuttle and others, 2002; Giles and others, 2009
Buckingham, Nevada	<50	0.005	17.5	40.7	–0.01	–0.01	2.2	60	–0.005	Tuttle and others, 2002; Giles and others, 2009
Buckingham, Nevada	1,600	0.007	18.5	705	4.08	–0.01	3.2	274	0.32	Tuttle and others, 2002; Giles and others, 2009
Buckingham, Nevada	<50	0.005	17.4	3.9	0.01	0.01	2.4	43	–0.005	Tuttle and others, 2002; Giles and others, 2009
Buckingham, Nevada	19,000	0.008	23.9	2,400	23.9	0.04	14.7	0	1.84	Tuttle and others, 2002; Giles and others, 2009
Buckingham, Nevada	<50	0.007	11.2	9.2	0.01	0.04	3	26	–0.005	Tuttle and others, 2002; Giles and others, 2009
Buckingham, Nevada	<50	0.007	5.33	1.1	0.08	0.4	3.9	20	0.01	Tuttle and others, 2002; Giles and others, 2009
Buckingham, Nevada	3,300	0.007	79.2	4,800	0.03	–0.01	2.9	555	0.01	Tuttle and others, 2002; Giles and others, 2009
Buckingham, Nevada	52	0.005	21.5	21.4	0.05	0.3	4.5	167	–0.005	Tuttle and others, 2002; Giles and others, 2009
Buckingham, Nevada	53,000	0.015	200	12,900	93.8	<1	<10		9.3	Tuttle and others, 2002; Giles and others, 2009
Buckingham, Nevada	140,000	0.012	674	32,600	317	1.3	26.1		45.6	Tuttle and others, 2002; Giles and others, 2009
Buckingham, Nevada	71	0.01	66.9	913	0.04	0.01	3.1	619	0.007	Tuttle and others, 2002; Giles and others, 2009
Buckingham, Nevada	<50	0.006	9.21	1.8	0.01	0.03	2.6	41	–0.005	Tuttle and others, 2002; Giles and others, 2009

Appendix 2. pH and dissolved metal concentrations of waters associated with arc-related porphyry molybdenum deposits and the Buckingham, Nevada molybdenum-rich porphyry copper deposit for comparison.—Continued

[mg/L, milligrams per liter; $CaCO_3$, calcium carbonate; µg/L, micrograms per liter; -, not reported or not analyzed; <, less than. Elemental abbreviations: Al, aluminum; As, arsenic; Cd, cadmium; Co, cobalt, Cr, chromium; Cu, copper; Fe, iron; Hg, mercury; Mn, manganese; Mo, molybdenum; Ni, nickel; Pb, lead; Se, selenium; Zn, zinc]

Deposit	Water type	pH	Alkalinity (mg/L $CaCO_3$)	Al (µg/L)	As (µg/L)	Cd (µg/L)	Co (µg/L)	Cr (µg/L)	Cu (µg/L)
Buckingham, Nevada	no known mining-related disturbances upgradient or upstream from the sampling site; tributary to Little Cottonwood Creek; field site 98NV027	8	152	13	7.5	46	0.02	0.16	<0.01
Buckingham, Nevada	potential mining-related disturbances upgradient or upstream from the sampling site; confluence of sites 98NV-026 and 98NV-027; field site 98NV028	8	112	19	19.9	35	0.02	0.13	<0.01
Buckingham, Nevada	no known mining-related disturbances upgradient or upstream from the sampling site; Elder Creek; field site 98NV029	8	117	<10	4.55	36.1	–0.01	0.08	<0.01
Buckingham, Nevada	no known mining-related disturbances upgradient or upstream from the sampling site; Elder Creek; field site 98NV030	8	119	<10	4.89	34.9	–0.01	0.08	<0.01
Buckingham, Nevada	no known mining-related disturbances upgradient or upstream from the sampling site; Elder Creek; field site 98NV031	8	121	<10	7.85	34.8	–0.01	0.08	<0.01
Buckingham, Nevada	no known mining-related disturbances upgradient or upstream from the sampling site; tributary to Elder Creek; field site 98NV032	8	80	26	31.6	23.3	0.02	0.07	<0.01
Buckingham, Nevada	no known mining-related disturbances upgradient or upstream from the sampling site; unnamed ephemeral drainage on west side of Elder Canyon; field site 98NV033	8	34	140	71.8	16.4	0.04	0.07	0.03
Buckingham, Nevada	no known mining-related disturbances upgradient or upstream from the sampling site; same drainage, downstream of site 98NV033; field site 98NV034	8	41	15	15	19.7	0.01	0.07	<0.01
Buckingham, Nevada	undisturbed, seep from deposit	4.0	-	-	-	-	-	-	-
Buckingham, Nevada	undisturbed, seep near deposit boundary	7.4	-	-	-	-	-	-	-
Buckingham, Nevada	undisturbed, surface water upstream and within deposit (Long Canyon)	7.6–8.4	-	-	-	-	-	-	-
Average background freshwater in the United States		-	-	-	-	-	-	-	-
Median surface water of North America		-	-	-	-	-	-	-	-
Drinking water guideline		-	-		10	3	-	50	2,000
Aquatic ecosystem acute toxicity[1]		-	-	750	340	2	-	570	13
Aquatic ecosystem chronic toxicity[1]		6.5–9	-	87	150	0.25	-	74	9

Appendix 2. pH and dissolved metal concentrations of waters associated with arc-related porphyry molybdenum deposits and the Buckingham, Nevada molybdenum-rich porphyry copper deposit for comparison.—Continued

[mg/L, milligrams per liter; $CaCO_3$, calcium carbonate; µg/L, micrograms per liter; -, not reported or not analyzed; <, less than. Elemental abbreviations: Al, aluminum; As, arsenic; Cd, cadmium; Co, cobalt, Cr, chromium; Cu, copper; Fe, iron; Hg, mercury; Mn, manganese; Mo, molybdenum; Ni, nickel; Pb, lead; Se, selenium; Zn, zinc]

Deposit	Fe (µg/L)	Hg (µg/L)	Mn (µg/L)	Mo (µg/L)	Ni (µg/L)	Pb (µg/L)	Se (µg/L)	Sulfate (mg/L)	Zn (µg/L)	Reference
Buckingham, Nevada	<50	0.006	16.2	2.7	–0.01	0.02	2.4	47	–0.005	Tuttle and others, 2002; Giles and others, 2009
Buckingham, Nevada	<50	0.006	11.7	1.8	–0.01	0.03	2.4	43	–0.005	Tuttle and others, 2002; Giles and others, 2009
Buckingham, Nevada	<50	0.006	12.2	0.3	–0.01	0.02	2.3	41	–0.005	Tuttle and others, 2002; Giles and others, 2009
Buckingham, Nevada	<50	0.006	11.4	0.3	–0.01	0.02	2.1	33	–0.005	Tuttle and others, 2002; Giles and others, 2009
Buckingham, Nevada	<50	0.006	11.4	0.6	–0.01	0.02	2.1	34	–0.005	Tuttle and others, 2002; Giles and others, 2009
Buckingham, Nevada	<50	0.006	7.35	0.6	0.01	0.02	2	25	–0.005	Tuttle and others, 2002; Giles and others, 2009
Buckingham, Nevada	96	0.007	4.25	0.7	0.03	0.1	2.2	39	–0.005	Tuttle and others, 2002; Giles and others, 2009
Buckingham, Nevada	<50	0.006	5.17	0.4	0.01	0.1	3	54	–0.005	Tuttle and others, 2002; Giles and others, 2009
Buckingham, Nevada	-	-	-	-	-	-	-	-		Tuttle and others, 2002
Buckingham, Nevada	-	-	-	-	-	-	-	-		Tuttle and others, 2002
Buckingham, Nevada	-	-	-	-	-	-	-	-		Tuttle and others, 2002
Average background freshwater in the United States	-	-	-	1	-	-	-	-		Chappell and others, 1979
Median surface water of North America	-	-	-	1	-	-	-	-		Hem, 1985
Drinking water guideline	300	2	400	70	70	10	50	-	5,000	World Health Organization, 2008
Aquatic ecosystem acute toxicity[1]	-	1.4	-	-	470	65		-	120	U.S. Environmental Protection Agency, 2006
Aquatic ecosystem chronic toxicity[1]	1,000	0.77	-	-	52	2.5	5	-	120	U.S. Environmental Protection Agency, 2006

[1]Freshwater criterion for Cd, Cr (assume Cr (III)), Cu, Pb, Ni and Zn are hardness dependent and calculated based on a hardness of 100 mg/L $CaCO_3$. Al, Fe, and pH are nonpriority pollutants.

[2] Estimated concentration for Cu.

[3]Historic data for 1989–1990 from Cyprus Minerals Corp. included in EPA report.

Publishing support provided by:
Rolla Publishing Service Center, Rolla, Missouri, and
Denver Publishing Service Center, Denver, Colorado

For more information concerning this publication, contact:
Center Director, USGS Geology and Environmental Change Science Center
Box 25046, Mail Stop 980
Denver, CO 80225
(303) 236-5344

Or visit the Geology and Environmental Change Service Center Web site at:
http://esp.cr.usgs.gov/

This report is available at: *http://pubs.usgs.gov/sir/2010/5070/d*